GREENER AND FACILE APPROACHES TOWARDS SYNTHESIS OF ORGANIC SEMICONDUCTING MATERIALS

By

FATHIMA FAZNA PARY

Bachelor of Science in Chemistry
University of Kelaniya
Kelaniya, Sri Lanka
2013

Submitted to the Faculty of the
Graduate College of the
Oklahoma State University
in partial fulfillment of
the requirements for
the Degree of
DOCTOR OF PHILOSOPHY
December, 2020

GREENER AND FACILE APPROACHES TOWARDS SYNTHESIS OF ORGANIC SEMICONDUCTING MATERIALS

Dissertation Approved:

Dr. Toby L. Nelson

Dissertation Adviser

Dr. Kenneth D. Berlin

Dr. Richard A. Bunce

Dr. Gabriel A. Cook

Dr. Heather Fahlenkamp

ACKNOWLEDGEMENTS

First and foremost, I am grateful to the almighty God for giving me a wonderful life throughout my Ph.D. journey.

Next, I would like to thank my advisor Dr. Toby L. Nelson for his enormous support, guidance, motivation, and appreciation all the time. Thank you very much.. I could not have gone through this journey without your support, encouragement, and the nice environment you created in our lab.

I am also thankful to my advisory committee members Dr. K. Darrell Berlin, Dr. Richard Bunce, Dr. Gabriel Cook, and Dr. Heather Fahlenkamp for their valuable suggestions and support on my Ph.D. candidacy exam and my dissertation.

I would like to thank all my group members, Dr. Devang Khambhati, Dr. Raianna Hopson, Dr. Niradha Sachinthani, Dr. Santosh Adhikari, Martha Essandoh, Tharika Nirmani, Mohammad Ebqa'ai, and all the undergraduates for making a joyful and co-operative environment in the laboratory. Thank you very much for your support, advice, and suggestions all the time. Special thanks to Dr. Niradha Sachinthani for her support from the beginning to the end.

Most of my projects were conducted with a collaborative approach and I am grateful to all my collaborators including Dr. Jamal Musaev, Dr. Marimuthu Andiappan, and Dr. Eric Anslyn. Many thanks go to Ravi Teja from the Andiappan group for his support and nice collaboration with Cu (I) oxide nanoparticles mediated polymerization project.

I would also like to thank all the faculty and staff members of the chemistry department at Oklahoma State University.

I am taking this opportunity to thank my teachers and mentors at the University of Kelaniya Sri-Lanka, who guided and motivated me towards this position.

At last but not least, I would like to offer my sincere gratitude to my family. My husband, Shafraz Jinnah who dedicated his valuable time because of me. Without your unceasing support, motivation, and suggestions I could never complete my Ph.D. My loving two little daughters, Izma Shafraz and Yaara Shafraz you both were really supportive to me; you were my secret of stress-free Ph.D. life. My parents; Hussain Pary and Jesmin Mubarak, and my loving sister Rukshana Pary; your scarification and continuous prayer made my Ph.D. journey a success.

Name: FATHIMA FAZNA PARY

Date of Degree: DECEMBER, 2020

Title of Study: GREENER AND FACILE APPROACHES TOWARDS SYNTHESIS OF ORGANIC SEMICONDUCTING MATERIALS

Major Field: CHEMISTRY

Abstract: Organic semiconductors (OSCs) are carbon-based materials that exhibit semiconducting properties and can be classified as π-conjugated small molecules and polymers. Over the past few decades, OSCs have attracted many fields due to their diverse range of applications in electronics, such as organic light-emitting diodes, organic photovoltaics, organic field-effect transistors, and sensors. These organic semiconductors offer several advantages over conventional semiconductors since they can be processed from solution at low temperature, have good mechanical flexibility and tunability, and have good electrical and chemical properties. With the worldwide demand for energy and technology, there is a critical need to design and synthesize high performing organic semiconductors that are robust, tunable optical, electrical, and physical properties. A major limitation associated with the organic semiconducting materials is their syntheses. Most of the synthetic approaches require many steps, rely on stoichiometric amounts of toxic metallic reagents, and result is the formation of large amounts of toxic byproducts. Therefore, a key challenge is to develop green methods and create strategies to synthesize semiconducting materials in a manner that reduces cost, waste, environmental impact, and improve safety.

In this regard, my researches were focused on the utilization of C-H direct arylation strategy, Cu_2O nanoparticles mediated oxidative homocoupling polymerization, synthesis of conjugated polymers using energy-efficient and aerobic conditions, and solid-state synthesis of conjugated polymers promoted by ball milling.

TABLE OF CONTENTS

Chapter Page

I. INTRODUCTION 1

1.1 ORGANIC SEMICONDUCTORS 1
1.2 CLASSIFICATION OF ORGANIC SEMICONDUCTORS 4
1.2.1 Conjugated small molecules 4
1.2.2 Conjugated polymers 5
1.3 STRATEGIES TO DESIGN HIGH-PERFORMANCE OSCs 6
1.4 CONVENTIONAL SYNTHETIC TOOLS FOR CONJUGATED SMALL MOLECULES AND POLYMERS 9
1.4.1 Stille cross-coupling reaction 10
1.4.2 Suzuki-Miyaura reaction 10
1.4.3 Sonogashira reaction 10
1.5 GREENER SYNTHETIC TOOLS FOR CONJUGATED MOLECULES 11
1.5.1 Direct heteroarylation polymerization 12
1.5.2 Green solvents 12
1.5.3 First-row transition metal catalysts 13
1.5.4 Energy efficient and aerobic reaction conditions 13
1.5.5 Microwave irradiation 13
1.5.6 Ball milling 14

II. PROGRESS TOWARDS REGIOSELECTIVE COPPER MEDIATED DIRECT ARYLATION OF BENZODITHIOPHENE-S,S-TETRAOXIDE: MECHANISTIC INSIGHT AND FURTHER UTILIZATION 16

2.1 INTRODUCTION 16
2.2 SYNTHESIS OF NOVEL BENZODITHIOPHENE-S,S- TETRAOXIDE BASED CONJUGATED POLYMERS VIA C-H DIRECT ARYLATION POLYMERIZATION (DArP) 17
2.2.1 COPPER MEDIATED C-H DArP 17
2.2.1.1 RESULTS AND DISCUSSION 17
2.2.2 ATTEMPTED SYNTHESIS OF BENZODITHIOPHENE-S,S-TETRAOXIDE BASED NOVEL CONJUGATED POLYMERS VIA Pd CATALYZED DArP 19
2.2.2.1 RESULTS AND DISCUSSION 19

Chapter Page

2.3 MECHANISTIC INSIGHT OF REGIOSELECTIVE COPPER MEDIATED DIRECT ARYLATION OF BENZODITHIOPHENE-S,S-TETRAOXIDE ..20
2.3.1 RESULTS AND DISCUSSION 20
2.4 ATTEMPTED DIVERSIFICATION STUDIES OF COPPER MEDIATED C-H DIRECTARYLATION OF BDTT 24
2.4.1 RESULTS AND DISCUSSION 24
2.5 COPPER (I) OXIDE NANOPARTICLE MEDIATED C-H DIRECT ARYLATION OF BDTT 26
2.5.1 RESULTS AND DISCUSSION 26
2.6 SYNTHESIS AND OPTICAL PROPERTIES OF BDTT BASED DONOR-ACCEPTOR CONJUGATED POLYMERS 27
2.6.1 RESULTS AND DISCUSSION 27
2.7 CONCLUSION 31
2.8 EXPERIMENTAL SECTION 31
2.8.1 Materials 31
2.8.2 Instrumentation 32
2.8.3 Synthesis 32
2.8.4 Spectra 35

III. COPPER (I) OXIDE NANOPARTICLE-MEDIATED SYNTHESIS OF POLYPHENYLENEDIETHYNYLENES 38

3.1 INTRODUCTION 38
3.2 RESULTS AND DISCUSSION 39
3.2.1 Evidence for homogeneous catalytic pathway 43
3.3 CONCLUSION 46
3.4 EXPERIMENTAL SECTION 46
3.4.1 General methods and materials 46
3.4.2 Polymer synthesis and characterization 47
3.4.3 Spectra 47

IV. “BENCHTOP” SYNTHESIS OF CONJUGATED POLYMERS VIA Pd/Cu Co-CATALYSIS 50

4.1 INTRODUCTION 50
4.2 RESULTS AND DISCUSSION 51
4.2.1 Reaction scope towards the heteroaromatic system 53
4.2.2 Attempted synthesis of donor-acceptor conjugated polymers via Pd/Cu co-catalysis 54
4.3 CONCLUSION 55
4.4 EXPERIMENTAL SECTION 55
4.4.1 Materials 55
4.4.2 Instrumentation 55
4.4.3 Synthesis procedures 55

Chapter Page

4.4.4 Spectra....58

V. MECHANOCHEMICAL APPROACH TOWARDS SYNTHESIS OF POLYFLUORENE-CO-BENZOTHIADIAZOLE VIA SUZUKI CROSS COUPLING POLYMERIZATION....60

5.1 INTRODUCTION....60
5.2 RESULTS AND DISCUSSION....62
5.3 CONCLUSION....66
5.4 EXPERIMENTAL....66
5.4.1 Materials....66
5.4.2 Instrumentation....66
5.4.3 Synthesis....67
5.4.4 Spectra....68

VI. CONCLUSIONS AND FUTURE DIRECTIONS....70

6.1 INTRODUCTION....70
6.2 CHAPTER 2: CONCLUSION AND FUTURE DIRECTIONS....70
6.3 CHAPTER 3: CONCLUSION AND FUTURE DIRECTIONS....71
6.4 CHAPTER 4: CONCLUSION AND FUTURE DIRECTIONS....71
6.5 CHAPTER 5: CONCLUSION AND FUTURE DIRECTIONS....72

REFERENCES....73

LIST OF TABLES

Table Page

2.1 Further reaction optimization towards lowering aryl iodide loadings 17

2.2 Reaction optimization of copper-mediated C-H direct arylation polymerization of BDTT.....18

2.3 Control experiments for Cu-mediated C-H direct arylation of BDTT 21

2.4 Control experiments for Cu-mediated C-H direct arylation of BDTT 22

2.5 Attempted reaction conditions for the monoarylation of BDTT core.....25

2.6 Structural properties of polymers.....28

2.7 Optical properties of the synthesized polymers 30

3.1 Optimization of Cu_2O NPs mediated Glaser polymerization of **1a**.....40

3.2 Optimization of Cu_2O NPs mediated Glaser polymerization of **1b**.....41

4.1 Optimization of "Benchtop" synthesis of PF via Pd/Cu co-catalysis 52

4.2 Structural properties of the polymers.....53

5.1 Effect of varying frequency on isolated yield and number average molecular weight.....63

5.2 Effect of K_2CO_3 loading on synthesis of PFBT.....72

5.3 Comparison of solid-state synthesis of PFBT promoted by BM and solution-state synthesis PFBT and effect of Pd catalyst 64

Table Page

5.4 Effect of varying milling time on isolated yield and number average molecular weight.....65

LIST OF FIGURES

Figure Page

1.1 Schematic representation of electronic orbitals of excited-state carbon, Sp^3 hybridization, sp^2 hybridization, and *sp* hybridization.....2

1.2 σ- and π- bond formation within an ethene molecule 3

1.3 The delocalization of π electrons and electron cloud formation.....1

1.4 Bandgap formation.....4

1.5 Examples of conjugated organic small molecules used in various electronic devices.....5

1.6 Examples of conjugated organic polymers used in various electronic devices....6

1.7 Orbital interaction of donor and acceptor moieties leading to a small bandgap in a D-A architecture.....7

1.8 Aromatic and quinoid forms of (a) poly(p-phenylene), (b) poly(p-phenylenevinylene), (c) polythiophene, (d) polyisothianapthene.....8

1.9 Catalytic cycle of transition-metal catalyzed reactions 9

Figure Page

1.10 Representative ball mills 15

2.1 Diversification of BDTT core with different aryl groups.....24

2.2 A) Absorbance spectra of polymers in solution ($CHCl_3$, solid lines) and thin-film B) Fluorescence spectra of polymers in solution.....29

2.3 Polymer solutions that have been irradiated under A) normal light, and B) UV (365 nm).....30

3.1 (a) A representative TEM image of the Cu_2O nanoparticles(34 ± 4nm). (b) Comparison of experimental and computational measurement of UV-Vis extinction spectrum for Cu_2O nanoparticles for the particle size 34 nm. (c) The X-ray diffraction pattern of the Cu_2O NPs 39

3.2 GPC traces of the synthesized polymers (a) obtained for the conditions outlined in Table 3.1. (b) obtained for the conditions outlined in Table 3.2 42

3.3 UV-Vis extinction spectra of the polymerization reaction, measured at different time intervals.....44

3.4 The HR-ESI-MS spectrum measured in negative ion mode for the reaction mixture obtained from polymer **1b**. and proposed possible copper complex....45

3.5 (a) predicted ESI-MS spectrum for the proposed copper complex 3.4 a (b) predicted ESI-MS spectrum for the proposed copper complex 3.4 b…….45

4.1 “Benchtop” synthesis of PF, PC, PSiF, and PIDTT via Pd/Cu co-catalysis.....51

5.1 Representative ball mill 61

LIST OF SCHEMES

Scheme Page

1.1 Representative scheme for C-H direct arylation polymerization.....12

2.1 Copper mediated C-H direct arylation of BDTT with aryl iodides 16

2.2 Synthesis of PBDTT-Th via copper-mediated C-H direct arylation polymerization 18

2.3 Proposed polycondensation of benzo[1,2-b:4,5-b]dithiophene-1,1,5,5-tetraoxide (BDTT) and 4,7-Dibromobenzo[*c*]-1,2,5-thiadiazole (BTz) to PBDTT-BTz.....20

2.4 Control experiments; understand the mechanism of regioselective C-H direct arylation of BDTT.....20

2.5 Presentation of the predicted mechanism of copper-mediated C-H direct arylation of DBT in the presence of CuI, phenanthroline, K_3PO_4, and Ag_2CO_3 23

2.6 Attempted monoarylation of BDTT core using conditions outline in Table 2.5 24

2.7 Attempted one-pot diarylation of the BDTT core 25

2.8 Cu_2O NPs mediated C-H direct arylation of BDTT 26

2.9 Synthesis of BDTT based novel donor-acceptor conjugated polymers.....27

Scheme Page

3.1 Synthesis of poly (2,5-dialkoxy-1,4-phenylenediethynylenes) 40

4.1 “Benchtop” top synthesis of PF using the conditions outlined in Table 4.1.....52

4.2 “Benchtop” synthesis of PC, PSiF, and PIDTT via Pd/Cu co-catalysis 53

4.3 Attempted donor-acceptor polymer synthesis via Pd/Cu co-catalysis under “benchtop” conditions.....54

5.1 Mechanochemical synthesis of PFBT via Suzuki cross-coupling polymerization 62

5.2 Effect of varying milling time on isolated yield and number average molecular weight.....65

6.1 Synthesis of polyfluorene-*co*-thienylbenzothiadiazole in the ball mill 72

CHAPTER I

INTRODUCTION

1.1 ORGANIC SEMICONDUCTORS

Semiconductors are materials that can partially conduct electric current. The conductivity of a semiconductor is somewhere between that of an insulator and a conductor. Semiconductors are widely employed in the manufacture of various kinds of electronic devices such as transistors, diodes, and integrated circuits. Semiconductors are divided into two classes such as organic semiconductors and inorganic semiconductors.[1] Organic semiconductor (OSCs) are carbon-based materials that exhibit optical and electronic properties.[2] OSCs offer the opportunity to fabricate low cost, lightweight, flexible electronics, and optoelectronic devices.[3] Due to these advantages, during the past few decades OSCs have gained substantial attention for their use in organic light-emitting diodes (OLEDs),[4-5] organic photovoltaics (OPVs),[6-7] organic field-effect transistors (OFETs),[8] and electronic sensory devices.[9]

Most of the organic compounds are considered insulators whereas some of the organic compounds exhibit semiconducting properties. The conductivity of organic semiconducting materials relies on a conjugated system throughout the structure. The series of alternating single and double bonds form a conjugated system.[1]

A neutral carbon atom has six electrons. Two electrons are in tightly bound in a *1s* orbital and the other four valence electrons are in *2s* orbital and *2p* orbital as in $2s^2$ and $2p^2$ configuration. As shown in Figure 1.1, the excited state 2s orbital and 2p orbitals undergo three different hybridizations such as sp^3, sp^2, and *sp* to lower their energy. The hybridization of one *2s* orbital and three *2p* orbitals form four sp^3 hybridized orbitals, these orbitals being arrange in tetrahedral geometry (Figure 1.1 a). Similarly, hybridization of one *2s* orbital and two *2p* orbitals form three sp^2 hybridized orbitals and one unhybridized *p* orbital which results in trigonal planer geometry (Figure 1.1 b). As shown in Figure 1.1c, the hybridization of one *2s* orbital and one *2p* orbital form two hybridized *sp* orbitals and two unhybridized *p* orbitals and these arrange in a linear geometry.[10]

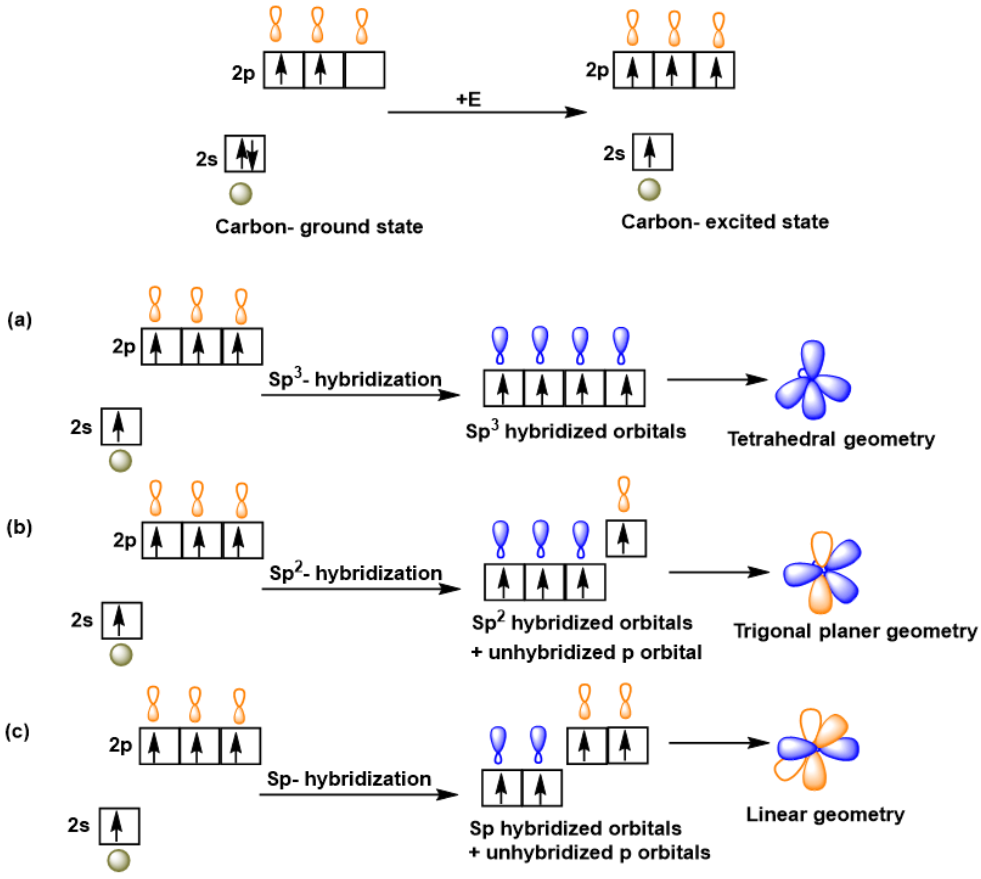

Figure 1.1: Schematic representation of electronic orbitals of excited-state carbon, sp^3 hybridization, sp^2 hybridization, and *sp* hybridization.[10]

As mentioned above, in a conjugated system alternating carbon-containing single bonds and double bonds are present in their molecular structure. The structure is created by σ bonds formed between carbon sp^2orbitals, and the formation of π bond with unhybridized *p* orbitals which are perpendicular to the plane of the molecule (eg: Figure 1.2 shows the σ- and π- bonding within an ethene molecule).[1] The overlapping of perpendicular *p* orbitals creates a delocalized π electron system within the molecule and which can be represented as an electron cloud (Figure 1.3).

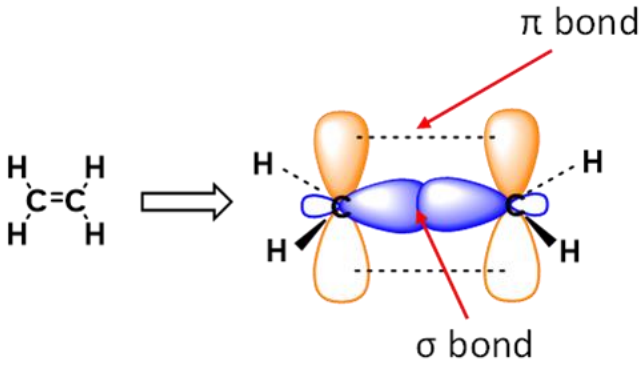

Figure 1.2: σ- and π-bond formation within an ethene molecule.

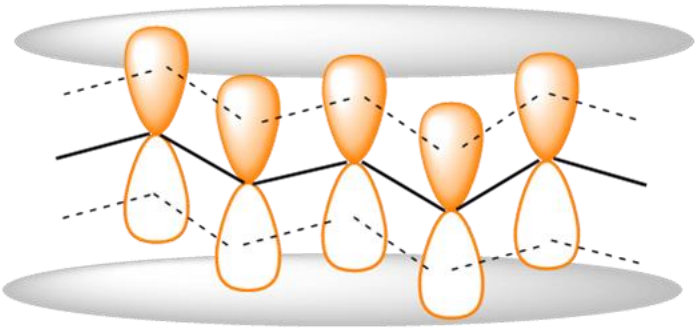

Figure 1.3: The delocalization of π electrons and electron cloud formation.

The properties of OSCs are a result of its band structure. According to the Hückel theory, when atomic orbitals are combined, molecular orbitals are formed. In the ethylene molecule, a combination of two perpendicular *p* orbitals form a π-bonding molecular orbital and π-antibonding molecular orbital (Figure 1.4). For a small-molecule like ethylene, the gap between π-bonding (π) molecular orbital and π-antibonding molecular orbital (π*) is large. As shown in Figure 1.4, when

more atoms are combined more molecular orbitals are formed, and the gap between the highest occupied molecular orbital (HOMO) and lowest unoccupied molecular orbital (LUMO) is reduced. In polyacetylene, a large number of orbitals are formed, and the energy difference between them becomes very small. Thus, forming continuous bands of energy. The energy gap between the HOMO and LUMO determines the bandgap (E_g). OSCs have a bandgap less than 3.2 eV and can absorb in the near UV to IR region.[1, 5, 11]

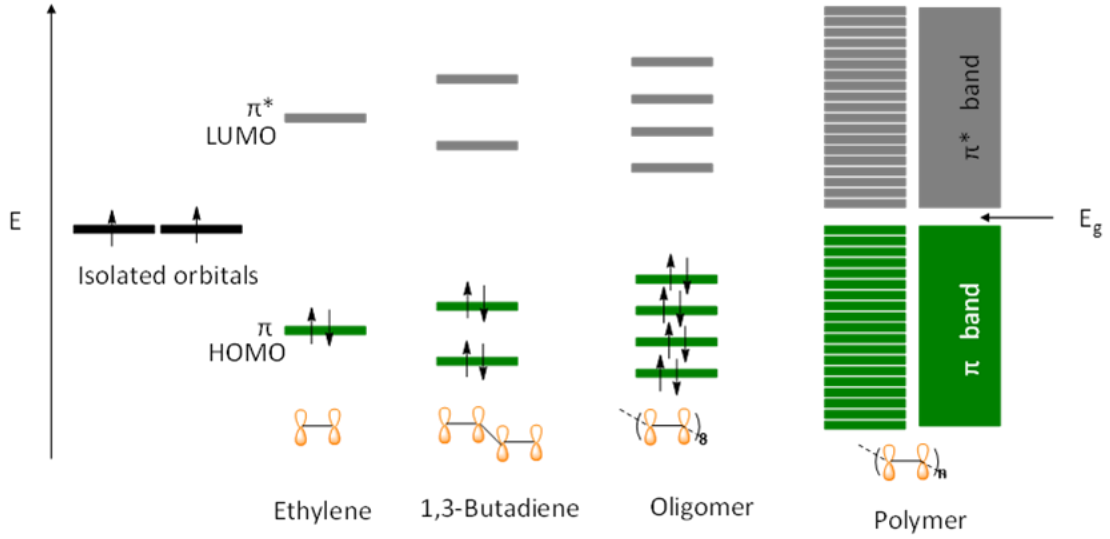

Figure 1.4: Band gap formation[11]

1.2 CLASSIFICATION OF ORGANIC SEMICONDUCTORS

There are two major classes of OSCs: conjugated small molecules and conjugated polymers.

1.2.1 Conjugated small molecules

Conjugated small molecules can be either a single molecule or an oligomer. These molecules have well defined molecular weights, structural homogeneity, and high purity. Some of the conjugated small molecules are highly crystalline and have limited solubility in common organic solvents. Therefore, techniques, such as thermally evaporated vapor deposition, are used to fabricate electronic devices. Figure 1.5 shows some of the important conjugated small molecules used in

electronic devices. As examples: 4,4'-di(9*H*-carbazol-9-yl)-1,1'-biphenyl (CBP) and 1,3-di(9*H*-carbazol-9-yl)benzene (mCP)[12-13] are the host materials used in the emissive layers of the organic light-emitting diodes. Bathcuprinone[14] and pentacene[15] are commonly used compounds in organic field-effect transistors. Sexithienyl and pentacene are the most popular molecules for organic thin-film transistors.[16]

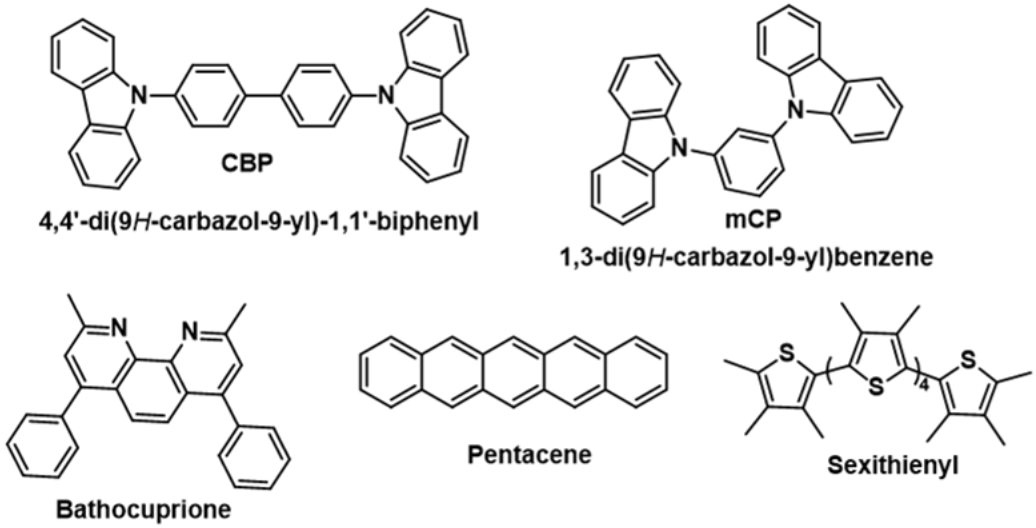

Figure 1.5: Examples of conjugated organic small molecules used in various electronic devices.

1.2.2 Conjugated polymers

Conjugated polymers have an extended π conjugation throughout the entire backbone. This extended conjugation along the backbone enables proper charge transportation and optical absorption by these polymers. Polyacetylenes, polyynes, and polyarylenes are important classes of polymers that have applications in a variety of organic electronics, such as in OLEDs, OPVs, OFETs, and sensory devices.[1, 4, 7, 17-18] Figure 1.6 show some examples of conjugated polymers that have been utilized in electronic devices.

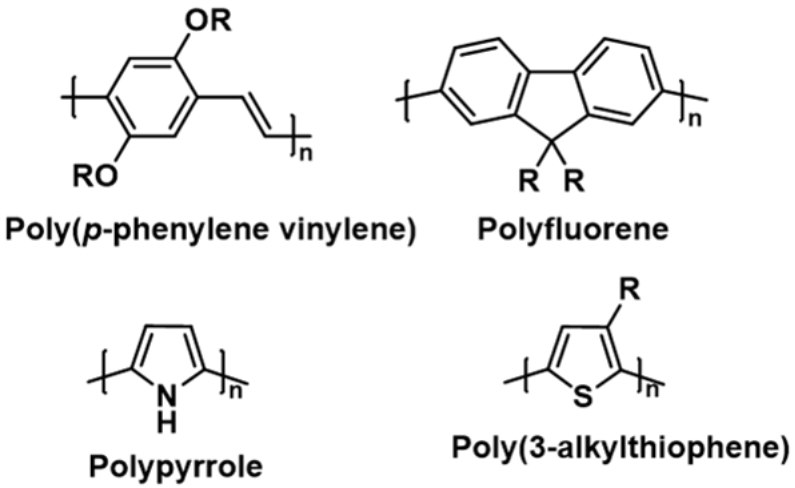

Figure 1.6: Examples of conjugated organic polymers used in various electronic devices.

Electrons and holes are the major charge carriers in semiconductors. Based on these major charge carriers, OSCs can be further classified as p-type and n-type materials. Generally, p-type OSCs holes are the main charge carriers, and such p-types are prepared from electron-donating π conjugated systems. In contrast, with n-type OSCs electrons are the main charge carrier, and these are prepared from electron-accepting π systems.[19-20] These two systems are important for the fabrication of electronic devices.[19]

1.3 STRATEGIES TO DESIGN HIGH-PERFORMANCE OSCs

The working principle of semiconductor devices crucially depends on the energy levels of conductive and valence bands. In OSCs, accurate energy level tuning of frontier orbitals (HOMO and LUMO) is necessary to optimize device efficiency.[21]

Electron-rich building blocks have higher energy HOMO levels, and electron-poor building blocks have low energy LUMO levels. Thus, the most common strategy to create p-type OSCs is to utilize electron-rich moieties whereas n-type OSCs are to utilize electron-poor moieties. Furthermore, by incorporation of electron-donating or electron-withdrawing groups into the conjugation system, the energy level of frontier orbitals can be tuned. The common electron-donating groups that have been

employed are alkoxy groups, amino groups, etc. and common electron-withdrawing groups that have been employed are nitriles, fluorides, and imides, etc. [6]

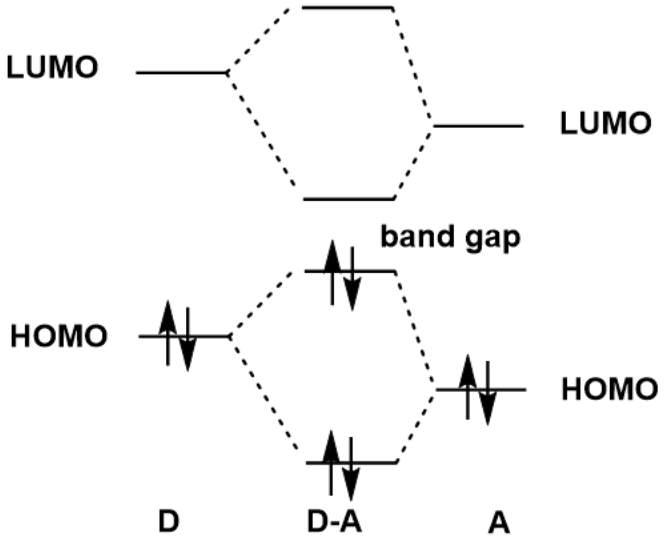

Figure 1.7: Orbital interaction of donor and acceptor moieties leading to a small bandgap in a D-A architecture.

A more powerful strategy in designing high-performance OSCs is to alternate a conjugated electron-rich donor (D) unit and electron-deficient acceptor unit (A) in the same polymer backbone. This D-A architecture has been utilized in both p-type and n-type high performing OSCs. This results due to an alternating D-A structure which has properties of both donor and acceptor moieties. As shown in Figure 1.7, the interaction of HOMO segments of both D and A moieties creates a new high lying HOMO energy level whereas interaction of LUMO segments of D and A creates a new low lying LUMO energy level resulting in a new low bandgap.[11, 22]

Furthermore, the bandgap of the conjugated systems can be engineered by the alternation of the bond length of the molecules.[6] There are two possible resonance structures for a conjugated system (Figure 1.8): aromatic form (aromaticity is maintained with confined π electrons) and quinoid form (delocalization of π electrons along the conjugated system converts double bonds into single bond character and single bonds into double bond character). Compared to an aromatic form, the quinoid

structure has a low bandgap because adopting a quinoid structure needs the destruction of aromaticity and a loss in the stabilization energy.[6] As the quinoid character increases band gap decrease linearly. A reduction in aromaticity in the conjugated system allows a greater tendency to adopt a quinoid form through π electron delocalization. As shown in Figure 1.8 (a), due to the high degree of aromaticity in the benzene ring polyphenylene has a high bandgap (3.3 eV). However, the insertion of double bonds between the benzene rings dilutes the effect of benzene rings and reduce the aromaticity (Figure 1.8 b). Hence the bandgap of polyphenylenevinylene was reduced (2.5 eV). Furthermore, thiophene has lower aromaticity than benzene, and thus the bandgap was low (2 eV). Another strategy is using a fused ring system that favors the quinoid form rather than the aromatic form (Figure 1.8 d).[6]

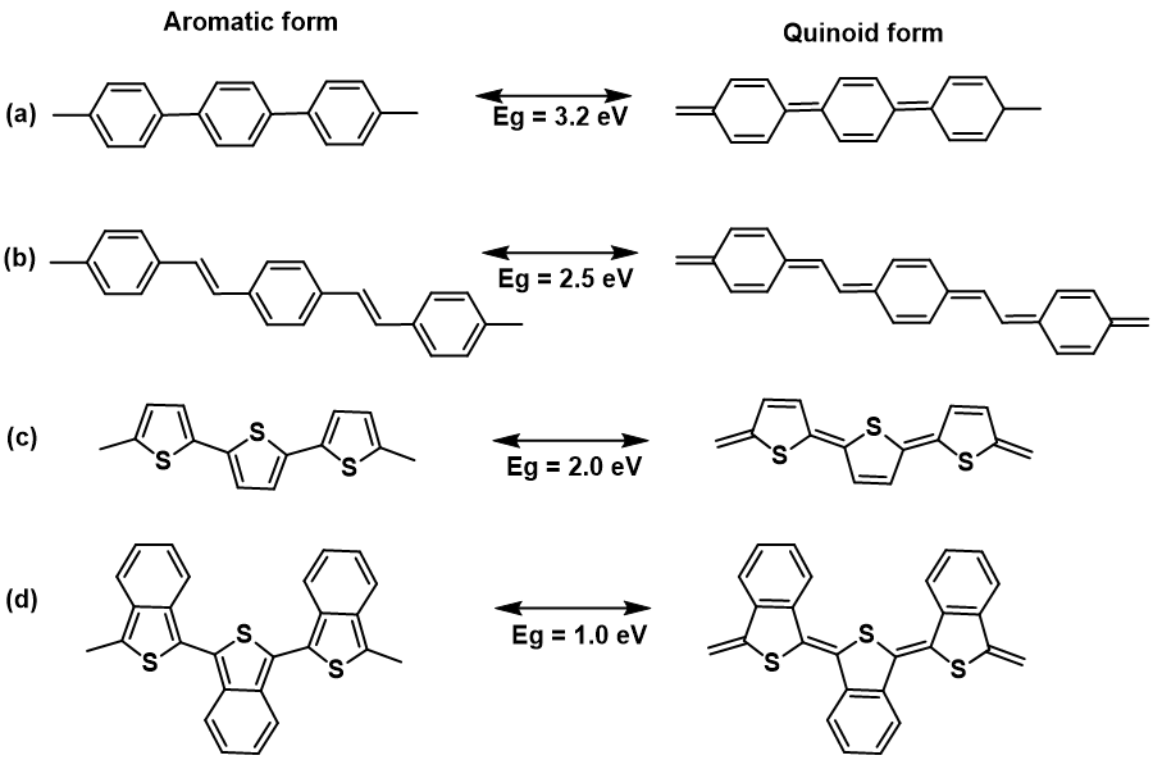

Figure 1.8: Aromatic and quinoid forms of (a) poly(p-phenylene), (b) poly(p-phenylenevinylene), (c) polythiophene, (d) polyisothianapthene.[6]

Another important consideration for OSCs is solubility. To ensure the solution-processability, the targeted polymers should possess good solubilities in organic solvents. Owing to strong π-π stacking interactions, most of the conjugated polyaromatics become highly insoluble. The introduction of alkyl side chains provides steric repulsion and prevent π-π interactions. Branched alkyl chains enhance the solubility more effectively than the linear chain counterparts.[6]

1.4 CONVENTIONAL SYNTHETIC TOOLS FOR CONJUGATED SAMLL MOLECULES AND POLYMERS

The construction of π-conjugated small molecules and polymers relies essentially on C-C bond formation between two unsaturated carbons. In this regard, transition-metal-catalyzed cross-coupling reactions play a vital role.

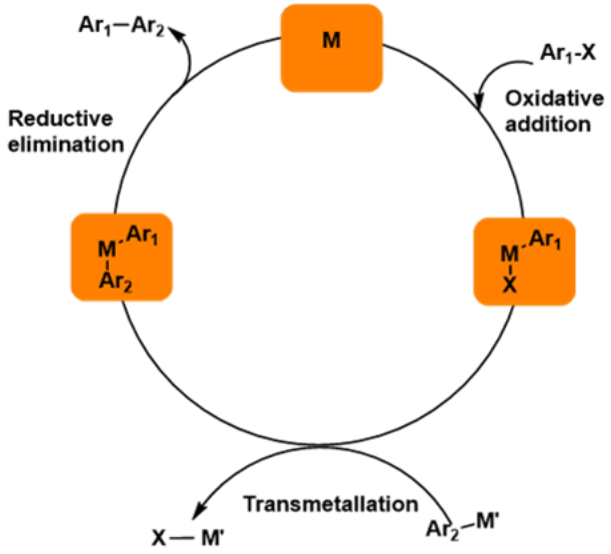

Figure 1.9: Catalytic cycle of transition-metal catalyzed reactions.

As shown in Scheme 1.9, generally these reactions involve transition-metal catalyzed oxidative addition across the carbon-halide (C-X) bond of an electrophile and then transmetalation with the main group nucleophile, followed by a reductive elimination step resulting in C-C bond formation. The most commonly used transition-metal catalysts are palladium or nickel-based complexes. The

organometallic nucleophiles often involve are Grignard reagents (Kumada-Corriu), stannyl (Stille), boron reagents (Suzuki-Miyaura), or copper (Sonogashira).

1.4.1 Stille cross-coupling reaction

The Stille cross-coupling reaction occurs between nucleophilic organostannes and organic halides or pseudo halides. The Stille polymerization has risen to prominence in the field of conjugated polymers owing to its broad scope and reliability.[23] However, when running-large scale reactions, there are some environmental issues. Such include the necessity of lithiating monomers to add trialkylstannyl groups and the toxicity of organostannane compounds. The stoichiometric generation of trialkyltin bromide presents an added cost and environmental externality.[24]

1.4.2 Suzuki-Miyaura reaction

The Suzuki coupling involves the reaction of an organoborane with an aryl halide to result in a coupled product in a palladium-catalyzed reaction. Among a variety of coupling reactions, the Suzuki has attracted great attention, as it is compatible with a wide range of functional groups.[25] The Suzuki reaction is in some aspects environmentally more friendly than a Stille reaction.[23] Also, organoboronates possess high thermal and chemical stability, are relatively inert toward moisture and oxygen.[25]

However, for a large-scale synthesis, the base, water, and phase transfer catalyst required for the typical Suzuki reaction add significant complexity to the reaction set up, and sometimes multiphase reactions are slower and more difficult to mix.[23]

1.4.3 Sonogashira reaction

The reaction of an aryl or vinyl halide with a terminal alkyne to form enynes or aryl alkynes is termed the Sonogashira coupling reaction.[26] This reaction is commonly catalyzed by a palladium catalyst in the presence of a copper co-catalyst and an amine base. The Sonogashira is one of the

most important and widely employed sp^2–sp C-C bond formation reactions in organic synthesis, due to its ability to form strong C(sp^2)-C(sp) bonds under relatively mild conditions, Songashira coupling reactions have been used for the synthesis of conjugated macromolecules.[26]

1.5 GREENER SYNTHETIC TOOLS FOR CONJUGATED MOLECULES

The field of organic electronics is rapidly growing due to substantial interest in semiconducting materials. As mentioned in the previous section, π-conjugated polymers have been synthesized mainly by traditional metal-catalyzed step-growth polymerization and also chain-growth polymerization methodologies. In spite of their great versatility, there are some limitations associated with such processes. These reactions require pre-functionalization of monomers which can lead to many steps, require stoichiometric amounts of reagents and produce stoichiometric amounts of toxic metallic by-products. Therefore, the development of both economically and environmentally feasible methodologies are highly desirable. In this regard, the application of green chemistry principles towards the synthesis of organic semiconducting materials play an important role.

Green chemistry is the design of chemical products and processes that reduce or eliminate the use and generation of hazardous substances and waste.[27] Green chemistry relies on a set of 12 principles that can be used to design or re-design molecules, materials, and chemical transformations to be safer for human health and the environment.[27-28] The 12 principles of green chemistry can be summarized as follows: 1) prevent waste; 2) be atom economical; 3) design less hazardous chemical syntheses; 5) use safer solvents; 6) design for energy efficiency; 7) use renewable feedstocks; 8) reduce derivatization; 9) use selective catalysis; 10) design chemicals that can degrade after use; 11) monitor reactions in real-time for pollution prevention; 12) apply safer chemistry for accident prevention. In the following sections, some of the emerging green strategies (chemical and physical) for organic semiconducting polymer synthesis will be discussed.

1.5.1 Direct hetaroarylation polymerization

Recently, C-H direct arylation polymerization (DArP) has become a viable sustainable alternative to the traditional cross-coupling polymerizations and offers tremendous potential for atom efficient synthetic protocol.[27, 29-30] This coupling requires only one monomer to be pre-functionalized and avoids the productions of toxic metallic byproducts (Scheme 1.1). However, controlling the regioselectivity of this reaction is challenging due to the possible activation of multiple C-H bonds. Hence, achieving regioselectivity would greatly broaden the scope of direct arylation reactions.[27, 31]

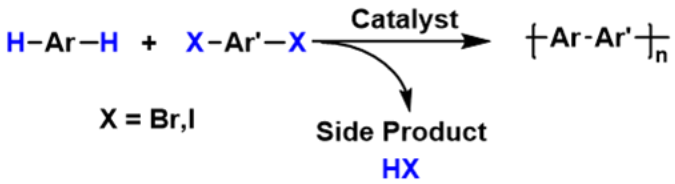

Scheme 1.1: Representative scheme for C-H direct arylation polymerization.

While the scope of DArP is still being explored and expanded, high-performing conjugated polymers have been already synthesized using this methodology.[32-38]

1.5.2 Greener solvents

When considering greener syntheses, particular attention should be focused on solvents, which are a major input in the synthetic process and typically comprise a large fraction of the waste generated. Cross-coupling reactions are often conducted in highly polar solvents, such as in dimethylformamide (DMF), dimethylacetamide (DMA), tetrahydrofuran (THF), pyridine, and chlorinated solvents because these solvents solubilize many monomers and resulting polymers.[27] However, these solvents cause high risk towards human health and environmental problems and rank high in the list of harmful chemicals because of their high volatility and toxicity.[27] Therefore,

the use of alternative green and sustainable solvents (eg: 2-methyltetrahydofuran, cyclopentyl methyl ether, anisole) are encouraged.[27, 31, 39-43]

1.5.3 First-row transition metal catalysts

Most of the catalysts used for synthesizing π-conjugated polymers rely heavily on precious metals, such as palladium, ruthenium, rhodium, and iridium-based catalysts. These metal catalysts are not only toxic but also expensive due to their low natural abundance which leads to the increased cost of semiconducting polymers.[27] Catalysts based on first-row transition metals, such as nickel, copper, cobalt, and iron, have attracted industry and academia due to their high natural abundancies and biocompatibility. Recent studies have demonstrated utility of first-row transition metal-based conjugated polymer synthesis, especially using nickel and copper catalysts.[37, 44-46]

1.5.4 Energy efficient and aerobic reaction conditions

Most of the conjugated polymer syntheses require an input of energy (heat). Scalability is a significant issue when reactions require high energy input for syntheses. Furthermore, high reaction temperatures are often the source of byproducts, which require extra purifications and contribute to the cost of synthesis.[27] Therefore, to maintain energy efficiencies for semiconducting polymer synthesis, mild or room temperature is desired.[47-49] Moreover, if the reactions can tolerate aerobic conditions, that can bypass the need for energy-efficient deoxygenation or can avoid long purges to achieve air-free environments. So far, few conjugated polymerization reactions have been performed under aerobic conditions.[50-51]

1.5.5 Microwave irradiation

Microwave (μW) irradiation is a green source of heating and is based on dielectric heating.[52] The heating rate and the efficiency of heating depending on the dielectric properties and the relaxation times of the reaction mixture.[28, 52] Thus the use of μW absorbing solvents, such as

dimethylformamide (DMF), methanol, acetone, and water, results in very fast heating compared to using toluene, CCl_4, or aliphatic hydrocarbons.[28] The use of μW irradiation as an alternative heat source is becoming more popular in organic syntheses due to major reaction time reductions,[53-54] greater control of the reaction conditions,[55], and in many cases higher yields were obtained.[56] In recent years, the application of μWs in polymerization reactions is increasing.[52, 57-58] Specifically, the synthesis of conjugated polymers by μW-assisted coupling reactions is becoming attractive,[52, 59-60] as it shows a clear economic advantage over conventional heating.[52]

1.5.6 Ball milling

In a general, solution-state organic reaction, solvents compose more than 50% of the mass used, and roughly 90% of the waste produced.[61] This situation increases serious concerns about its impact on the environment and human health. The recent demand for green chemistry has produced a renewed interest in solid-state synthesis.[62] However, thermal activation of concentrated reactive systems might lead to the formation of many byproducts,[63] and thus involve many purification steps. In this regard mechanical activation of solid reactions are attractive.[63] Ball milling is expected to be the technique that leads this charge. Ball milling is a procedure in which solid reactants are placed inside a vessel, in the absence of a solvent, along with ball bearing(s). The vessel is sealed and placed inside the milling apparatus whereby it is agitated. The high-speed agitation provides sufficient kinetic energy to the ball to initiate a reaction. Ball milling reactions are theorized to react in a two-step process. First is the activation step, the point at which the particles are reduced to a size suitable for reaction. Second is the initiation step, the point at which ball collisions cause a chemical reaction to occur. There are various aspects that govern the rate of these two steps. These steps are dependent upon the mechanical operation of the mill, the mechanics of individual collisions, the chemical process, structural changes in the reagents and defect formations. Factors such as milling time, milling speed, ball to powder ratio (i.e. mass of

the solids to the mass of the balls), atmosphere and temperature of the mill all play an integral role in this novel technique.

The most commonly used ball mills are shaker mills and planetary mills. These vary in the motion that causes mixing.[64] In a shaker ball mill, the jars undergo a simple back-and-forth oscillation (Figure 1.10 a). In contrast, in planetary mills, the cylindrical jars spin around their main axis while rotating eccentrically about the sun wheel axis (Figure 1.10 b).[63-64]

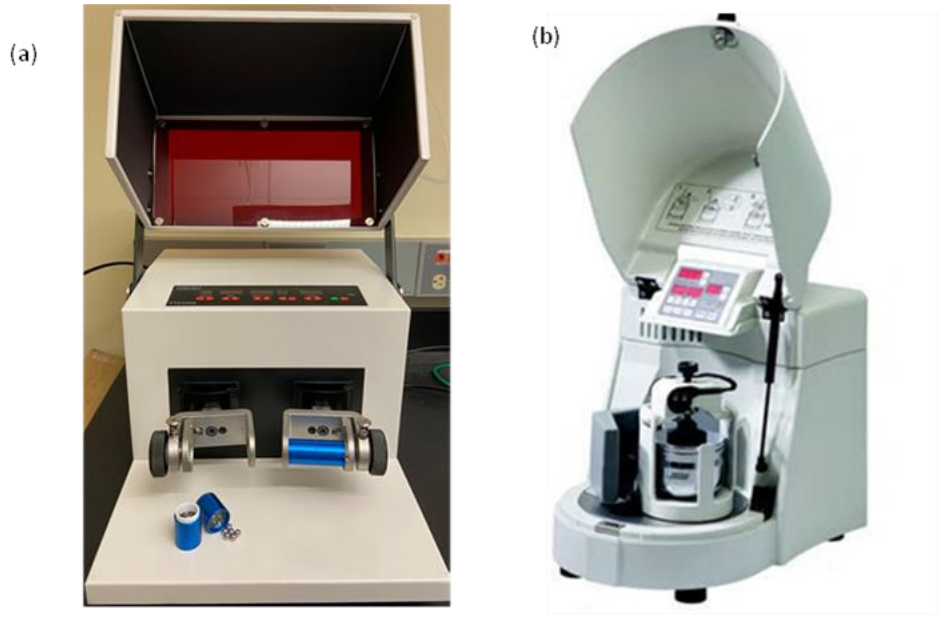

Figure 1.10: Representative ball mills (a) shaker ball mill. (b) planetary ball mill (FRITSCH PULVERISETTE 6).

In the recent past, the mechanochemistry promoted by ball milling has been successfully utilized in many organic reactions, such as in amide couplings,[65] Witting reactions,[66-67] and metal-catalyzed cross-coupling reactions.[68-73] In comparison with small molecule synthesis, the synthetic polymerization promoted by ball milling,[74-79] especially conjugated polymer synthesis has been relatively unexplored.[76-79]

CHAPTER II

PROGRESS TOWARDS REGIOSELECTIVE COPPER MEDIATED DIRECT ARYLATION OF BENZODITHIOPHENE-S,S-TETRAOXIDE: MECHANISTIC INSIGHT AND FURTHER UTILIZATION

2.1 INTRODUCTION

Heterocycle building blocks, such as benzodithiophene, benzobisthiazoles, and benzobisoxazoles are major components for the field of organic electronic devices like organic light-emitting diodes, organic photovoltaics, batteries, and organic field-effect transistors.[80-83] Benzo[1,2-b:4,5-b'] dithiophen-1,1,5,5-tetraoxide (benzodithiophene-S,S-tetraoxide (BDTT)) is an electron-poor heterocycle and excellent building block for the synthesis of electron-accepting materials. However, BDTT has seen limited utility as a building block for the synthesis of organic semiconductors.[84-85] This lack of effort is likely due to the difficulties of precursor syntheses for carbon-carbon cross-coupling reactions that result in low yields.[85]

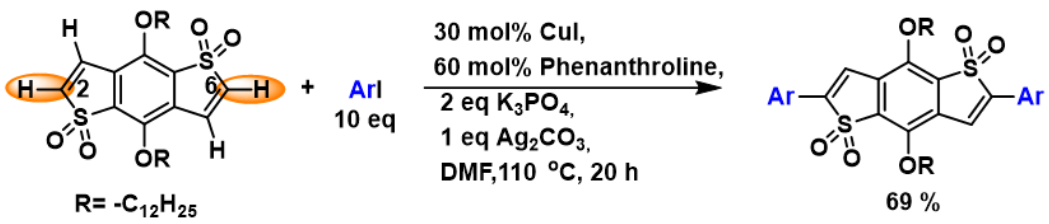

Scheme 2.1: Copper mediated C-H direct arylation of BDTT with aryl iodides.[86]

Our group has developed an efficient methodology for the regioselective synthesis of 2,6 -diarylbenzodithiophene-*S,S*-tetraoxide via copper-mediated C-H direct arylation using a mild base, a ligand, and a silver salt additive (Scheme 2.1).[86] The method demonstrates a broad scope with good to excellent isolated yields. This reaction opens a path for the efficient utilization of electron-poor heterocycles in organic semiconductor design. In this chapter, further utilization and mechanistic insight will be discussed.

2.2 SYNTHESIS OF NOVEL BENZODITHIOPHENE-*S,S*-TETRAOXIDE BASED CONJUGATED POLYMERS VIA C-H DIRECT ARYLATION POLYMERIZATION (DArP)

2.2.1 COPPER MEDIATED C-H DArP

2.2.1.1 RESULTS AND DISCUSSION

We were interested in expanding this methodology towards the synthesis of conjugated polymers. According to the Carothers equation,[87] to achieve high molecular weights, the two monomers should be in equimolar quantities. However, under previously optimized conditions, we couldn't achieve the desired diarylated product at lower aryl iodide loadings. Therefore, further optimization was carried out. As shown in Table 2.1, when the reaction temperature was increased to 140 ℃, the desired diarylated product was obtained with the equimolar ratio of the starting materials (Table 2.1, entry 3).

Table 2.1: Further reaction optimization towards lowering the aryl iodide loadings.

Entry	**2-Iodothiophene (eq)**	**Yield (%)**
1	10	73
2	3	84
3	2	84

As discussed above, BDTT has been less utilized as a building block for developing n-type OSCs despite being an electron-poor heterocycle with promise for the development of n-type materials.[85-86, 88-89] To the best of our knowledge limited studies were carried out for BDTT-based donor-acceptor polymer synthesis.[86, 90-91] Here we have taken the first attempt to synthesize BDTT-based novel donor-acceptor polymer synthesis via C-H DArP.

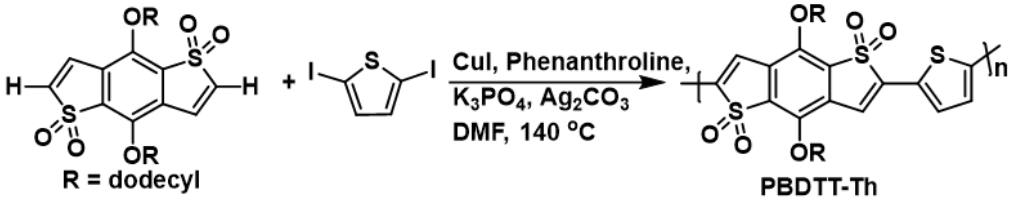

Scheme 2.2: Synthesis of PBDTT-Th via copper-mediated C-H direct arylation polymerization.

Table 2.2: Reaction optimization of copper-mediated C-H direct arylation polymerization of BDTT

Entry	**CuI (mol%)**	**Phen (mol%)**	**Ag_2CO_3 (eq)**	**K_3PO_4 (eq)**	**M_n[a] (Da)**	**Đ[a]**	**Yield**
1	30	60	1	2	3579	1.3	20%
2	30	60	3	2	2303	1.1	60%

[a] Determined by GPC using polystyrene standards.
Đ = Polydispersity index

The synthesis of polymer, PBDTT-Th was carried out in a sealed reaction vial under argon atmosphere. After 48 h, the reaction mixture was precipitated in methanol, and Soxhlet extraction was done with methanol, acetone, and chloroform to yield a bluish-purple solid. Initially, we applied the conditions which have been developed for the small molecules (Table 2.2, entry 1). This resulted in low molecular weight oligomers (3.6 kDa) in low yield (20 %). The next reaction was carried out with three equivalents of Ag_2CO_3 (Table 2.2, entry 2). Surprisingly, the yield increased significantly but M_n decreased to 2.3 kDa. During this time, we changed focus to a detailed mechanistic investigation of this methodology since it might help us understand the

reaction and better optimize the reaction conditions for polymerization. This project was postponed for future studies.

2.2.2 ATTEMPTED SYNTHESIS OF BENZODITHIOPHENE-*S*,*S*-TETRAOXIDE (BDTT) BASED NOVEL CONJUGATED POLYMERS VIA Pd CATALYZED DArP:

2.2.2.1 RESULTS AND DISCUSSION

While we were exploring the synthesis of BDTT-based conjugated polymers using our methodology, we also attempted to synthesize BDTT based n-type semiconductor polymers via a Pd catalyzed C-H DArP strategy. Our study was initiated by exploring DArP for benzo[1,2-b:4,5-*b*]dithiophene-1,1,5,5-tetraoxide (BDTT) with 4,7-dibromobenzo[*c*]-1,2,5-thiadiazole (BTz) for the formation of poly-BDTT-BTz (Scheme 2.3). These preliminary experiments were initiated based on previously reported ligand-enabled Pd catalyzed C-H direct arylation polymerization.[92-95] As shown in Scheme 2.3, we examined the polymerization in the presence of palladium acetate (30 mol%), phosphine ligand (60 mol%), potassium carbonate (2 eq), and pivalic acid (2 eq). The reaction was performed in a sealed reaction vessel in DMF at 80 °C for 48 h. Readily available bulky tri-*tert*-butyl phosphine was selected for the first run. Based on previous literature, the next two experiments were carried out with aryl phosphenes, tri(o-tolyl) phosphine, and tris (4-methoxy phenylphosphine).[93-95] After 48 hours, the reaction mixture was precipitated in methanol. These experiments resulted in the black insoluble precipitate. Due to insolubility, further analysis could not be done. We assumed that the insolubility might be due to high molecular weight and π-π stacking of the polymer chains. Then we elected to perform a control experiment to synthesize a BDTT based small molecule using 2-bromothiophene (Thiophene-BDTT-Thiophene) by applying the same reaction conditions. Unfortunately, we obtained a black color gummy product, and ^{1}H NMR spectrum was inconclusive.

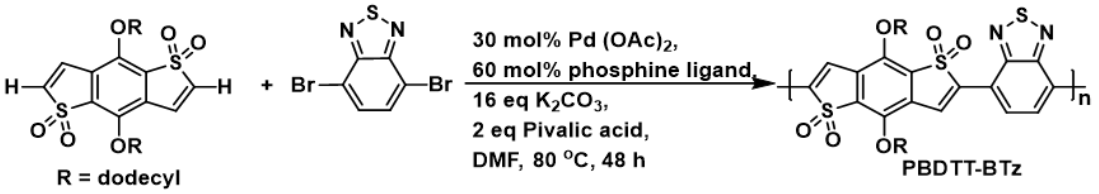

Scheme 2.3: Proposed polycondensation of benzo[1,2-*b*:4,5-*b*]dithiophene-1,1,5,5-tetraoxide (BDTT) and 4,7-Dibromobenzo[*c*]-1,2,5-thiadiazole (BTz) to PBDTT-BTz.

While exploring these experiments, Punzi et al. reported a solvent-free Pd-catalyzed C-H arylation of BDTT for small molecules.[96] They have observed moderate yields with the methyl or dimethyl substituted aryl coupling partners and low yields with either electron-rich or electron-poor aryl coupling partners. They also mentioned that partial decomposition in the BDTT was observed in the reaction media.[96] Therefore, further optimizations were not done.

2.3 MECHANISTIC INSIGHT OF REGIOSELECTIVE COPPER MEDIATED DIRECT ARYLATION OF BENZODITHIOPHENE-S-S-TETRAOXIDE.

2.3.1 RESULTS AND DISCUSSION

The lack of an in-depth understanding of mechanistic details, role of catalyst, ligand, base, and additive makes a broader application of the reaction limited. Therefore, to gain an insight into the mechanism, control experiments and computational studies were carried out (Scheme 2.4).

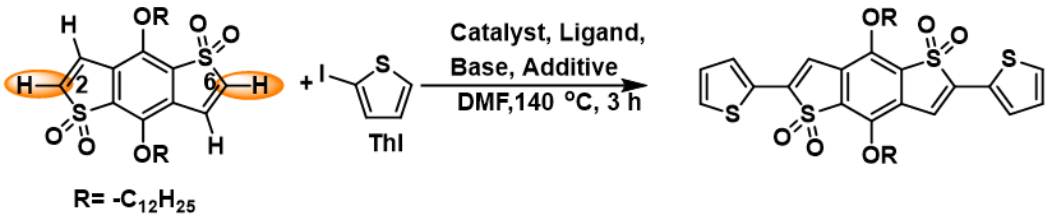

Scheme 2.4: Control experiments to understand the mechanism of regioselective C-H direct arylation of BDTT.

Table 2.3: Control experiments for Cu-mediated C-H direct arylation of BDTT.

Entry	Catalyst	Ligand	Base	Additive	Result
1	-	-	K_3PO_4	Ag_2CO_3	a
2	CuI	-	K_3PO_4	Ag_2CO_3	trace SM, a
3	-	Phen	K_3PO_4	Ag_2CO_3	a
4	CuI	Phen	-	-	SM
5	CuI	Phen	K_3PO_4	-	b
6	CuI	Phen	-	Ag_2CO_3	b

a = Complicated mixture which could not be analyzed

SM = starting material

b = desired product

Control experiments were carried out in the presence and absence of each catalyst, ligand, base, and additive to probe the reaction mechanism as it relates to the role of catalyst, ligand, base, additive, nucleophile, and electrophile. First, we focused on the importance of CuI and phenanthroline (Table 2.3, entries 1,2,3). The first run was carried out in the absence of both CuI and phenanthroline. In this experiment, neither the desired product nor the starting material was obtained. TLC analysis showed a dark brown spot on the baseline and ^{1}H NMR was inconclusive. The second experiment was carried out in the presence of CuI and the absence of phenanthroline. The ^{1}H NMR showed a trace amount of starting material (BDTT) and other unidentified products. The third run was carried out in the absence of CuI. Here also, the result obtained was inconclusive. Next, we altered the conditions with K_3PO_4 and Ag_2CO_3 (Table 2.3, entries 4, 5, and 6). In the absence of both K_3PO_4 and Ag_2CO_3, starting materials were obtained (BDTT and ThI). Surprisingly, the desired diarylated product formed when the reaction was carried out in the presence of K_3PO_4 and in the absence of Ag_2CO_3 with a low yield of 29% (Table 2.3, entry 5). Similarly, when the reaction was carried out in the presence of Ag_2CO_3 and the absence of K_3PO_4, the diarylated product formed with a moderate yield of 36% (Table 2.3, entry 6).

Table 2.4: Control experiments for Cu mediated C-H direct arylation of BDTT.

Entry	Metal source	Phen (mol %)	K_3PO_4 (eq)	Additive (1 eq)	Yield
1	CuBr (30)	60	2	Ag_2CO_3	80%
2	$CuBr_2$ (30)	60	2	Ag_2CO_3	11%
3	$ZnCl_2$ (30)	60	2	Ag_2CO_3	SM, a
4	CuI (30)	60	2	$AgOSO_2CF_3$	63%
5	CuI (30)	60	2	$AgSbF_6$	50%

a = Complicated mixture which could not be analyzed,

SM = starting material

The next set of experiments were carried out with different metal sources and silver salts (Table 2.4). We were interested to see whether iodide is crucial for the reaction. Therefore, reaction one was carried out with copper (I) bromide (Table 2.4, entry 1). The desired product was obtained with a high isolated yield (80%). Next, we focused on the oxidation state of the copper. The second experiment was done in the presence of copper(II) bromide. The desired product was obtained with a low isolated yield (11%). With these results in hand, we wanted to focus on whether copper was crucial for the reaction. The third run was carried out in the presence of Zn(II) chloride (Table 2.4, entry 3). Unreacted BDTT was obtained and a product that could not be identified. The next set of experiments were carried out with different silver salts (Table 2.4, entries 4 and 5). In these experiments, the desired product was obtained with moderate isolated yields.

To understand the reaction mechanism in detail, computational experiments were carried out in collaboration with Prof. Djamaladdin Musaev at Emory University. We studied the aryl coupling between 4,7-dimethoxybenzo[b]thiophen 1,1-dioxide (DBT) (model of BDTT) and phenyl iodide in the presence of CuI, phenanthroline, K_3PO_4, and Ag_2CO_3. Scheme 2.5 represents the schematic diagram of the predicted mechanism. In the first step, iodide-to-base ligand exchange occurred in the prereaction complex (Phen)CuI). The process has a very small energy barrier and is highly

exergonic. Then, the resulting intermediate coordinates substrate (DBT) and deprotonates the reactive C-H bond via the acid-base mechanism. It was shown that the sulfonyl oxygens in the DBT interact with the cation of the base to bring the substrate and base close to each other. The Cu-center of the catalyst plays an anchoring role. The deprotonation of the substrate by Ag_2CO_3 presents a larger free energy barrier than K_3PO_4. Hence, K_3PO_4 is a more effective base for deprotonation of DBT. Then, aryl iodide (Ar-I) addition and carbon-carbon coupling take place. As shown in Scheme 2.5, in the presence of K_3PO_4, the reaction occurs via a copper-mediated nucleophilic substitution pathway. This requires a significant free energy barrier. In contrast, in the presence of Ag_2CO_3, Ar-I activation and C-C coupling proceed via oxidative addition of Ar-I on Ag^+, followed by reductive elimination. This process requires a free energy barrier smaller than copper-mediated nucleophilic substitution.[97]

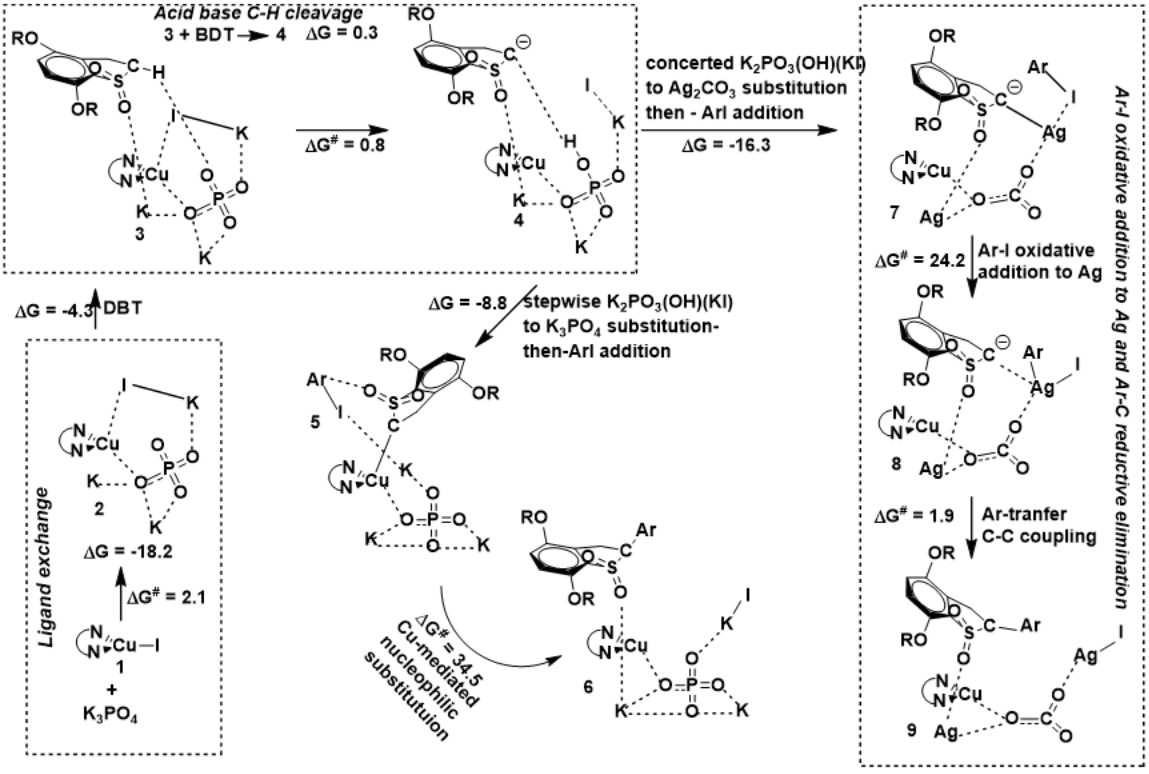

Scheme 2.5: Presentation of the predicted mechanism of copper-mediated C-H direct arylation of DBT in the presence of CuI, phenanthroline, K_3PO_4, and Ag_2CO_3.[97]

The above experimental and computational studies show that Cu(I)-phen complex is important for the reaction initiation. The K_3PO_4 and Ag_2CO_3 play key roles in the reaction mechanism. These key findings were published.[97]

2.4 ATTEMPTED DIVERSIFICATION STUDIES OF COPPER MEDIATED C-H DIRECT ARYLATION OF BDTT

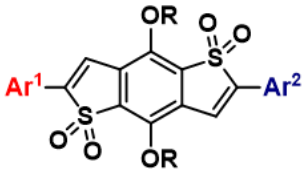

Figure 2.1: Diversification of BDTT core with different aryl groups.

2.4.1 RESULTS AND DISCUSSION

The electronics of the BDTT core is very important for its semiconducting properties and potential application. The optical and electronic properties of this core can be tuned by diversification of the aryl groups attached to the BDTT core. The aim was to develop a library of functionalized BDTTs with different aryl groups at the 2- and 6-positions (Figure 2.1). Here, we took 2-iodothiophene (ThI) and phenyl iodide (PhI) as our model coupling partners. The first approach was to carry out monoarylation and then couple the second aryl group (Scheme 2.6). Monoarylation reactions were performed by varying different parameters as shown in Table 2.5. However, diarylated products were obtained under every reaction condition employed.

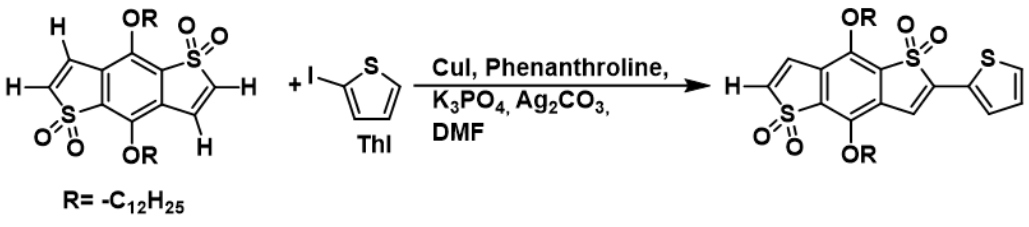

Scheme 2.6: Attempted monoarylation of BDTT core using conditions outline in Table 2.5.

Table 2.5: Attempted reaction conditions for the monoarylation of BDTT core.

Entry	ThI (eq)	CuI (mol%)	Phen (eq)	K_3PO_4 (eq)	Ag_2CO_3 (eq)	Temperature (°C)	Result
1	1	30	60	2	1	140	Diarylation
2	1	30	60	1	0.5	140	Diarylaion, a
3	1	30	60	1	0.5	80	Diarylation SM, a

a = Complicated mixture which could not be analysed
SM = starting materials

Next, we experimented by adding both aryl groups (PhI and ThI) simultaneously. Surprisingly, TLC and ^{1}H NMR analyses indicated that the product obtained was a combination of Ph-BDTT-Ph and Th-BDTT-Th (Scheme 2.7).

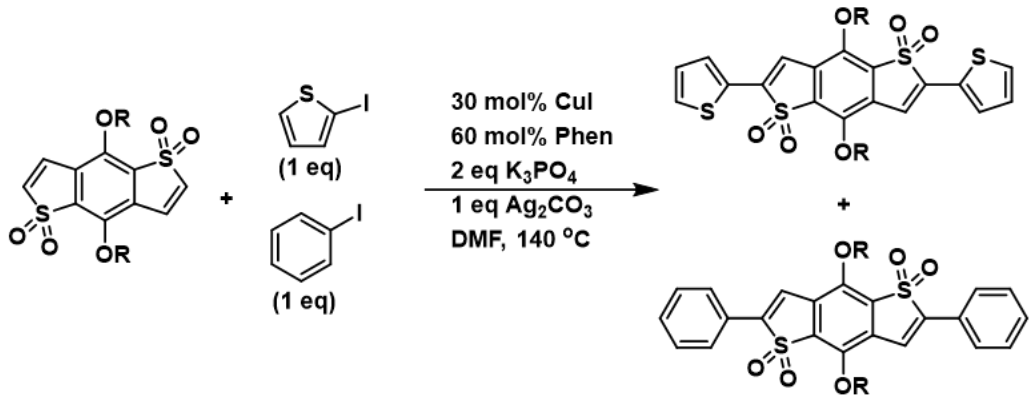

Scheme 2.7: Attempted one-pot diarylation of the BDTT core.

2.5 COPPER (I) OXIDE NANOPARTICLE MEDIATED C-H DIRECT ARYLATION OF BDTT

2.5.1 RESULTS AND DISCUSSION

In recent years copper and copper-based nanocatalysts have been employed in various cross-coupling reactions due to their stability and availability.[98-100] To the best of our knowledge, limited studies were carried out for copper oxide nanoparticles mediated C-H bond arylation.[101-103] In this study, copper (I) oxide nanoparticles (Cu_2O NPs) were used for the regioselective C-H bond functionalization of BDTT. The Cu_2O NPs were obtained from the Andiappan group (School of Chemical Engineering Oklahoma State University). Optimization of the reaction conditions for the Cu_2O NP-mediated arylation of BDTT was performed using 2-iodothiophene as an aryl coupling partner (Scheme 2.8).

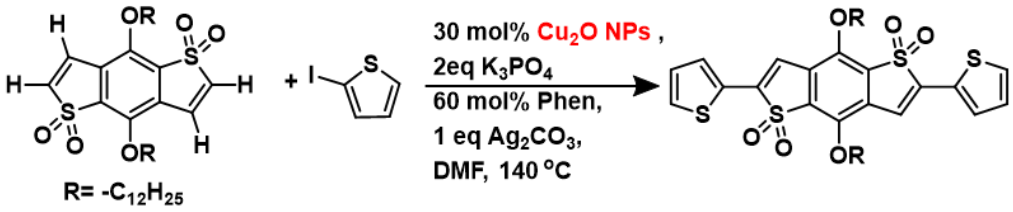

Scheme 2.8: Cu_2O NPs mediated C-H direct arylation of BDTT.

As shown in Scheme 2.8, for the first experiment we applied the same conditions which were developed earlier for the CuI mediated C-H direct arylation, and the reaction proceeded for 3 h. We determined the trace amounts of the desired product and other impurities. In the next experiment, the reaction was stopped after 30 min. TLC and ^{1}H NMR analysis indicated the formation of the desired product and residual starting materials. Thus, the reaction time was increased to 1.5 h. TLC and ^{1}H NMR analyses showed the formation of the desired product with the isolated yield of 60%. According to the results we obtained, it was concluded that, in the presence of Cu_2O NPs, the reaction was faster, but when the reaction proceeded further, product

might undergo decomposition. With these conditions in hand, the substrate scope and reaction pathway will be studied.

2.6 SYNTHESIS AND OPTICAL PROPERTIES OF BDTT BASED DONOR-ACCEPTOR CONJUGATED POLYMERS.

2.6.1 RESULTS AND DISCUSSION

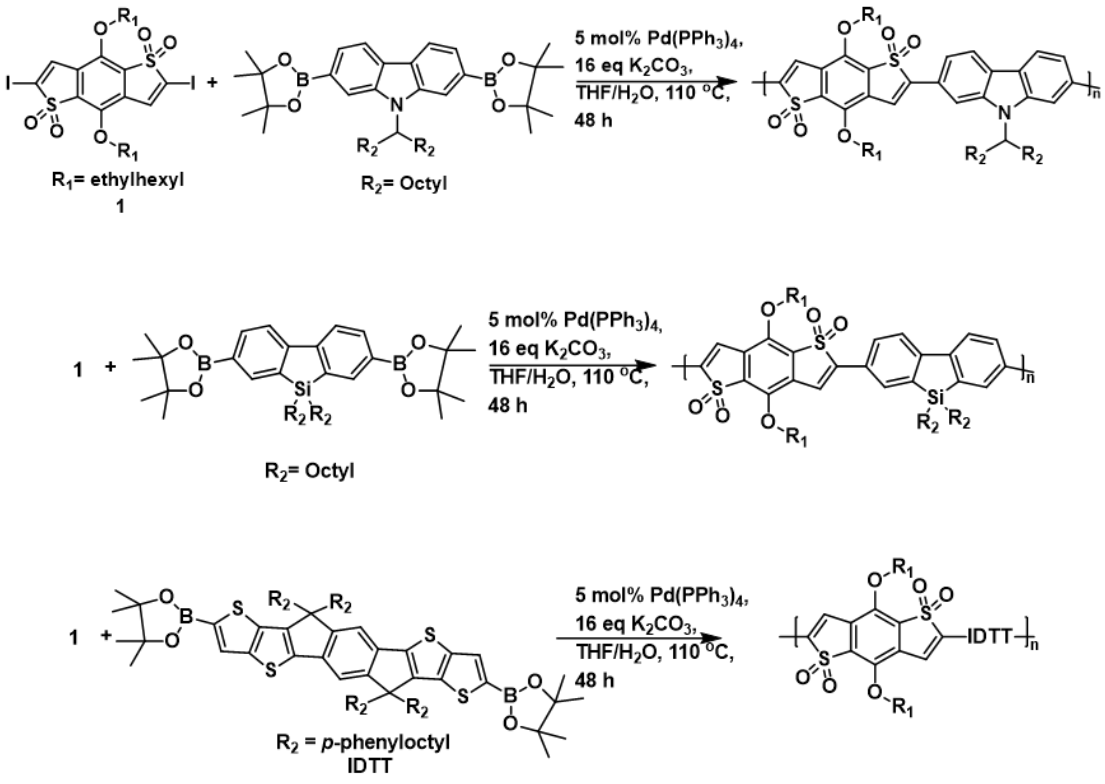

Scheme 2.9: Synthesis of BDTT based novel donor-acceptor conjugated polymers.

Recently, our group has reported the functionalization of BDTT via the C-H iodination strategy.[91] This opens an entry to direct incorporation of this electron-deficient BDTT moiety in the conjugated system in making high performing OSC materials. Here we show the utilization of this iodinated BDTT moiety in the donor-acceptor polymer system. Carbazole, silafluorene, and IDTT (6,6,12,12-tetrakis(4-hexylphenyl)-6,12-dihydro-dithieno[2,3-*d*:2',3'-*d*']-*s*-indaceno[1,2-*b*:5,6-*b*']

dithiophene) are well-known materials for high performing OSCs.[104-106] We attempted to synthesize PBDTT-C, PBDTT-SiF, and PBDTT-IDTT by reacting compound **1** with (9-heptadecanyl)-9*H*-carbazole-2,7-diboronic acid bis(pinacol) ester, 9,9-dioctyl-9*H*-9-silafluorene-2,7-bis(boronic acid pinacol ester), and 6,12-dihydro-6,6,12,12-tetrakis(4-octylphenyl)-2,8-bis(4,4,5,5-tetramethyl-1,3,2-dioxaborolan-2-yl)dithieno[2,3-*d*:2′,3′-*d*′]-*s*-indaceno[1,2-*b*:5,6-*b*′]dithiophene, respectively, under Suzuki copolymerization conditions (Scheme 2.9). The results are summarized in Table 2.6. After Soxhlet purification, PBDTT-C was obtained in high yield and with a high number average molecular weight (90%, 31 kDa). Although PBDTT-SiF was obtained in good yield (60%) and with a very high number average molecular weight (123 kDa), a little gelation was observed in the polymer product and the proton NMR was inconclusive due to gelation. The gel formation may be due to inappropriate reaction conditions for the synthesis of PBDTT-SiF. The PBDTT-IDTT was obtained in low yield and low number average molecular weight (16%, 3.0 kDa) (because of the low molecular weight hereafter this will be referred to as BDTT-IDTT oligomer). This low yield and low molecular weight might be due to the steric hindrance of the IDTT molecule, and the strong π-π interaction may cause low solubility in THF/water solvent system. We will explore different parameters to synthesize PBDTT-SiF and PBDTT-IDTT with better structural properties.

Table 2.6: Structural properties of polymers.

Polymer	**M_n [a] (kDa)**	**M_w [a] (kDa)**	**Đ [a]**	**% Yield**
PBDTT-C	31	71.3	2.3	90
PBDTT-SiF	123	332.1	2.7	60
BDTT-IDTT oligomer	3.0	5.0	1.7	16

[a] Determined by GPC using polystyrene standards.
Đ = polydispersity index

The optical properties of the products were determined using UV-Vis absorption spectroscopy (in $CHCl_3$ and thin films) and with fluorescence spectroscopy (in $CHCl_3$). The absorption and fluorescence spectra of the products are shown in Figure 2.2, and the results are summarized in Table 2.7.

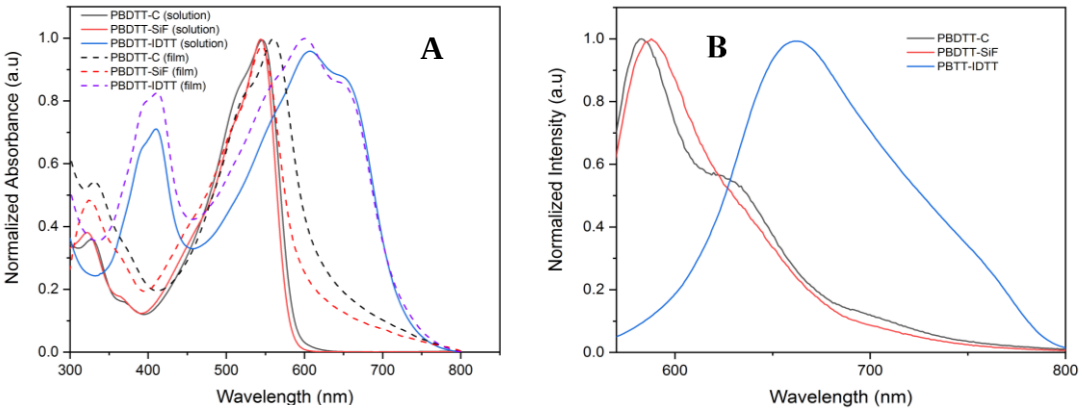

Figure 2.2: A) Absorbance spectra of polymers in solution ($CHCl_3$, solid lines) and thin film (cast from $CHCl_3$, dashed lines). B) Fluorescence spectra of polymers in solution ($CHCl_3$). The excitation wavelengths were 548 nm, 546 nm, and 610 nm for PBDTT-C, PBDTT-SiF, and BDTT-IDTT oligomer respectively.

As shown in Figure 2.2 A, the polymers exhibited two characteristic absorption bands. Most of the donor-acceptor architectures show these two types of prominent absorption peaks.[107-108] The peaks near 325-400 nm can be assigned to π-π* transition whereas the peaks near 550-650 nm are due to intramolecular charge transfer (ICT) between the donor and acceptor moieties.[108] Compared to the absorption maximum of PBDTT-C and PBDTT-SiF (λ_{max} = 548 nm and 546 nm respectively), the absorption maximum of BDTT-IDTT oligomer (λ_{max} = 602 nm) is more broadened and redshifted. This can be due to large ICT effects in the BDTT-IDTT based polymers than that of BDTT-C and BDTT-SiF based polymers. The absorption spectra of the thin films are generally similar in shape to those of dilute solution spectra. A hypsochromically shifted spectrum was observed in the BDTT-IDTT oligomer. This might be due to pre-aggregation in solution because of the strong intermolecular interaction of the large fused and rigid conjugated system.[109] The fluorescence spectra of the compounds were obtained in dilute $CHCl_3$ solution. The PBDTT-C showed maximum emission at 583 nm, the PBDTT-SiF showed emission at 587nm, and BDTT-IDTT

oligomer showed the maximum emission at 661 nm, where the excitation wavelength was 548 nm, 546 nm, and 610 nm, respectively.

Table 2.7: Optical properties of the synthesized polymers

Polymer	Media	λ_{abs}[a] (nm)	λ_{ems}[a] (nm)	E_g^{opt} (eV)[b]
PBDTT-C	$CHCl_3$	548	583	1.96
	Film	560		
PBDTT-SiF	$CHCl_3$	546	587	2.03
	Film	546		
BDTT-IDTT oligomer	CHCl3	610	661	1.65
	Film	602		

[a] Measured in dilute chloroform. [b] Measured from the tangent drawn at the onset of absorption.

The optical bandgaps were deduced from the absorption spectra of the thin films. The wavelengths corresponding to the absorption were measured at the intersection of the leading-edge tangent with the x-axis. The onset absorptions of PBDTT-C, PBDTT-SiF, and BDTT-IDTT oligomer are 630 nm, 610 nm, and 747 nm respectively; thus, the optical band gaps (E_g^{opt}) are 1.96 eV, 2.03 eV, and 1.65 eV, respectively (Table 2.7). The polymers that have been irradiated under normal light and UV are shown in Figure 2.3.

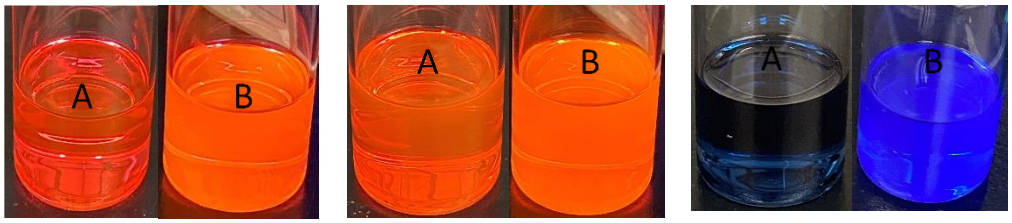

PBDTT-C PBDTT-SiF BDTT-IDTT oligomer

Figure 2.3: Polymer solutions that have been irradiated under A) normal light, and B) UV (365 nm).

2.7 CONCLUSION

Experimental and detailed theoretical studies revealed the base (K_3PO_4) and additive (Ag_2CO_3) play crucial roles in copper-mediated regioselective C-H direct arylation of BDTT. Currently, copper-mediated C-H DArP of BDTT resulted in low molecular weight oligomers. Further optimization will be carried out to improve the structural properties. Under the attempted conditions, diversification of BDTT was not successful; the homo diarylated product was obtained. Utilizing 2,6-diiodo BDTT, BDTT based novel donor-acceptor conjugated polymers were synthesized via Suzuki cross-coupling polymerization. The optical properties of the materials indicate donor-acceptor architecture and low optical band gaps.

2.8 EXPERIMENTAL SECTION

2.8.1 Materials

Benzodithiophene-S,S-tetraoxide (BDTT) was synthesized according to the previously reported procedure.[84,86,110] Aryl iodides, 2,5-diiodothiophene, 4,7-dibromobenzo[c]-1,2,5-thiadiazole were purchased from Oakwood chemicals. Copper halides, 1,10-phenanthroline, K_3PO_4, and silver salts were purchased from Sigma-Aldrich, Alfa Aesar, and Oakwood chemicals and were used as received. Compound **1** (Scheme 2.9) was synthesized according to the literature procedure.[91] (9-heptadecanyl)-9*H*-carbazole-2,7-diboronic acid bis(pinacol) ester, 9,9-dioctyl-9*H*-9-silafluorene-2,7-bis(boronic acid pinacol ester), and 6,12-dihydro-6,6,12,12-tetrakis(4-octylphenyl)-2,8-bis(4,4,5,5-tetramethyl-1,3,2-dioxaborolan-2-yl)dithieno[2,3-*d*:2′,3′-*d*′]-*s*-indaceno[1,2-*b*:5,6-*b*′]dithiophene were purchased from Sigma-Aldrich and used as received. Anhydrous DMF and anhydrous THF were obtained from a solvent purification system under argon.

2.8.2 Instrumentation

^{1}H NMR spectra were measured on a Bruker Avance 400 MHz instrument. Number average molecular weight (M_n) and polydispersity (Đ) were determined by gel permeation chromatography (GPC) using a Waters pump with a Waters 2410 refractive index detector. THF was used as an eluent at 35 °C with a flow rate of 1.0 mL min^{-1}. The instrument was calibrated with polystyrene standards and data were analyzed using Breeze software. UV-Vis and fluorescence spectra were recorded on a Cary 5000 UV–Vis NIR spectrophotometer and a Cary Eclipse fluorescence spectrophotometer, respectively. Absorption measurements were obtained using compounds in $CHCl_3$ solutions and thin films. Fluorescence measurements were obtained in $CHCl_3$.

2.8.3 Synthesis

C-H direct arylation, the general procedure for small molecule synthesis:

In a glovebox, was placed 4,8-didodecyloxybenzo[1,2-b;3,4-b']dithiophene-S,S-dioxide (50 mg, 0.080 mmol) in a 10 mL reaction tube, followed by the aryl iodide (0.160 mmol), CuI (4.6 mg, 0.024 mmol), 1,10-phenanthroline (8.7 mg, 0.048 mmol), K_3PO_4 (34.9 mg, 0.160 mmol), Ag_2CO_3 (22.1 mg, 0.080 mmol), and dry DMF (2 mL). The reaction color was dark brown to green. The reaction vials were sealed, taken out of the glovebox, and stirred at 140 ℃ for 3.5 h. The color of the reaction turned a darker brown. The reaction mixture was allowed to cool to room temperature, poured into water, and extracted with ethyl acetate. The resulting solution was washed with deionized water (5 x 15 mL), brine (2 x 15 mL), and dried ($MgSO_4$). The solvents were removed with rotatory evaporation. Further purification was obtained by dissolving the crude product in dichloromethane:methanol (1:1) and followed by rotary evaporation to precipitate the product. The suspension was then filtered and washed with cold methanol to obtain the pure product.

Th-BDTT-Th : red color solid, yield 86%, ^{1}H NMR (400 MHz, $CDCl_3$): δ 7.71 (dd, 2H), 7.51 (dd, 2H), 7.22–7.15 (m, 4H), 4.48 (t, 4H), 1.93 (p, 4H), 1.58–1.52 (m, 4H), 1.43–1.24 (m, 32H), 0.88 (t, 6H).

Copper mediated C-H direct arylation polymerization.

Synthesis of PBDTT-Th: In the glovebox, was placed 4,8-didodecyloxybenzo[1,2-b;3,4-b']dithiophene-S,S-dioxide (50 mg, 0.080 mmol) in a 10 mL reaction tube, followed by the 2,5-diiodothiophene (27 mg, 0.0.080 mmol), CuI (4.6 mg, 0.024 mmol), 1,10-phenanthroline (8.7 mg, 0.048 mmol), K_3PO_4 (34.9 mg, 0.160 mmol), Ag_2CO_3 (22.1 mg, 0.080 mmol), and dry DMF (4 mL). The reaction vial was sealed, taken out of the glovebox, and stirred at 140 ℃ for 48 h. The color of the reaction turned a bluish purple. The reaction mixture was precipitated in methanol and then Soxhlet extraction was carried out with methanol, hexane, and chloroform. Finally, the chloroform extraction was evaporated to dryness to yield a purple product. Yield 20%. ^{1}H NMR (400 MHz, $CDCl_3$): δ 7.71 (b, 2H), 7.32 (b, 2H), 4.52 (b, 4H), 1.93 (b, 4H), 1.82-0.87 (b, 42H)

Palladium-catalyzed C-H direct arylation polymerization:

Attempted synthesis of PBDTT-BTz: In a glovebox, was placed 4,8-didodecyloxybenzo[1,2-b;3,4-b']dithiophene S,S-dioxide (25 mg, 0.040 mmol) in a 10 mL reaction tube, followed by 4,7-dibromobenzo[c]-1,2,5-thiadiazole (11.8 mg, 0.04 mmol), $Pd(OAc)_2$ (2.69 mg, 0.012 mmol), a phosphine ligand (0.024 mmol), K_2CO_3 (88 mg, 0.64 mmol), and pivalic acid (4 mg, 0.04 mmol). The reaction vial was sealed, taken out of the glovebox, and stirred at 140 ℃ for 48 h. After the allotted time, the reaction mixture was precipitated in methanol which resulted in an insoluble black solid. Further analysis could not be carried out due to the insolubility of the product.

General procedure for the Suzuki cross-coupling polymerization: To a 10 mL oven-dried reaction tube, were placed 4,8-bis(ethylhexyloxy)-2,6-diiodobenzo[1,2-*b*:4,5-*b*']dithiophene 1,1,5,5-tetraoxide (Compound 1) (25 mg, 0.033 mmol), bis(boronic pinacol ester) functionalized

monomers (0.033 mmol), $Pd(PPh_3)_4$ (2 mg, 0.00164 mmol), and K_2CO_3 (72 mg, 0.525 mmol) inside a glove box. The reaction vial was sealed and taken out of the glove box. Dry THF (1 mL) and degassed water (1 mL) was added to the mixture using a syringe. The reaction vessel was heated at 110 ℃ for 48 h. The reaction mixture was cooled to room temperature, and 6 N HCl (8 mL) was added to the reaction vial. The crude product was extracted into ethyl acetate (15 mL x 3). The organic layer was washed with saturated sodium chloride (15 mL x 2) and dried (Na_2SO_4). The solvent was evaporated, and the resulting residue was redissolved in THF (1.0 mL) and precipitated in methanol (15.0 mL). The resulting precipitate was filtered through a cellulose thimble, and Soxhlet purification was done using methanol, hexane, and chloroform. Finally, the chloroform fraction was evaporated to dryness to yield the product.

PBDTT-C: Dark red color solid (27 mg, 90% yield). ^{1}H NMR (400 MHz, $CDCl_3$): δ 8.21-7.55 (b, 8H), 4.53 (b, 1H), 4.51 (b, 4H), 1.96-0.81(b, 37 H), 0.81-0.79 (b, 6H). M_n = 31 kDa, PDI = 2.3.

PBDTT-SiF: Orange color solid (19 mg, 60% yield). M_n = 123 kDa, PDI = 2.7

BDTT-IDTT oligomer: Dark blue solid (10 mg, 18% yield). ^{1}H NMR (400 MHz, $CDCl_3$): δ 7.55-7.29 (b, 6H), 7.18-7.06 (b, 16H), 4.4 (b, 4H), 2.54 (b, 8H), 1.85 (b, 2H), 1.3-0.8 (b, 88H). M_n = 3.0 kDa, PDI = 1.7.

2.8.4 Spectra

^{1}H NMR of BDTT

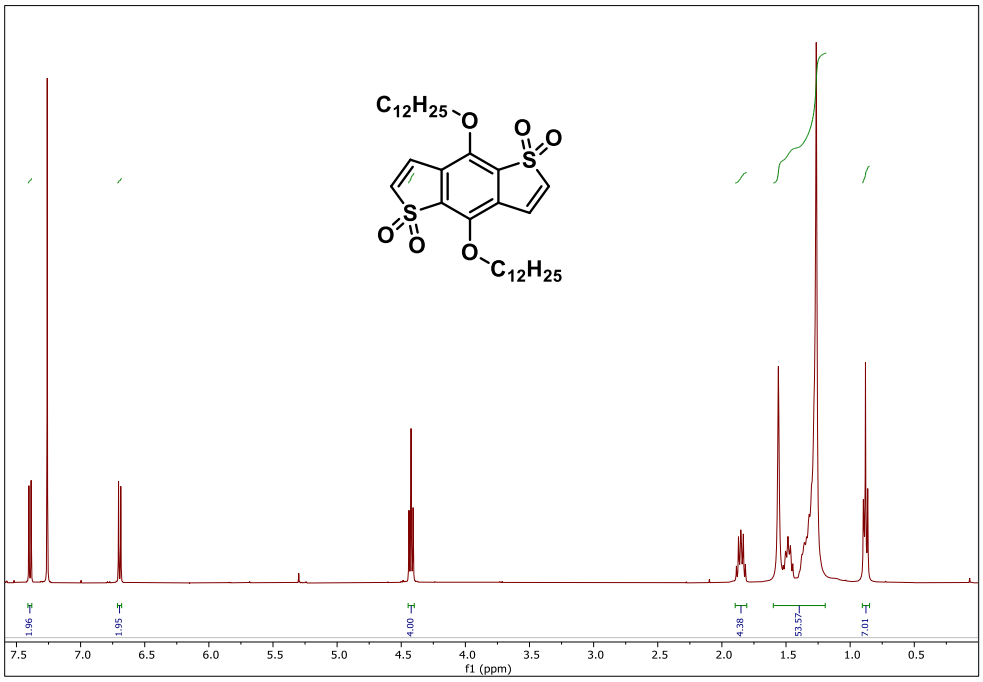

^{1}H NMR of Th-BDTT-Th

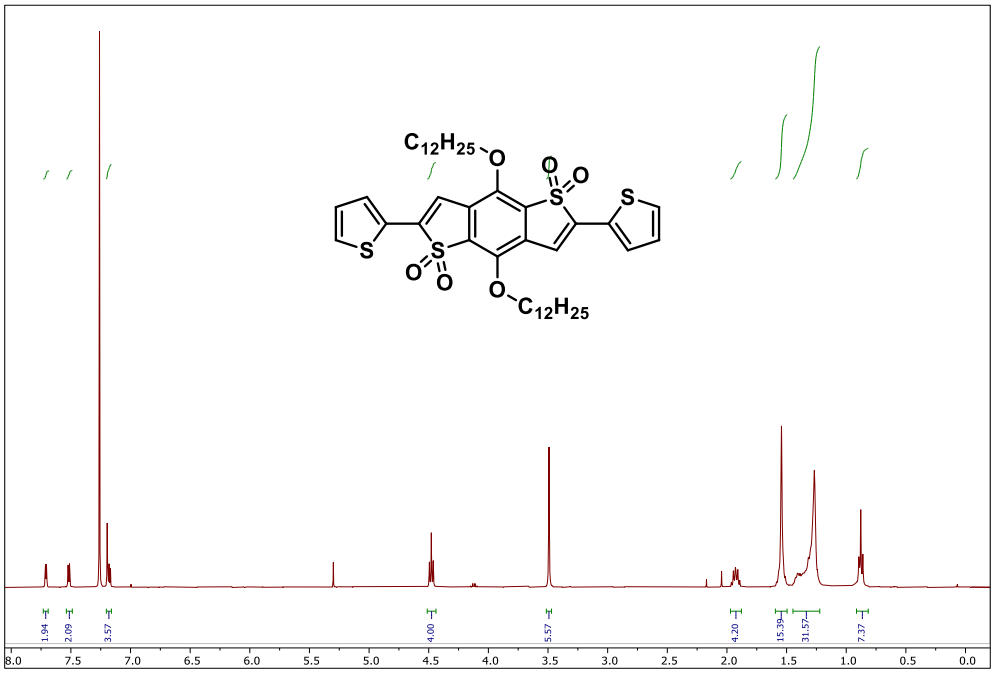

^{1}H NMR of PBDTT-Th

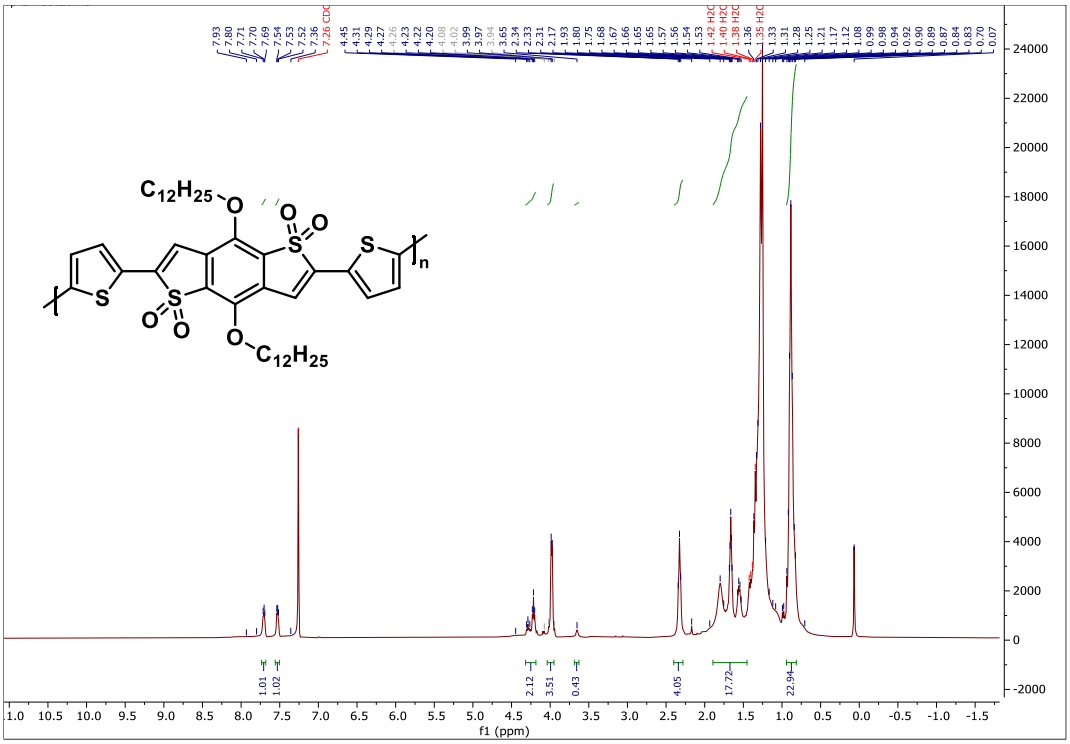

^{1}H NMR of PBDTT-C

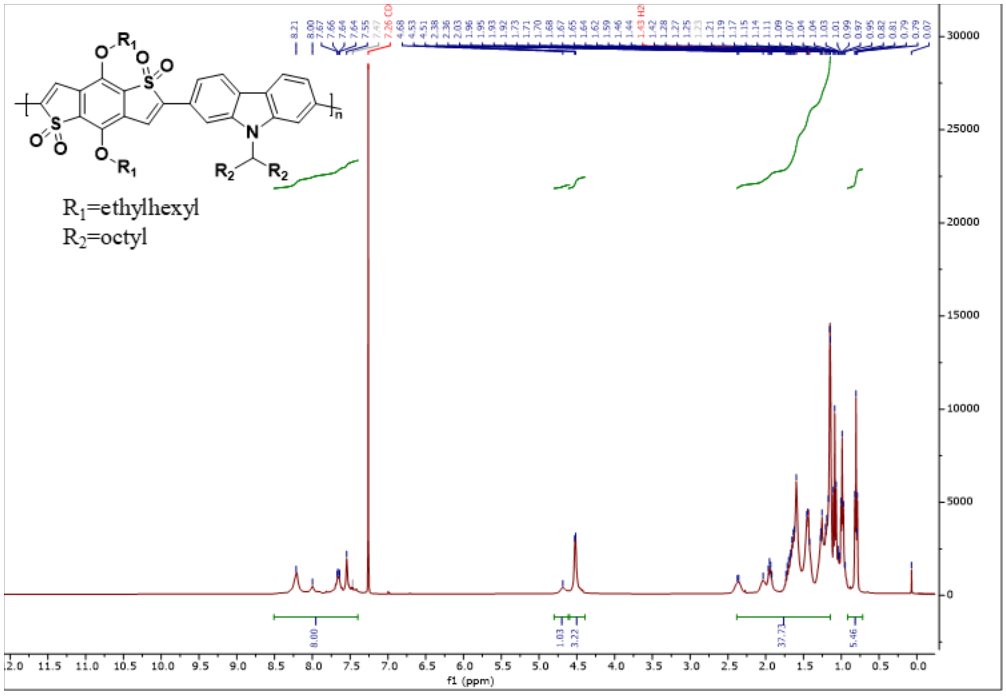

^{1}H NMR of BDTT-IDTT oligomer

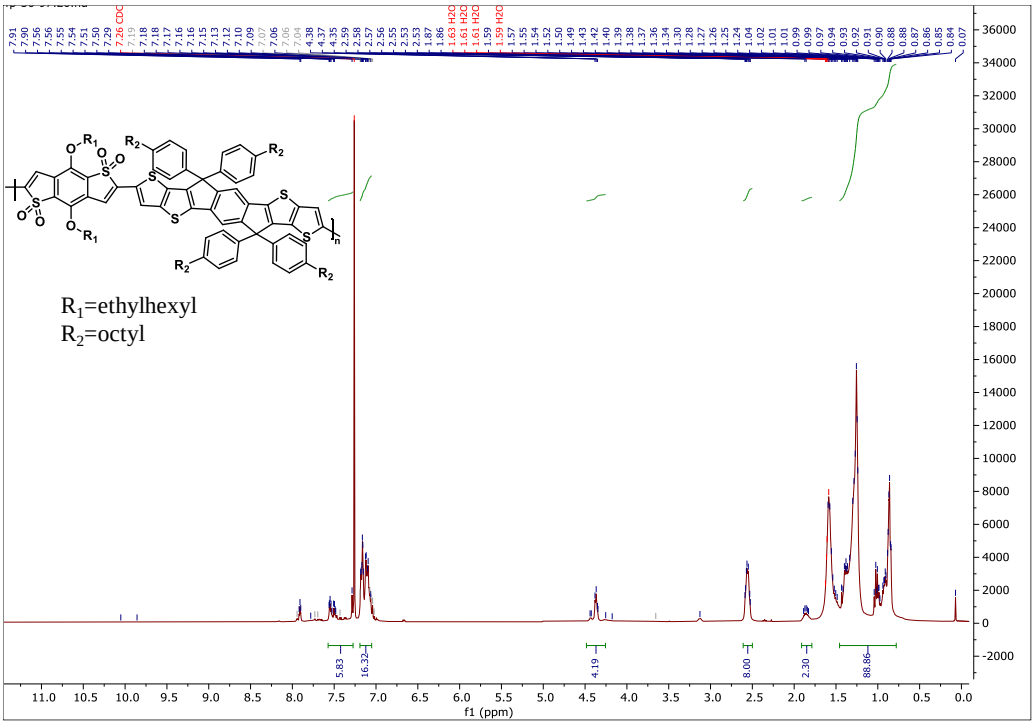

CHAPTER III

COPPER (I) OXIDE NANOPARTICLE-MEDIATED SYNTHESIS OF POLYPHENYLENEDIETHYNYLENES

3.1 INTRODUCTION

Recently metallic nanoparticles (NPs) have been widely used as catalysts in the field of organic synthesis due to their high reactivity, recyclability, and sustainability.[111-114] Metal NPs are of great scientific interest as they often exhibit different reactivities from their corresponding bulk materials because of their different sizes and shapes.[115] Metal NPs- catalyzed reactions are advantageous over conventional metal-catalyzed reactions in terms of high reactivity, low catalyst loading, and shorter reaction times.[112] The metal NPs have high surface-to-volume ratios that provide a large number of active sites compared to their heterogeneous counterparts. The higher zeta potential of metal NPs prevents aggregation thereby increasing the dispersity and stability in most chemical environments.[116] Due to growing environmental concerns, copper has gained substantial attention in organic synthesis because of its environmentally benign nature, high natural abundance, low cost, and minimal toxicity.[112,117] Copper and copper-based NPs have received tremendous attention from industry and academia because of their unique properties and applications in many areas of science.[112]

Conjugated oligo-poly yines are an important class of materials which have applications in electronic and photonic devices, such as in light-emitting diodes (LED)s, liquid crystal displays, thin-film transistors, and nanoscale molecular wires.[118-120] Generally, these polymers were synthesized via homogeneous palladium-catalyzed and copper-catalyzed coupling reactions in the presence of ligands and external oxidants.[121-122]

In this project, we present the Cu_2O NPs-mediated synthesis of poly(2,5-dialkoxy-1,4-phenylenediethynylene) under ligand-free conditions and using air as oxidant. In collaboration with the Andiappan group in the School of Chemical Engineering, we demonstrated that the polymerization reaction proceeded via a homogeneous catalytic pathway.

3.2 RESULTS AND DISCUSSION

Recently, Andiappan and co-workers reported a Cu_2O NPs-mediated homocoupling of phenylacetylene.[123] We were interested in expanding this methodology towards the polymerization routes via Cu_2O NPs-mediated homocoupling approach under ligand-free conditions and using atmospheric air as oxidant.

For these polymerization experiments, the Cu_2O NPs synthesis and characterization were done in the Andiappan lab (Figure 3.1 a-c).[123]

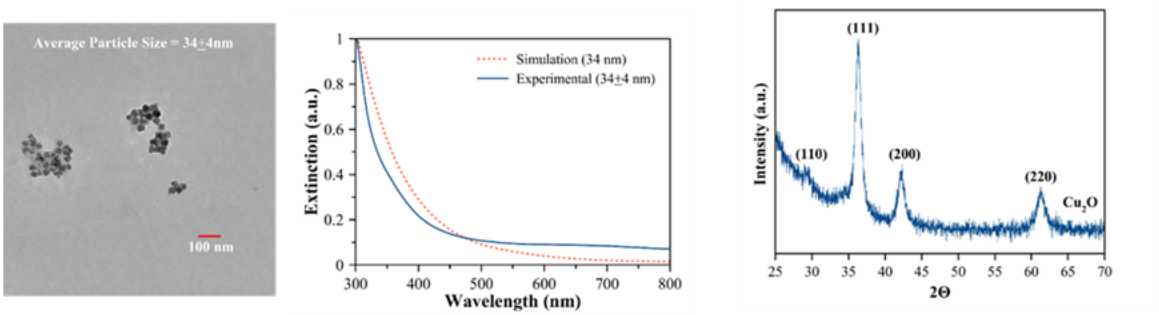

Figure 3.1: (a) A representative TEM image of the Cu_2O nanoparticles(34±4nm). (b) Comparison of experimental and computational measurement of UV-Vis extinction spectrum for Cu_2O nanoparticles for the particle size 34 nm. (c) The X-ray diffraction pattern of the Cu_2O NPs.[123]

Herein, we demonstrate Cu_2O NPs-mediated Glaser polymerization of 2,5-dialkoxyphenylen-1,4-diethynylenes (Scheme 3.1) with reasonable yields and moderate number average molecular weight M_n values. The utilization of air as the oxidant under ligand-free conditions of the Cu_2O NPs have led to a cost-effective and environmentally friendly process.

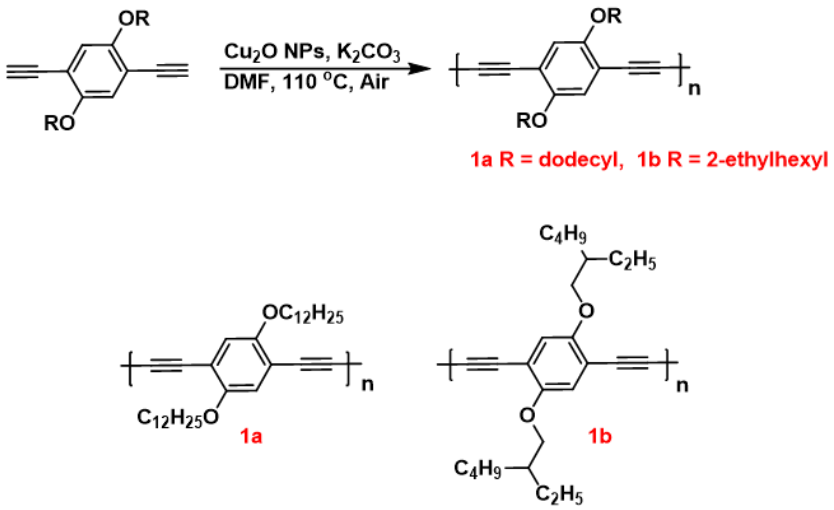

Scheme 3.1: Synthesis of poly (2,5-dialkoxy-1,4-phenylenediethynylenes).

Table 3.1: Optimization of Cu_2O NPs mediated Glaser polymerization of **1a**.

Entry	Cu_2O NPs (mol%)	K_2CO_3 (eq)	Solvent	Yield (%)	M_n[a] (kDa)	Đ[a]
1	50	4	DMF	88	1.1	1.4
2	50	16	DMF	75	3.3	1.6
3	5	16	DMF	25	1.6	1.3
4	25	16	DMF	33	2.3	1.2
5	50	16	DMF/DCB	90	3.0	1.6

[a] Determined by GPC in THF using polystyrene standards.
Đ = polydispersity index

Initially, we employed the conditions that the Andiappan group had optimized for the homocoupling of phenylacetylene which was two equivalents of K_2CO_3 and 50 mol% of Cu_2O NPs in DMF. However, these reaction conditions resulted in polymer **1a** with a low molecular weight

and a 70% yield. Hence, we increased the amount of base to four equivalents based on a previously reported polymerization (Table 3.1, entry 1).[124] The desired polymer was obtained in good yield (88%) but possessed a low value of M_n. Additional base (16 eq, Table 3.1, entry 2) was needed to improve the M_n values (3.3 kDa). We sought to probe the catalyst loading (Table 3.1, entries 2-4). Lower catalyst loading resulted in a significant lowering of the yield. As shown in Table 3.1, catalyst loadings of 25 mol% and 5mol% resulted in low isolated yields and with only a slight decrease in M_n values (entries 3 and 4). In general, relatively low M_n values were observed for the polymers shown in Table 3.1 (entries 1-4) which can probably be attributed to the poor polymer solubility in DMF. Indeed, the reaction mixture became opaque as the reaction proceeded, and deposition was observed on the wall of the reaction vessel which could result from a heterogeneous reaction and hindrance of the polymer chain growth. Considering these results, we anticipated that the addition of 1,4 dichlorobenzene (DCB) would improve the M_n with increased solubility (Table 3.1, entry 5). Unfortunately, the deposition on the reaction tube was observed, and the M_n values remained almost the same (3.0 kDa).

Table 3.2: Optimization of Cu_2O NPs mediated Glaser polymerization of **1b.**

Entry	**Cu_2O NPs (mol%)**	**K_2CO_3 (eq)**	**Solvent**	**Yield (%)**	**M_n[a] (kDa)**	**Đ[a]**
1	50	4	DMF	50	8.6	2.1
2	50	16	DMF	40	9.0	4.5
3	5	16	DMF	25	5.4	1.7
4	25	16	DMF	40	9.8	4.5
5	50	16	DMF/DCB	48	11.2	3.8

[a] Determined by GPC in THF using polystyrene standards.
Đ = polydispersity index

In an attempt to enhance the solubility, a second polymer derivative was prepared that incorporated branched 2-ethylhexyloxy side chains. The data for polymer **1b** was summarized in Table 3.2. In contrast to the dodecyloxy analogue, **1a**, poly (1,4-bis((2-ethylhexyl) oxy)-2,5-di(prop-1-yn-1-yl)

benzene), **1b** afforded higher M_n values ranging from 5-11 kDa (Table 3.2, entries 1-5) and in all cases large polydispersities were observed. Similarly, the previous literature showed that, for this type of homopolymer, the M_n values obtained were ranged from 5-14 kDa with large polydispersities.[121-122] The polymer yields obtained were comparatively low (Table 3.2, entries 1-5) but after solvent washes, we observed a yellowish-red material that remained in the Soxhlet thimbles. We assume the material to be insoluble higher molecular weight polymers. Structure characterization was done using ^{1}H NMR spectroscopy, and the spectra were in good agreement with those previously reported.[121-122]

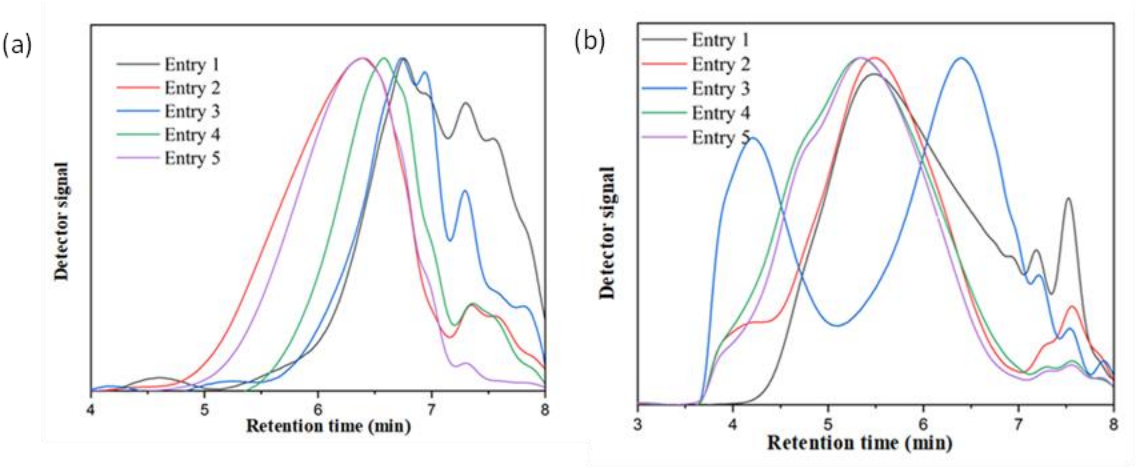

Figure 3.2: GPC traces of the synthesized polymers (a) obtained for the conditions outlined in Table 3.1. (b) obtained for the conditions outlined in Table 3.2.

The Gel permeation chromatography (GPC) traces of the polymerization reactions are shown in Figure 3.2. The peaks show the polymer distribution based on the reaction conditions. Figure 3.2 (a) represents the distributions of polymer **1a**. Here, under the conditions mentioned in Table 3.1, entry 1, the polymer distribution was not smooth,and several humps at higher retention times were observed which is indicative of different sizes of oligomer formation (Figure 3.2 a, entry 1, black line). However, in entry 2 (red line), a nice Gaussian curve was obtained, which showed the normal distribution of molecular weights which is indicative of further growth of polymers at high base loading (16 eq, Table 3.1, entry 2). As mentioned in Table 3.1, entries 3 and 4, the lowering loading of Cu_2O NPs shifted the GPC traces towards lower molecular weights. Entry 3 (blue line), shows

the presence of oligomers with different molecular weights. whereas entry 4 (green line) shows oligomers with narrower size distribution. In entry 5 (purple line), a similar trend is observed as in entry 2.

For the polymer **1b**, Figure 3.2 b, entry 1(black line) shows the normal distribution of the polymers compared to Figure 3.2 a, entry 1. This might be due to the increased solubility of the branched alkoxy chain. As mentioned in Table 3.2, entry 2, higher base loading was favorable for the reaction. The GPC trace shows growing high molecular weight polymers at lower retention time (~ 4 min) (Figure 3.2, entry 2, red line). Lowering the Cu_2O NPs loadings shifted the peaks towards higher retention times. When 5 mol % of Cu_2O NPs were used (Table 3.2, entry 3), a significant bimodal polymer distribution was displayed which is indicative of the formation of higher molecular weight polymers as well as the presence of low molecular weight oligomers (Figure 3.2 b, entry 3, blue line). Due to the low concentration of Cu_2O NPs, further polymer growth might be hindered. However, when Cu_2O NPs loading was increased to 25 mol %, normal distribution was observed (Figure 3.2 b, entry 4, green line) which indicates further growth of polymers compared to entry 3. In entry 5 (purple line), a slight shoulder peak was observed around 4.5 min. However overall distribution was normal and similar to entry 3.

3.2.1 Evidence for homogeneous catalytic pathway

Andiappan and coworkers previously reported that in the presence of K_2CO_3, the Cu_2O nanoparticles mediate the homocoupling of phenylacetylene (PA) via a homogeneous catalytic pathway.[123] Based on UV-Vis extinction spectra and electrospray ionization mass spectrometry (ESI-MS), they have shown that *in-situ* formation of homogeneous copper complexes via PA-induced leaching of Cu_2O NPs surface atoms. The leaching of Cu_2O NPs was also confirmed using Transition Electron Microscopy (TEM).[123] We hypothesized that a similar mechanism might be

involved with the polymerization reaction. We have carried out UV-Vis spectroscopic studies and ESI-MS studies for the polymerization reactions.

UV-Vis extinction spectra of the polymerization reaction are shown in Figure 3.3. Aliquots from the reaction mixture were taken at different time intervals. Based on the literature, the peaks at 346 nm and 424 nm correspond to the starting monomer and the polymer, respectively.[121] The new extinction peak around 450-475 nm might be associated with the homogenous copper complexes.

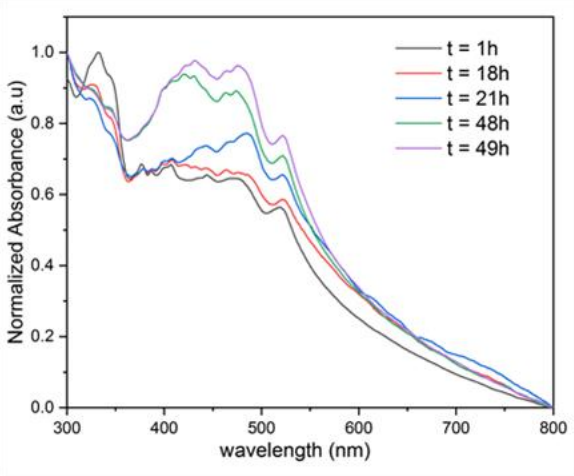

Figure 3.3: UV-Vis extinction spectra of the polymerization reaction, measured at different time intervals

To further confirm and gain an insight into the signature of the homogeneous copper complexes, we also performed ESI-MS analysis for the reaction mixtures. The representative ESI-MS spectra obtained for the polymer samples are shown in Figure 3.4 a and b.

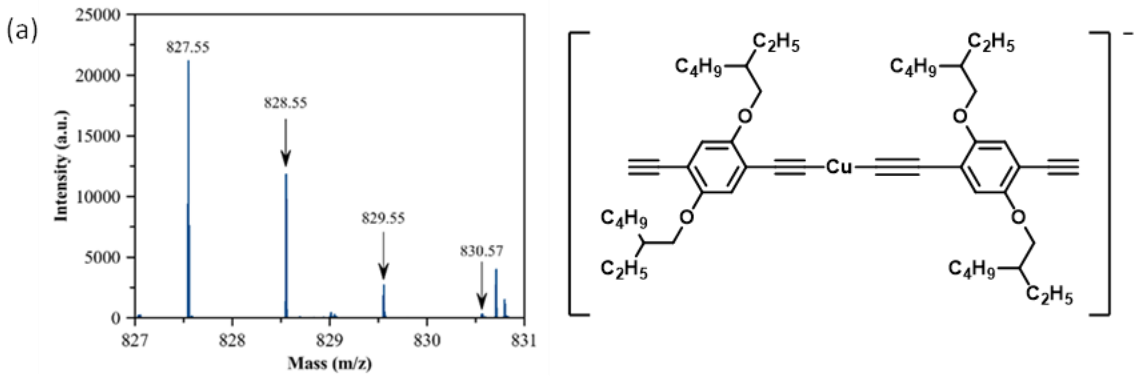

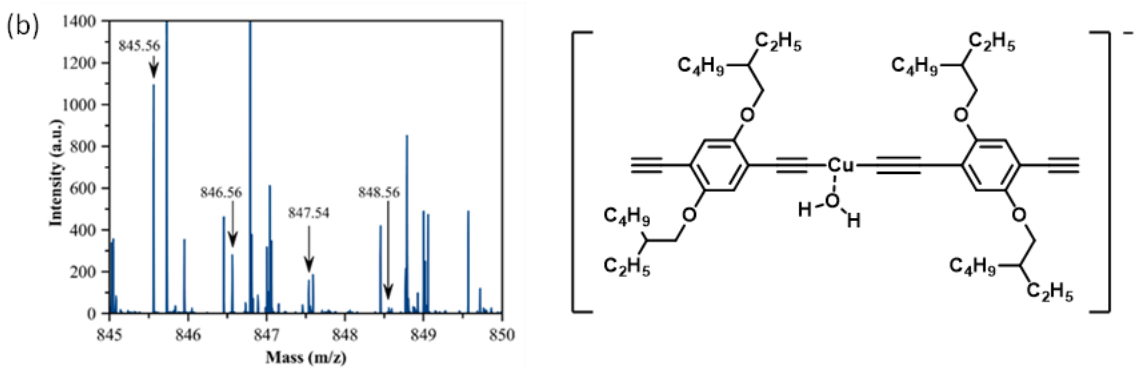

Figure 3.4: (a and b) The HR-ESI-MS spectrum measured in the negative ion mode for the reaction mixture obtained from polymer **1b,** and proposed possible copper complex.

In accordance with the experimental ESI-MS spectra in Figure 3.4 (a) and (b), we propose two possible homogeneous copper complexes (shown in Figure 3.4 (a) and (b)) for the polymerization reaction **1b**. Furthermore, we have obtained predicted ESI-MS spectra for the proposed structures from the literature[125] and the experimental spectra were a good match with the predicted spectra (Figure 3.5 a and b).

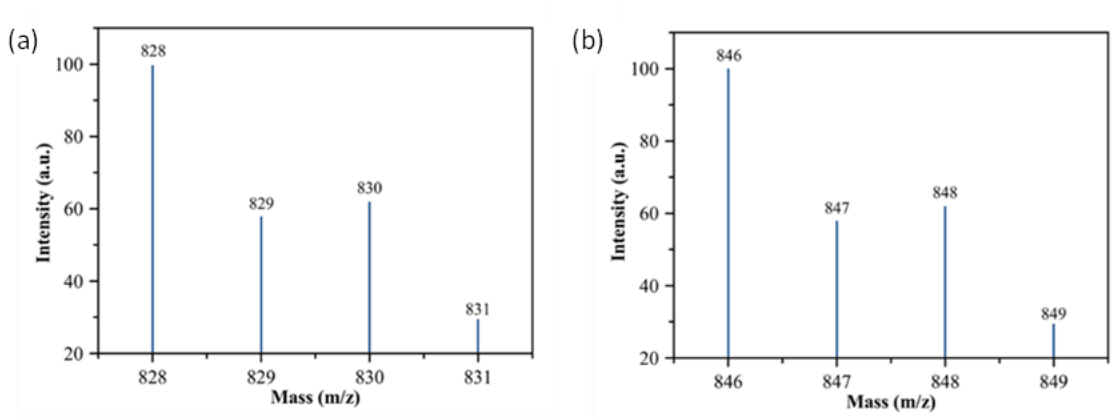

Figure 3.5: (a) predicted ESI-MS spectrum for the proposed copper complex 3.4 a. (b) predicted ESI-MS spectrum for the proposed copper complex 3.4 b

3.3 CONCLUSION

In this project, we have synthesized Cu_2O nanoparticles-mediated poly(2,5-dialkoxy-1,4-phenylenediethynylene) under ligand-free conditions and using ambient air as oxidant. This methodology is environmentally benign and cost-effective in contrast to traditional methods. The addition of branched alkoxy side chains increases the solubility, thereby improving the molecular weights of the polymers. Andiappan and co-workers have shown that during the C-C homocoupling reaction, Cu_2O NPs undergo leaching to form in-situ homogeneous copper complexes, and the reaction occurs via a homogeneous catalytic pathway.[123] We assume a similar mechanism may occur during the polymerization reaction. Using UV-Vis extinction spectra and ESI-MS spectra, we have shown the formation of homogeneous copper complexes during the polymerization.

3.4 EXPERIMENTAL SECTION

3.4.1 General methods and materials:

All reagents were purchased and used as received from Fisher Scientific and VWR unless otherwise noted. Solvents were purchased from Fisher Scientific and were used without further purification. The monomers, 2,5-dialkoxy-1,4-phenylenediethynylenes were synthesized according to the literature.[126] ^1H NMR spectra were measured on a Bruker Avance 400 MHz instrument. Number average molecular weight (M_n) and polydispersity (Đ) were determined by gel permeation chromatography (GPC) using a Waters pump with a Waters 2410 refractive index detector. THF was used as an eluent at 35 °C with a flow rate of 1.0 mL min^{-1}. The instrument was calibrated with polystyrene standards and data were analyzed using Breeze software. UV-Vis extinction spectra were recorded using an Agilent Cary 60 spectrophotometer. Electrospray ionization mass spectrometry (ESI-MS) spectra of the reaction mixture were collected on LTQ Orbitrap system with an ESI source.

3.4.2 Polymer synthesis and characterization: (1,4-Bis((2-ethylhexyl) oxy)-2,5-di(prop-1-yn-1-yl) benzene) (0.065 mmol), and K_2CO_3 (0.26 mmol) were weighed in air and then added to a 10 mL reaction vessel equipped with a stir bar. A suspension solution was prepared by adding Cu_2O NPs (0.033 mmol, 50 mol%) in DMF (2.5 mL) and was sonicated for 15 min. This suspension solution was added to the reaction vessel in the air, and the reaction vessel was sealed. It was noted that similar results were obtained in the presence of wet air, dry air or atmospheric air in the headspace of the reaction vessel. The reaction mixture was heated at 110 °C for 48 h and then cooled to room temperature and was precipitated in methanol (25 mL). The precipitate was filtered through a cellulose thimble and subjected to Soxhlet extraction with methanol, acetone, and chloroform. The polymer was isolated and dried under reduced pressure to yield a dark brownish-red polymer (polymer 1b) (12 mg, 50%). ^{1}H NMR (400 MHz, $CDCl_3$): δ 6.96 (s, broad, Ar-H), 3.87 (d, broad, -OCH_2), 1.79 (m, broad, -CH), 1.54-1.25 (m, broad, -CH_2), 0.96 (t, broad, -CH_3), 0.92 (t, -CH_3). M_n = 8.6 kDa, Đ = 2.1.

3.4. 3 Spectra

^{1}H NMR of 1,4-bis(dodecyloxy)-2,5-diethynylbenzene

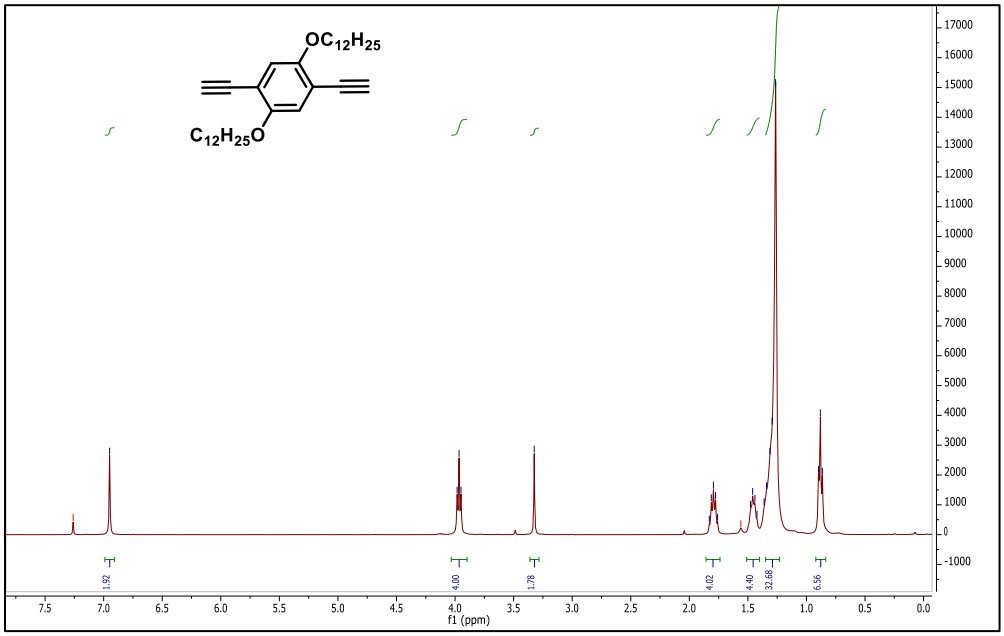

^{1}H NMR of 1,4-bis((2-ethylhexyl)oxy)-2,5-diethynylbenzene

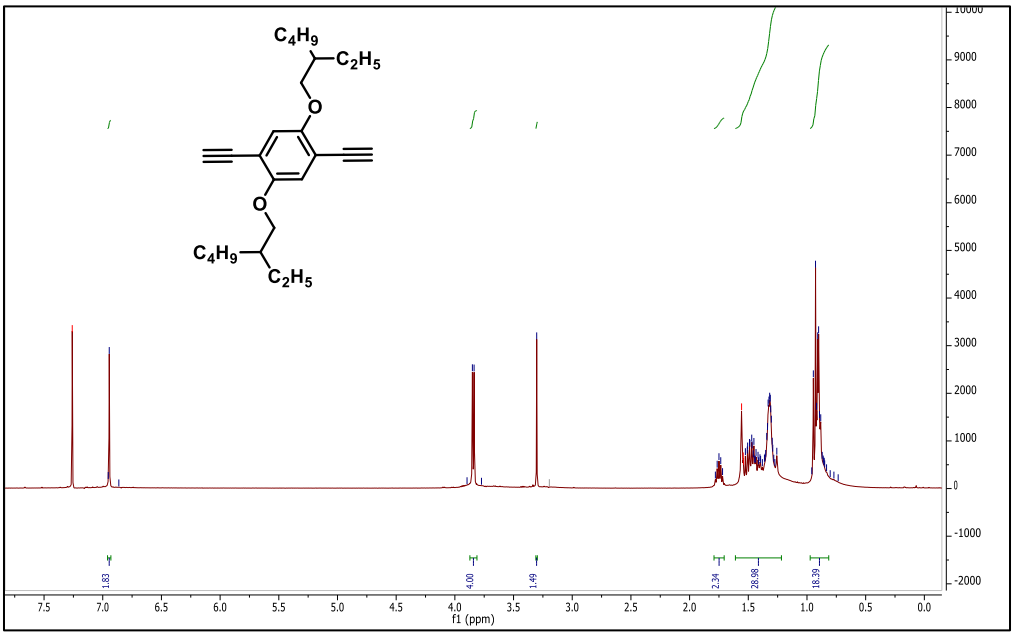

^{1}H NMR of poly (1,4-bis(dodecyloxy)-2,5-diethynylbenzene)

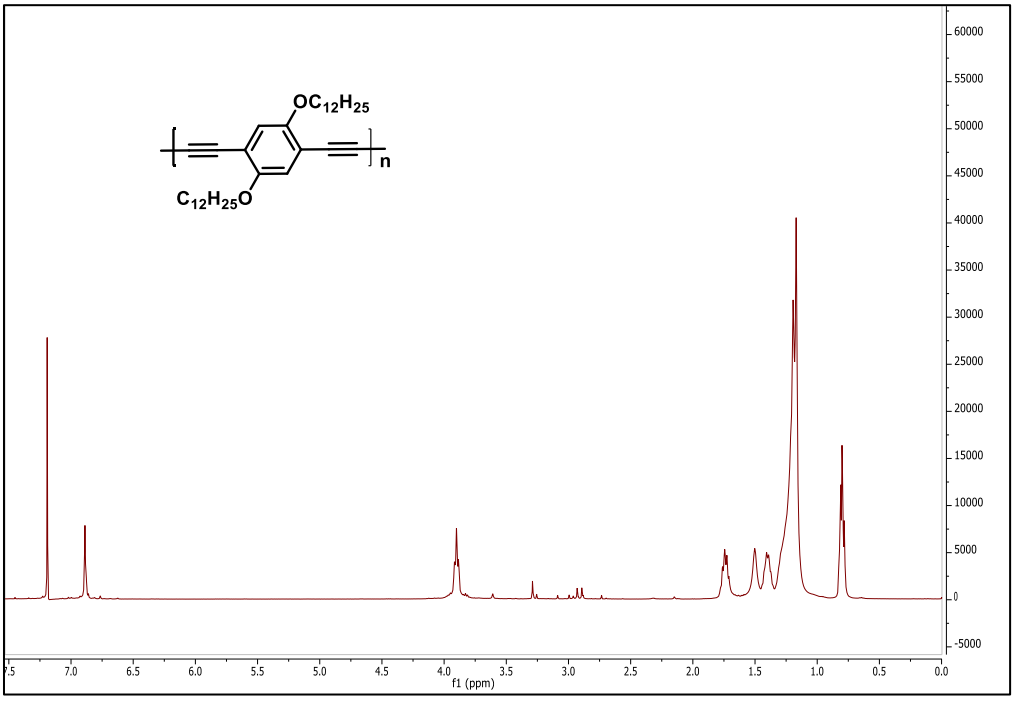

^{1}H NMR of poly(1,4-bis((2-ethylhexyl)oxy)-2,5-diethynylbenzene

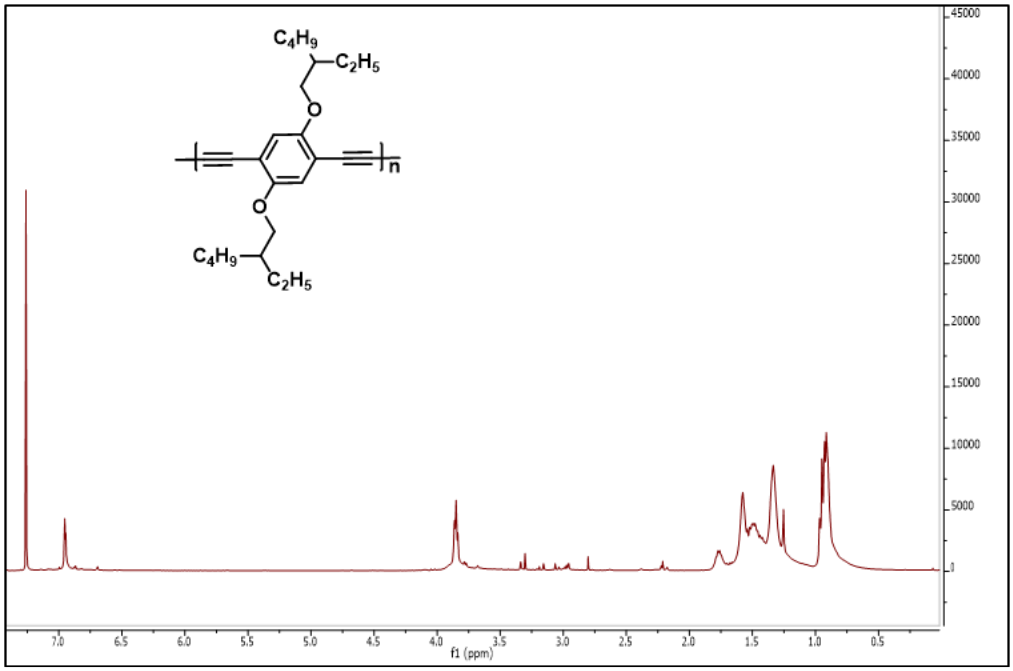

CHAPTER IV

"BENCHTOP" SYNTHESIS OF CONJUGATED POLYMERS VIA Pd/Cu Co-CATALYSIS

4.1 INTRODUCTION

Conjugated polymers containing aromatic rings in the backbone have attracted substantial attention due to their wide range of applications in many areas such as organic light-emitting diodes (OLEDs), organic field-effect transistors (OFETs), organic photovoltaics (OPVs), chemical sensors, and bioelectronics.[127-131] Aryl-aryl coupling reactions are central to the construction of π conjugated polymers. In the past, aryl-aryl coupling reactions were employed mostly via Stille-based coupling reactions which require aryl halide and organostannyl substituted coupling partners. However, organotin compounds and their byproducts are hard to remove and highly toxic.[132] In comparison to the Stille based reactions, the Suzuki reaction is in some aspects environmentally preferable.[133] Moreover, most of the aryl boronic acids and esters are now readily available from commercial sources. Nevertheless, a standard Suzuki coupling requires inert conditions.[134] According to literature, there have been several reports utilizing boronic acids in oxidative dimerization and polymerization.[135-138] But most reactions required oxygen conditions and phase transfer catalysts which add significant complexity to the reaction set up. To address these issues, Minus. et al. developed a new bimetallic methodology that exploits the distinct reactivities of palladium and copper to perform high yielding aryl-aryl dimerizations.

These couplings are facile and can be done by simple mixing components in an open vessel. In our lab, we demonstrate the utility of this methodology in the context of polymer synthesis involving polycarbazole (PC), polysilafluorene (PSiF), and poly 6,6,12,12-tetrakis(4-hexylphenyl)-6,12-dihydro-dithieno[2,3-*d*:2',3'-*d*']-s-indaceno[1,2-*b*:6,6-*b*']dithiophene (PIDTT) using energy-efficient and aerobic conditions (benchtop synthesis) (Figure 4.1).

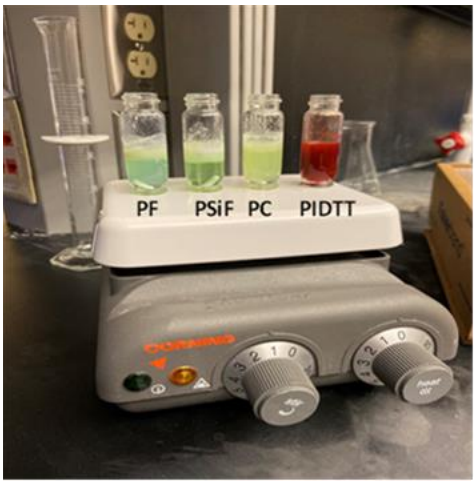

Figure 4.1: "Benchtop" synthesis of PF, PC, PSiF, and PIDTT via Pd/Cu co-catalysis.

4.2 RESULTS AND DISCUSSION

As mentioned above, Minus and coworkers have utilized benchtop aryl-aryl dimerizations. This methodology requires $Pd(OAc)_2$, $Cu(OAc)_2$, $B(OH)_3$ under air, in wet DMSO. Boric acid was used as an additive to facilitate the *in situ* deprotection of the boronate esters to the boronic acids.[139] Given these parameters, we were interested in extending this methodology towards the synthesis of conjugated polymers.

Our efforts have focused on the synthesis of polyfluorene (PF) using commercially available 9,9-dioctyl fluorene-2,7-diboronic acid bis (1,3-propendiol) ester as the monomer in Scheme 4.1.

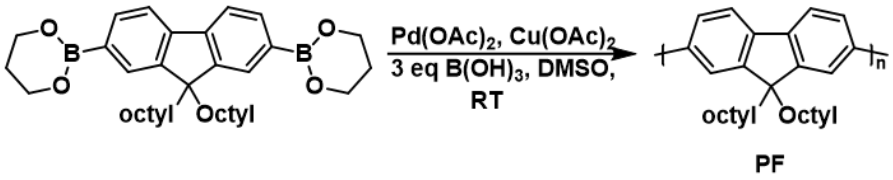

Scheme 4.1: "Benchtop" synthesis of PF using the conditions outlined in Table 4.1

Table 4.1: Optimization of "Benchtop" synthesis of PF via Pd/Cu co-catalysis.

Entry	$Pd(OAc)_2$ (mol %)	$Cu(OAc)_2$ (mol %)	Temperature	Time	%Yield	M_n[a] (kDa)	Đ[a]
1	2	4	RT	48 h	33	4.8	1.60
2	3	5	RT	48 h	44	6.8	1.91
3	3	5	50℃	48 h	17	5.3	1.52
4	6	10	RT	48 h	65	7.9	2.20
5	3	5	RT	96 h	35	4.6	1.63
6	6	10	RT	96 h	74	7.7	2.46

[a] Determined by GPC in THF using polystyrene standards.
Đ = polydispersity index

The focus of the optimization was catalysts loading, reaction temperature, and time as detailed in Table 4.1. The polymerization was performed in a reaction vessel (10 mL) at room temperature open to the air for the indicated time. Then the reaction mixture was precipitated in methanol and Soxhlet extraction was done with methanol, hexane, and chloroform. The chloroform fraction was evaporated and used in the calculation of molecular weights and yields of products. Initially, we altered the conditions used in the aryl-aryl dimerization (Table 4.1, entry 1). This resulted in moderate value for the number average molecular weight (M_n) and a low yield (4.8 kDa, 33%, respectively). Increasing the catalysts loading improved the yield and M_n (Table 4.1, entry 2). However, the addition of heat (Table 4.1, entry 3) was detrimental to the reaction and a lower yield was obtained (17%). The addition of heat could accelerate the reaction, and premature precipitation might have occurred. Next, we doubled the loadings of catalyst (Table 4.1, entry 4). This afforded

polymer products with high M_n and good yield (7.9 kDa, 65%, respectively). As shown in entries 5 and 6 (Table 4.1), increasing the reaction time to 96 h did not dramatically affect the yield and M_n values.

4.2.1 Reaction scope towards the heteroaromatic system.

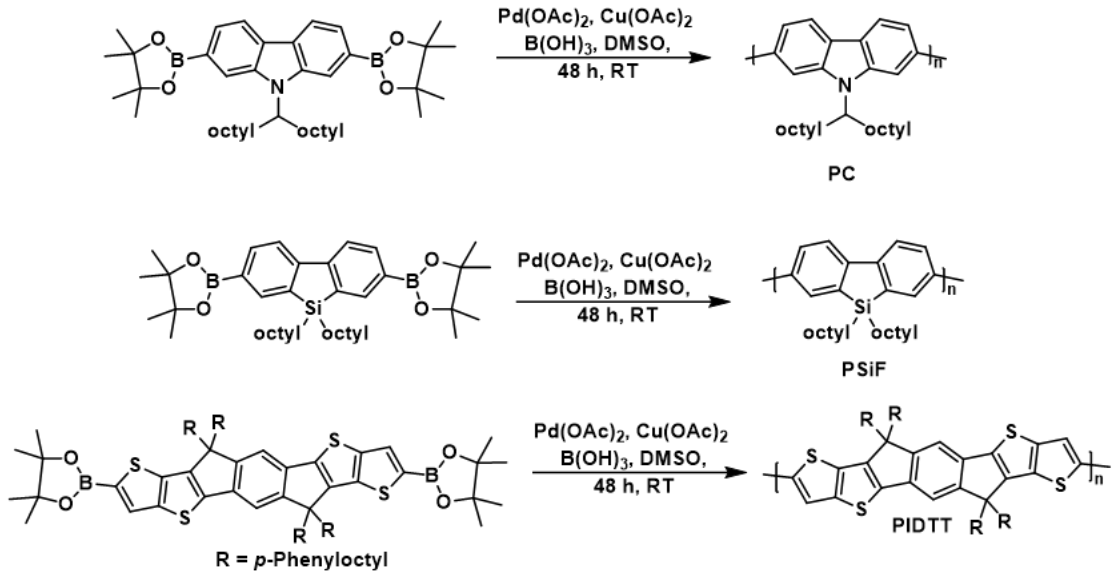

Scheme 4.2: "Benchtop" synthesis of PC, PSiF, and PIDTT via Pd/Cu co-catalysis.

Table 4.2: Structural properties of the polymers.

Polymer	**M_n[a] (kDa)**	**M_w[a] (kDa)**	**Đ[a]**	**Yield (%)**
PC	6.54	8.84	1.35	16
PSiF	4.90	7.12	1.75	16
PIDTT	4.64	9.69	2.09	22

[a] Determined by GPC in THF using polystyrene standards.
Đ = polydispersity index

We were further interested in exploring the polymerization reaction with heterocyclic aromatic systems. Carbazoles (C), silafluorene (SiF), and 6,6,12,12-tetrakis(4-hexylphenyl)-6,12-dihydro-dithieno[2,3-*d*:2',3'-*d'*]-s-indaceno[1,2-b:6,6-b']dithiophene (IDTT) are well known materials,

used in OSCs.[104-106] PC, PSiF, and PIDTT were successfully synthesized at room temperature from the analogs of diboronate esters (Scheme 4.2) and the results are summarized in Table 4.2. The isolated polymers of PC, PSiF, and PIDTT have M_n values of 6.5, 4.9, and 4.6 kDa, respectively. However, most of the colored material remained insoluble in the Soxhlet thimble after extraction. We assume the insoluble materials to be high molecular weight polymers.

4.2.2 Attempted synthesis of donor-accepter conjugated polymers via Pd/Cu co-catalysis under "benchtop" conditions.

π-Conjugated polymers with the alternating donor (electron-rich) and acceptor (electron-deficient) architecture (D-A) are particularly attractive due to the facile tunability of the electronic structures in their conjugated backbones, thus optoelectronic properties.[140-141] Therefore, we used our newly developed methodology towards donor-acceptor conjugated polymers.

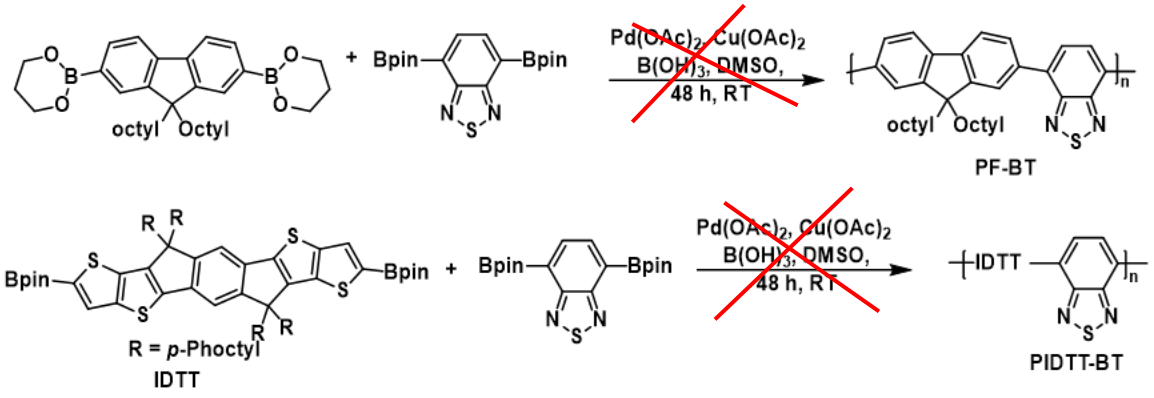

Bpin = pinacolborane

Scheme 4.3: Attempted donor-acceptor polymer synthesis via Pd/Cu co-catalysis under "benchtop" conditions.

As shown in Scheme 4.3, we attempted to synthesize PF-BT and PIDTT-BT using fluorene (F) and thiophene rich IDTT molecules as the donors and benzothiadiazole (BT) as the acceptor. Unfortunately, under the current reaction conditions, it appear to have either a homocoupling product or a degraded product. This might be due to the different electronic nature of the donor and acceptor core, which could not undergo coupling in the catalytic cycle. As we know, each condition

is substrate-dependent, and to utilize this methodology towards donor-acceptor conjugated polymer synthesis, further optimization might be needed.

4.3 CONCLUSION

Using Pd(II)/Cu(II) co-catalysis and diboronic acid precursors, we achieved benchtop access for conjugated organic polymers. We successfully synthesized PF, PC, PSiF, and PIDTT with reasonable M_n values.

4.4 EXPERIMENTAL SECTION

4.4.1 Materials

All starting monomers, $Pd(OAc)_2$ and $Cu(OAc)_2$, were purchased from Aldrich and used as received. Solvents were purchased from Fisher Scientific and used without further purification.

4.4.2 Instrumentation

^1H NMR spectra were measured on a Bruker Avance 400 MHz instrument. Number average molecular weight (M_n) and polydispersity (Đ) were determined by gel permeation chromatography (GPC) using a Waters pump with a Waters 2410 refractive index detector. THF was used as an eluent at 35 °C with a flow rate of 1.0 mL min^{-1}. The instrument was calibrated with polystyrene standards and data were analyzed using Breeze software.

4.4.3 Synthesis procedures

Poly (9,9-dioctylfluorene) (PF)

9,9-Dioctylfluorene-2,7-diboronic acid bis(1,3-propanediol) ester (100 mg, 0.179 mmol), $Pd(OAc)_2$ (2.4 mg, 0.011 mmol), $Cu(OAc)_2$ (3.2 mg, 0.0179 mmol) and boric acid (55 mg, 0.895 mmol) were added to a 10 mL reaction vessel equipped with a stir bar, followed by DMSO (2 mL). The reaction vessel was covered with a Kimwipe and stirring was continued at room temperature

for 48 h. The reaction mixture was precipitated in methanol (20 mL) to give and light-yellow precipitate. The resulting precipitate was filtered through a cellulose thimble and subjected to Soxhlet extraction with methanol, acetone, and chloroform. The solvent was removed to yield a green-yellow polymer (45 mg, 65%). ^{1}H NMR (400 MHz, $CDCl_3$): δ 7.66-7.86 (m, broad, 6H), 2.11 (t, broad, 4H), 1.09-1.26 (m, broad, 28H), 0.73 (t, broad, 6H). M_n = 7.9 kDa and Đ = 2.2.

Poly (9-(9-heptadecyl)-9*H*-carbazole) (PC)

9-(9-heptadecyl)-9H-carbazole-2,7-diboronic acid bis(pinacol) ester (200 mg, 0.30 mmol), $Pd(OAc)_2$ (3.4 mg, 0.015 mmol), $Cu(OAc)_2$ (5.5 mg, 0.03 mmol) and boric acid (56.4 mg, 0.9 mmol) were added to a 10 mL reaction vessel equipped with a stir bar followed by DMSO (4 mL). Then the reaction vessel was covered with a Kimwipe and stirred under room temperature for 48 h. The reaction mixture was precipitated in methanol (40 mL) to give an off-white precipitate. The resulting precipitate was filtered through a cellulose thimble and subjected to Soxhlet extraction with methanol, acetone, and chloroform. The solvent was removed to yield a green-brown polymer (20 mg, 16 %). ^{1}H NMR (400 MHz, $CDCl_3$): δ 7.62-8.28 (m, broad, 6H), 1.15-1.29 (m, broad, 28H), 0.81 (m, broad, 6H); M_n = 6.54 kDa and Đ = 1.4.

Poly (9,9-dioctyl-9*H*-9-silafluorene) (PSiF)

9,9-Dioctyl-9H-9-silafluorene-2,7-bis(boronic acid pinacol ester) (200 mg, 0.30 mmol), $Pd(OAc)_2$ (3.4 mg, 0.015 mmol), $Cu(OAc)_2$ (5.4 mg, 0.03 mmol) and boric acid (55.6 mg, 0.9 mmol) were added to a 10 mL reaction vessel equipped with a stir bar followed by DMSO (4 mL). Then the reaction vessel was covered with a Kimwipe and stirred under room temperature for 48 h. The reaction mixture was precipitated in methanol (40 mL) to give off- white precipitate. The resulting precipitate was filtered through a cellulose thimble and subjected to Soxhlet extraction with methanol, acetone, and chloroform. The solvent was removed to yield a green-brown polymer (20

mg, 16%). ^{1}H NMR (400 MHz, $CDCl_3$): δ 7.73-8 (m, broad, 6H), 1.18-1.29 (m, broad, 28H), 0.84 (m, broad, 6H); M_n = 4.90 kDa and Đ = 1.8.

Poly(6,6,12,12-tetrakis(4-octylylphenyl)-6,12-dihydro-dithieno[2,3-d:2′,3′-d′]-s-indaceno[1,2-b:5,6-b′]dithiophene) (PIDTT)

6,12-Dihydro-6,6,12,12-tetrakis(4-octylphenyl)-2,8-bis(4,4,5,5-tetramethyl-1,3,2-dioxaborolan-2-yl)dithieno[2,3-*d*:2′,3′-*d*′]-s-indaceno[1,2-b:5,6-*b*′]dithiophene (200 mg, 0.14 mmol), $Pd(OAc)_2$ (1.6 mg, 0.007 mmol), $Cu(OAc)_2$ (2.6 mg, 0.015 mmol) and boric acid (26.8 mg, 0.43 mmol) were added to a 10 mL reaction vessel equipped with a stir bar followed by DMSO (4 mL) was added to the reaction mixture. Then the reaction vessel was covered with a Kimwipe and stirred under room temperature for 48 h. The reaction mixture was precipitated in methanol (40 mL) to give off white precipitate. The resulting precipitate was filtered through a cellulose thimble and subjected to Soxhlet extraction with methanol, acetone, and chloroform. The solvent was removed to yield a dark red polymer (35 mg, 22 %). ^{1}H NMR (400 MHz, $CDCl_3$): δ. 7.37-7.46 (s, broad, 2H), 7.22-7.29 (s, broad, 2H) 6.96-7.15 (m, broad, 16H), 1.07-1.31(m, broad, 56H) 0.78 (m, broad, 12H); M_n = 4.64 kDa and Đ = 2.1.

4.4.4 Spectra

^{1}H NMR of PF

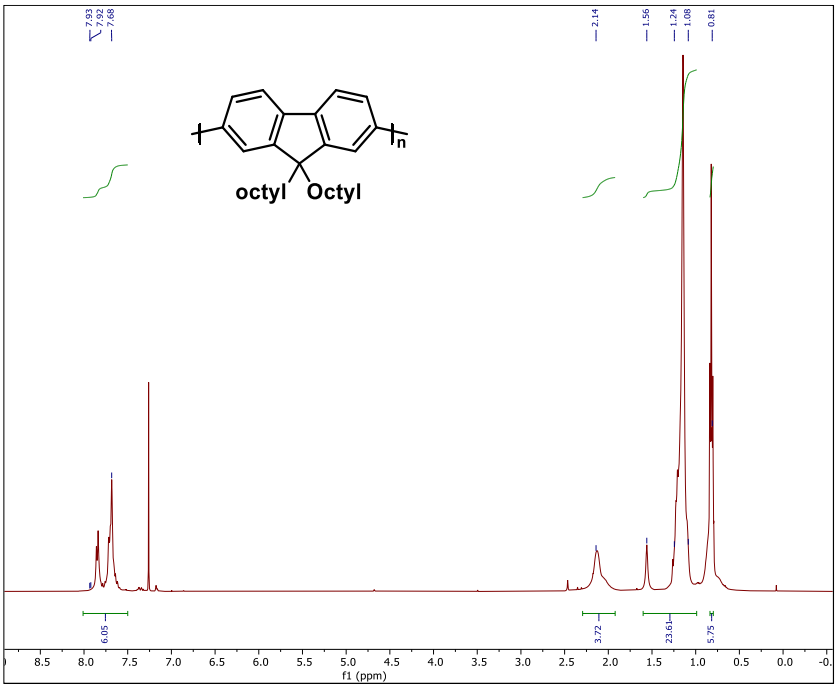

^{1}H NMR of PC

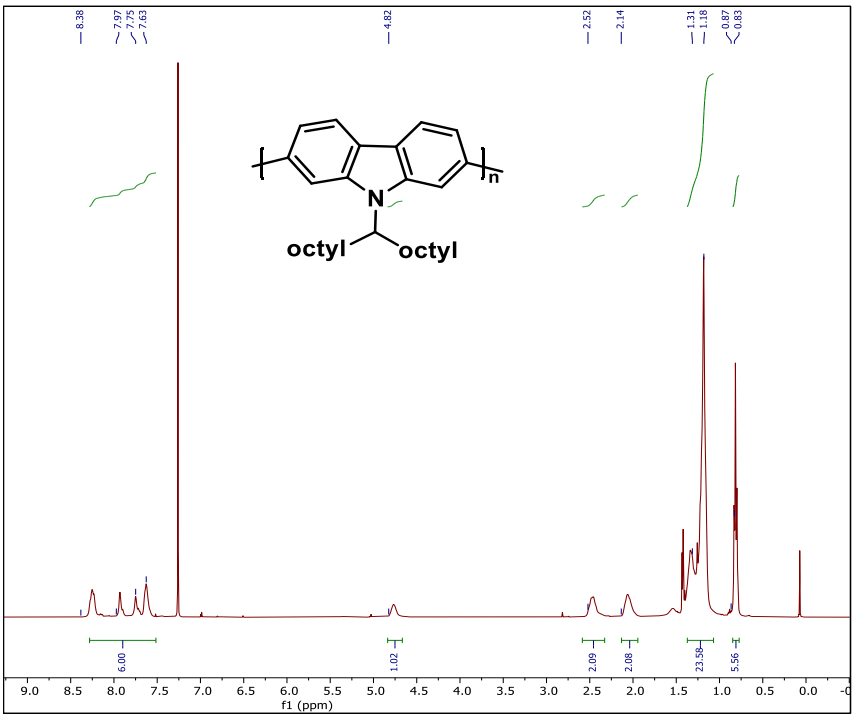

^{1}H NMR of PSiF

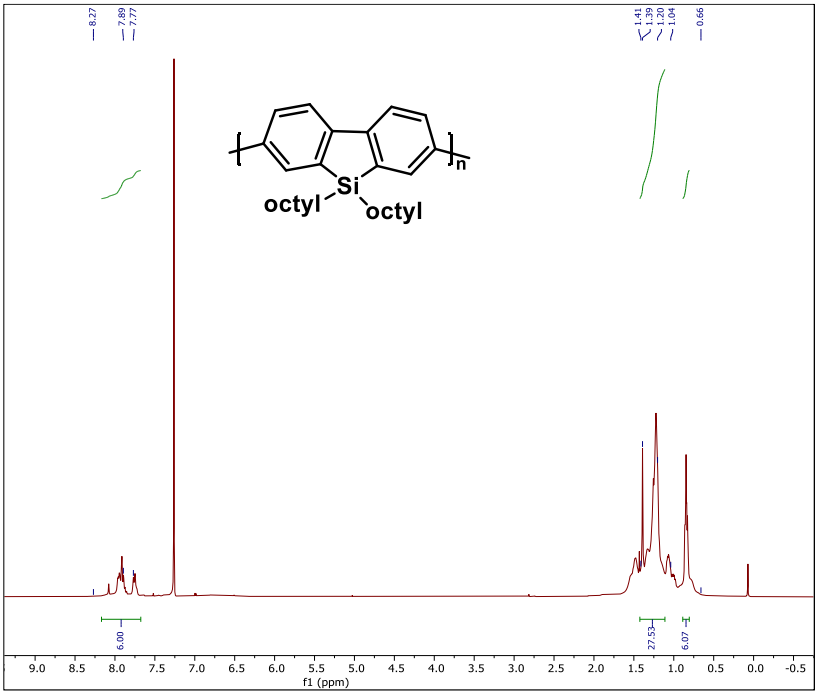

^{1}H NMR of PIDTT

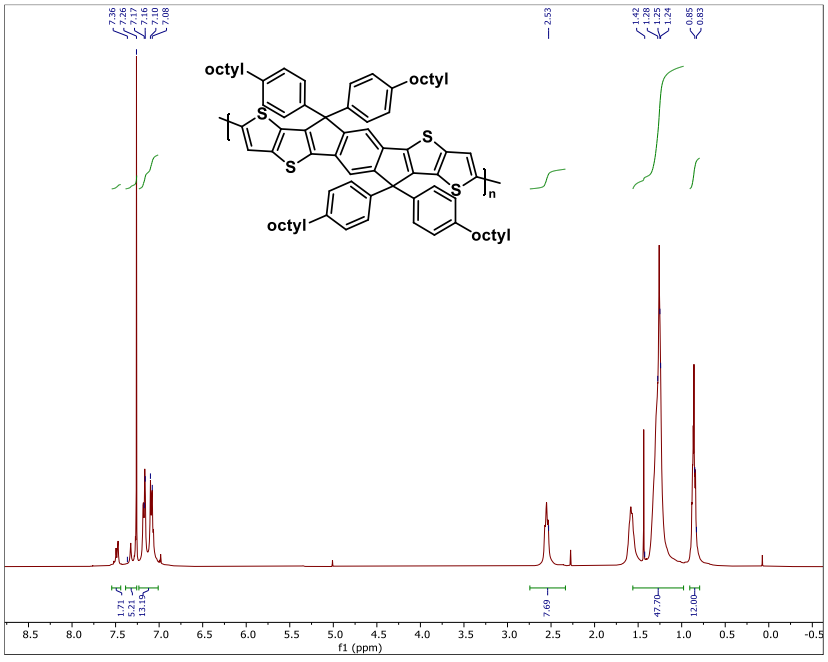

CHAPTER V

MECHANOCHEMICAL APPROACH TOWARDS SYNTHESIS OF POLYFLUORENE-*CO*-BENZOTHIADIAZOLE VIA SUZUKI CROSS COUPLING POLYMERIZATION

5.1 INTRODUCTION

'Mechanochemistry' refers to reactions, where solid state transformations occur, induced by the input of mechanical energy, such as by grinding in ball mills (Figure 5.1).[62] In 2019, the International Union of Pure and Applied Chemistry (IUPAC) identified mechanochemistry as one of 10 world-changing technologies.[142] Recently, the ball milling process has attracted considerable attention as it can provide efficient and environmentally-friendly (green and sustainable) alternatives to solution-based reactions.[143]

In the recent past, the impact of mechanochemistry in organic synthesis has been recognized and many organic transformations have been demonstrated in the literature. The utility of the mechanochemistry include amide couplings,[65] Wittig reactions,[66-67], and metal-catalyzed cross-coupling reactions.[68] These mechanochemical reactions provide advantages: consumed less energy, reacted more rapidly, required no solvent , and significantly reduced the amount of waste produced.[62]

Solvent-free syntheses of polymers under ball milling has blossomed in recent years,[76,78-79,144-146] but only a few approaches towards mechanochemical conjugated polymer syntheses have been undertaken.[76,78-79,146] Specifically, mechanochemical cross-coupling polymerization reactions have been relatively unexplored.[73,77]

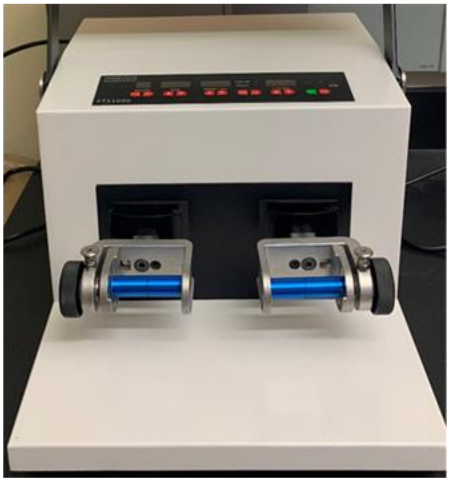

Figure 5.1: Representative ball mill

Fluorene-based π conjugated polymers have emerged as excellent materials for organic electronics.[147-150] Polyfluorene-based materials possess many desirable properties, such as high quantum yields, good film-forming, and hole-transporting properties.[150] The electronic properties of fluorene can be tuned by incorporating an electron-deficient monomer into the polymer backbone.[151-152] For this purpose, benzothiadiazole (BT) has been extensively used.[153-154] The incorporation of BT units into the polymer main chain allows the color tuning to the green region in the visible spectra. The polymer possessed high electron affinity and preferential electron transport properties compared to those of the polyfluorene homopolymers.[154] In this chapter, our approaches towards solid-state synthesis of polyfluorene-*co*-benzothiadiazole in the ball mill will be discussed.

5.2 RESULTS AND DISCUSSION

In our initial attempts at the solid-state synthesis of polyfluorene-*co*-benzothiadiazole (PFBT), promoted by ball milling, the monomers (9,9-dioctylfluorene-2,7-diboronic acid, 4,7-dibromobenzo[*c*]-1,2,5-thiadiazole), 10 mol% of $Pd(OAc)_2$, and 8 equivalents of K_2CO_3 were added to stainless steel (SS) milling jars along with the SS balls (Scheme 5.1). The solid reaction mixture was subjected to vibrational milling for 30 min in the high-speed ball milling (HSBM). After the milling time, the reaction was quenched by adding methanol (5 mL) to the jars which were then shaking manually for 30 seconds. The resulted slurry was precipitated in methanol, followed by filtering and washing the precipitate with methanol, acetone, and chloroform. The structural properties were characterized by ^1H NMR analysis and gel permeation chromatography (GPC).

Scheme 5.1: Mechanochemical synthesis of PFBT via Suzuki cross-coupling polymerization.

Table 5.1: Effect of varying frequency on isolated yield and number average molecular weight.

Entry	Frequency (rpm)	% Yield	M_n[a] (Da)	Đ[a]
1	1800	18	1771	1.38
2	1500	25	2192	1.36
3	1000	20	1802	1.38
4	600	50	2653	1.64

[a] Determined by GPC in THF using polystyrene standards.
Đ = polydispersity index

First, we conducted a series of solid-state polymerizations with varying milling frequencies (Table 5.1) using 10 mol% of $Pd(OAc)_2$ and 8 equivalents of K_2CO_3 (Scheme 5.1). For the above data, isolated yields and number average molecular weights (M_n) were obtained on the polymer after

manual washing with methanol, acetone, and chloroform. (In our preliminary studies our objective was to see whether there was a significant effect on yield and number average molecular weight by varying the vibrational frequency). Manual purification was done, where the polymer was filtered through a cellulose thimble and the solvents were manually poured through the thimble. This normally results in low M_n values compared to Soxhlet purification. As shown in Table 5.1, the M_n values and the yields were almost the same under the applied vibrational frequencies, except at 600 rpm, in which slight increase in the yield was obtained.

Table 5.2: Effect of K_2CO_3 loading on synthesis on PFBT in the ball mill.

Entry	**$Pd(OAc)_2$ (mol %)**	**K_2CO_3 (eq)**	**% Yield**	**M_n[a] (Da)**	**Đ[a]**
1	10	4	13	4939	1.3
2	10	8	25	5640	1.4
3	10	16	21	5556	1.4

[a] Determined by GPC in THF using polystyrene standards.

Compared to solution-based reactions, the solid-state nature of this method results in a high concentration of monomers.[78] Solid-state dilution of the monomers can be achieved by the addition of base.[78] Therefore, efforts were directed towards varying K_2CO_3 loading. As shown in Table 5.2, the reactions were carried out using 4 eq, 8 eq, and 16 eq of K_2CO_3 at 600 rpm for 30 min. (Note: the isolated yields M_n values were obtained after Soxhlet purification). Under the conditions applied, no significant differences were observed in the isolated yields or number average molecular weights. Furthermore, we tested Li_2CO_3, Na_2CO_3, and Cs_2CO_3 as bases for our solid-state synthesis of PFBT. No polymerizations were observed with these bases.

Table 5.3: Comparison of solid-state synthesis of PFBT promoted by BM and solution-state synthesis of PFBT and effect of Pd catalyst.

Entry	Catalyst (10 mol %)	Base (8eq)	Reaction media	Time	% Yield	M_n[a] (Da)	Đ[a]
1	$Pd(OAc)_2$	K_2CO_3	HSBM (600 rpm), RT	30 min	25	5640	1.4
2	$Pd(OAc)_2$	K_2CO_3	THF: Water reflux	48 h	43	2639	1.5
3	$Pd(PPh_3)_4$	K_2CO_3	HSBM (600 rpm)	30 min	5	5772	1.4
4	$Pd(PPh_3)_4$	K_2CO_3	THF: Water reflux	48 h	46	8477	2.8

[a] Determined by GPC in THF using polystyrene standards.

Next, we compared our solid-state Suzuki polymerization of PFBT with that of the solution-based Suzuki polymerization method. The results are summarized in Table 5.3. Based on the recent literature for the mechanochemical polymerization,[77, 78] the milling time was limited to 30 min. Since typical polymerization reactions in solution-state utilized a reaction time of 48 h, we carried out the wet reactions for 48 h. As shown in Table 5.3, entries 1 and 2, $Pd(OAc)_2$ was used as the catalyst. Under the conditions applied, a higher M_n value was obtained via the ball milling product compared to that of solution-state synthesis. In contrast, the isolated yield of polymer was relatively low in the solid-state reaction. We changed the catalyst to $Pd(PPh_3)_4$, and the polymerization was carried out in both solid and solution states under argon. (Table 5.3, entries 3-4). The isolated yield of ball milling product was dramatically decreased compared to entry 1. However, the M_n values remained almost the same in both reactions. In contrast, under the conditions we have used (Table 5.3), in the presence of $Pd(PPh_3)_4$, the solution state polymerization resulted in an increased M_n value compared to that of entry 2, where the isolated yield remained almost the same in entries 2 and 4.

To further optimize the ball milling methodology, milling times were varied. A series of polymerization reactions were performed for 60 min, 30 min, 15 min, 5 min, and 1 min at 600 rpm (which is the lowest vibrational frequency in our instrument).

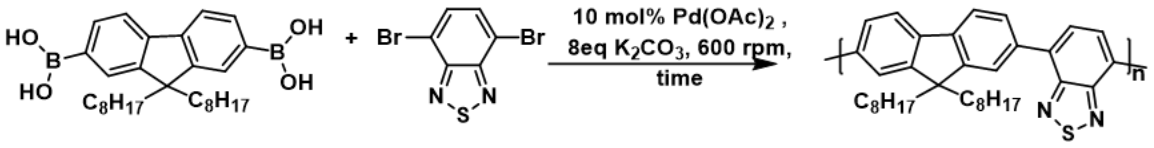

Scheme 5.2: Effect of varying milling time on isolated yield and number average molecular weight.

Table 5.4: Effect of varying milling time on isolated yield and number average molecular weight.

Entry	Time (min)	% Yield	M_n[a]	Đ[a]
1	60	27	5381	1.5
2	30	25	5640	1.4
3	15	24	5791	1.7
4	5	40	7350	1.7
5	1	36	7360	1.7

[a] Determined by GPC in THF using polystyrene standards.
Đ = polydispersity index

As mentioned above, for our initial optimizations the reactions were carried out for 30 min. As shown in Table 5.4, Entry 1, the reaction time was extended to 1 h, under the conditions used (Scheme 5.2) no significant improvement in isolated yield or number average molecular weight occurred. We probed the reaction conditions by lowering the milling time. As shown in Table 5.4, no significant improvement was observed when lowering the time from 30 min to 15 min. Surprisingly, further lowering the reaction time from 15 min to 5 min, a significant improvement in yield and number average molecular weight occurred. However, when the reaction proceeded for 1 min, a slight lowering of the yield was observed. According to the above data, under the reaction conditions shown in Scheme 5.4, the solid-state synthesis of PFBT promoted by ball

milling (via Suzuki cross-coupling polymerization) occurred as fast as 5 min with reasonable number average molecular weight. However, the yield obtained was low (40%). With an optimized time in hand, we will further explore the reaction at higher frequencies to investigate whether lower reaction times at higher frequencies facilitate the polymerization.

5.3 CONCLUSION

In this chapter, we have demonstrated simple, rapid, and solvent-free (green) methodology towards the synthesis of PFBT (via Suzuki cross-coupling polymerization) promoted by BM. We explored the influence of different parameters on the reaction and observed that the polymerization in BM is a rapid process. Based on the optimizations so far, we could obtain the desired polymer with a reasonable number of average molecular weight in as little as five minutes. With this optimized time in hand, further studies will be carried out to get a higher yield.

5.4 EXPERIMENTAL

5.4.1 Materials

9,9-Dioctylfluorene-2,7-diboronic acid and 4,7-dibromobenzo[*c*]-1,2,5-thiadiazole, and $Pd(OAc)_2$ were purchased from Sigma Aldrich. K_2CO_3 was purchased from Acros. All the reagents were used as received. When needed, THF was obtained from a solvent purification system under ultra-pure argon. Water was degassed under Argon. All the other solvents were used as received.

5.4.2 Instrumentation

The ball-milling experiments were carried out in FORM-TECH Scientific (FTS-100) instrument (65 Rue Saint-Paul Ouest, Unit 407,Montreal, (QC) H2Y 3S5 Canada). The ^1H NMR spectra were measured on a Bruker Avance 400 MHz instrument. Number average molecular weight (M_n) and polydispersity (Đ) were determined by gel permeation chromatography (GPC) using a Waters pump with a Waters 2410 refractive index detector. THF was used as an eluent at 35 °C with a

flow rate of 1.0 mL min^{-1}. The instrument was calibrated with polystyrene standards, and data were analyzed using Breeze software.

5.4.3 Synthesis

General experimental procedure for the synthesis of PFBT via solid-state Suzuki polymerization in the ball mill (5.4.3.1): To a stainless steel (SS) milling jar (5 mL) were added 9,9-dioctylfluorene-2,7-diboronic acid (100 mg, 0.209 mmol), 4,7-dibromobenzo[*c*]-1,2,5-thiadiazole (61.5 mg, 0.209 mmol), $Pd(OAc)_2$ (5.0 mg, 0.029 mmol) and K_2CO_3 (231 mg, 1.672 mmol) followed by SS balls (5 mm, 4 balls). The vial was sealed and placed in the vibrational ball mill and subjected to milling for 30 min at 600 rpm. After an allotted time, methanol (5 mL) was added to the jar which was shacken manually for 30 sec. The product was precipitated in methanol and the mixture was poured through a cellulose thimble and subjected to Soxhlet extraction with methanol, acetone, and chloroform. The chloroform extraction was solvent evaporated to obtain a dark brown color solid. Yield (28 mg, 25%). ^1H NMR (400 MHz, $CDCl_3$): δ 8.11-7.68 (b, 8H), 1.29-0.78 (b, 28H). M_n = 5640 Da, Đ =1.4.

Synthesis of PFBT via solution-state Suzuki polymerization: In an oven-dried (10 mL) Schlenk flask (equipped with a stir bar) were placed dioctylfluorene-2,7-diboronic acid (100 mg, 0.209 mmol), 4,7-dibromobenzo[*c*]-1,2,5-thiadiazole (61.5 mg, 0.209 mmol), $Pd(PPh_3)_4$ (24 mg, 0.0209 mmol) and K_2CO_3 (231 mg, 1.672 mmol) inside a glove box. A condenser was connected to the flask and sealed with a rubber septum. The apparatus was taken out of the glove box, and THF (4 mL) and degassed water (4 mL) was added. The reaction was refluxed for 48 h under an argon environment. The reaction mixture was added to 6 N HCl (15 mL), and the mixture was extracted with $CHCl_3$. The $CHCl_3$ fractions were combined and the solvent was evaporated. The product was precipitated in methanol and filtered through a cellulose thimble. Soxhlet extraction was done

with methanol, acetone, and chloroform to yield a brown-yellow solid. 46 % yield. ^{1}H NMR (400 MHz, $CDCl_3$): δ 8.11-7.68 (b, 8H), 1.29-0.78 (b, 28H). M_n = 8477 Da, Đ = 2.8.

5.4.4 Spectra

^{1}H NMR of solid-state synthesis of PFBT in ball mill

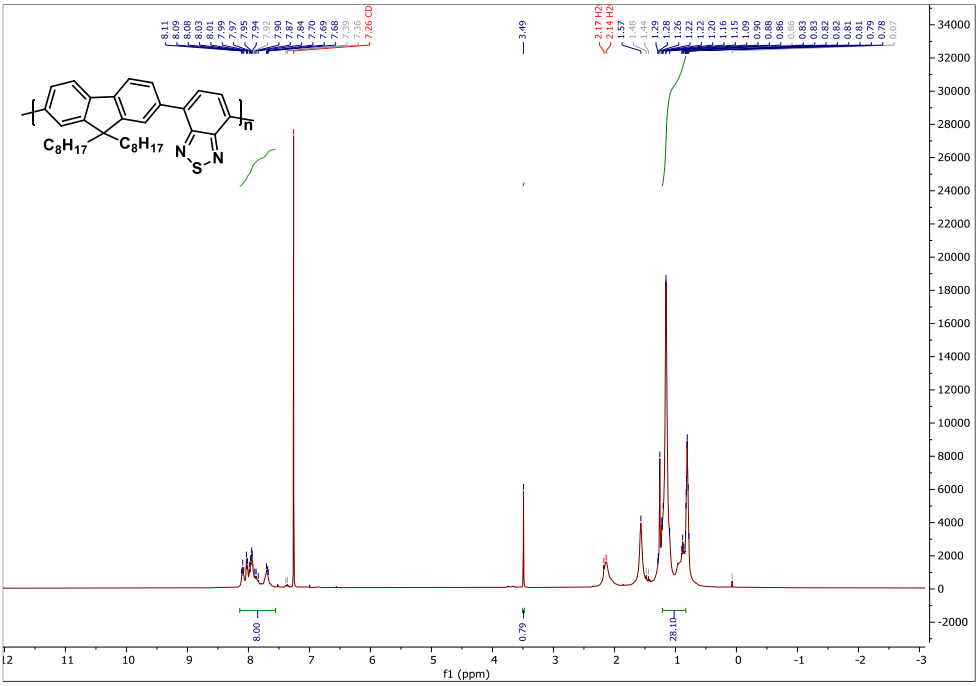

^{1}H NMR of solution-state synthesis of PFBT

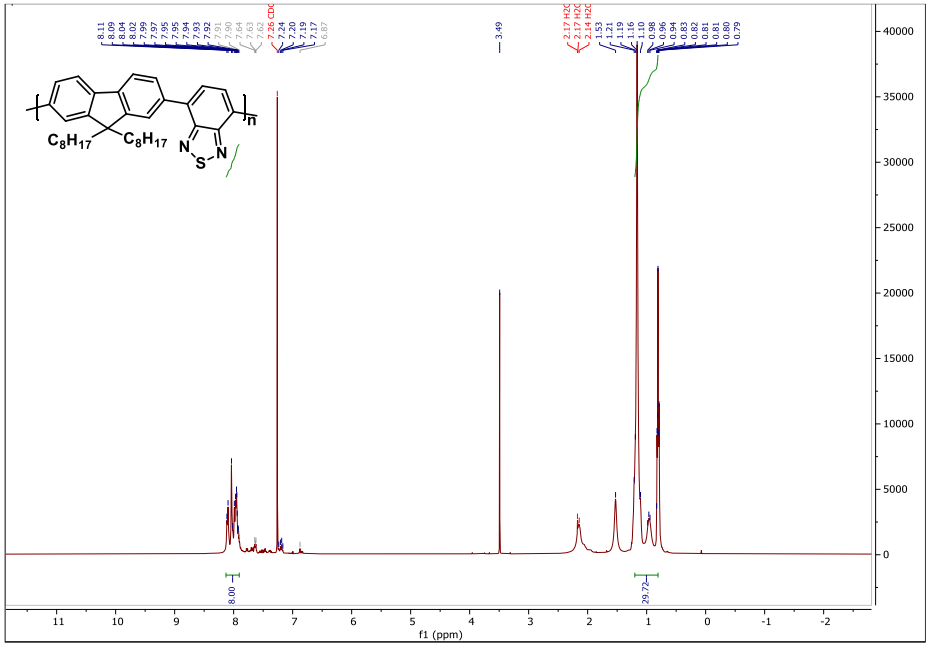

CHAPTER VI

CONCLUSIONS AND FUTURE DIRECTIONS

6.1 INTRODUCTION

In this chapter, I have summarized my projects and included some future directions.

6.2 CHAPTER 2: CONCLUSION AND FUTURE DIRECTIONS

Our research group developed a methodology towards copper-mediated, regioselective C-H direct arylation of benzodithiophene-S,S-tetraoxide (BDTT).[86] In this chapter, the mechanistic insight of this methodology and further utilization were discussed. The detailed experimental and theoretical studies showed that the base (K_3PO_4) and additive (Ag_2CO_3) have important role in the reaction.[97] We utilized this methodology towards C-H direct arylation polymerization. Current reaction conditions resulted in low molecular weight oligomers. To obtain high molecular weight polymers, future optimizations will be carried out by probing the use of CuI, K_3PO_4, and Ag_2CO_3. Furthermore, instead of DMF, greener and sustainable solvents, such as γ-valerolactone, 2-methyltetrahydrofuran, and cyclopentyl methyl ether will be used.[27]

Moreover, utilizing 2,6-diiodinated BDTT, BDTT-based novel donor-acceptor conjugated polymers (PBDTT-C, PBDTT-SiF, and PBDTT-IDTT) were synthesized via a Suzuki polycondensation. Under the current reaction conditions used for the synthesis of PBDTT-IDTT, low number average molecular weight (3 kDa) and low yield (16%) were obtained. The reaction conditions will be optimized to improve the yield and number average molecular weight. Furthermore, characterization of the polymers should be conducted for the optical, electronic, and physical properties.

6.3 CHAPTER 3: CONCLUSION AND FUTURE DIRECTIONS

In chapter 3, we synthesized poly(2,5-dialkoxy-1,4-phenylenediethynylene)s using a Cu_2O nanoparticle-mediated polymerization under ligand-free conditions and in air as oxidant via a Glaser polymerization. Compared to a dodecyloxy analog, incorporation of branched 2-ethylhexoxy side chains improved the solubility of the resulted polymer. Hence, higher molecular weights were obtained. The polymerizations were carried out using DMF as the solvent at 110 °C for 48 h. In the future, this polymerization reaction can be conducted in the ball mill under solvent-free grinding or solvent assisted grinding (adding a catalytic amount of solvent). Moreover, mechanochemical polymerization is faster than solution-state polymerization. Based on the previous literature from Andiappan and co-workers,[123] and the UV-vis extinction spectroscopy and ESI-MS data obtained from the polymerization reactions, we proposed this polymerization reaction might undergo via a homogeneous catalytic pathway. However, if the reaction is performed in the solid-state, the catalytic pathway might be different from the solution state and the process can be analyzed using UV-vis extinction spectroscopy and ESI-MS.

6.4 CHAPTER 4: CONCLUSION AND FUTURE DIRECTIONS

In Chapter 4, conjugated homopolymers, polyfluorene, polycarbazole, polysilafluorene, and poly 6,6,12,12-tetrakis(4-hexylphenyl)-6,12-dihydro-dithieno[2,3-*d*:2',3'-*d*']-*s*-indaceno[1,2-*b*:6,6-

b']dithiophene were synthesized under benchtop conditions (room temperature, open to air) via Pd/Cu co-catalysis. These polymerizations were carried out in DMSO for 48 h. In the future, these reactions can be synthesized in a more greener way under solvent-free conditions in a ball mill.

6.5 CHAPTER 5: CONCLUSION AND FUTURE DIRECTIONS

In chapter 5, polyfluorene-*co*-benzothiadiazole (PFBT) was synthesized under solvent-free conditions promoted by ball milling via a Sonogashira cross-coupling polymerization using 9,9-dioctylfluorene-2,7-diboronic acid and 4,7-dibromobenzo[*c*]-1,2,5-thiadiazole as the monomers. We have examined several parameters, such as the effect of vibrational frequency, base (K_2CO_3) loadings, catalysts, and milling time on the polymer yield and number average molecular weight. Based on the results, the polymerization occurred in five minutes at 600 rpm with a reasonable number average molecular weight (7.3 kDa), however in low yield (40%). Previous literature emphasized that the use of a mechanochemical Suzuki-Miyara reaction significantly improved the yield in the presence of liquid additive (liquid assisted grinding).[63] Ananikov and co-workers showed water can play a crucial role in the solid-state Suzuki cross-coupling reaction.[155] In the future, this reaction will be performed with liquid assisted grinding using water as an additive. Furthermore, optimizations will be carried out by changing the kinetic energy of the reaction via varying the sizes of the balls and the number of balls. With the optimized conditions in hand, high performing donor-acceptor conjugated polymers will be synthesized via mechanochemical Suzuki cross-coupling polymerization. Further, band-gap of the resulting polymer can be highly tuned by incorporating a thiophene ring into the benzothiodiazole unit.[156-158] In the future, a copolymer based on fluorene-*co*-thienylbenzothiadiazole can be synthesized via a solid-state Suzuki cross-coupling polymerization in the ball mill (Scheme 6.1).

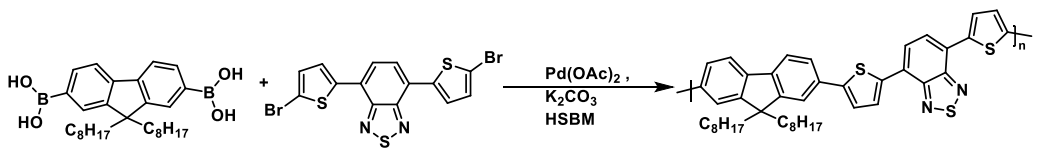

Scheme 6.1: Synthesis of polyfluorene-*co*-thienylbenzothiadiazole in the ball mill.

REFERENCES

1. Myers, J. D.; Xue, J., *Polym Rev*. **2012,** *52*, 1-37.

2. Zhao, X.; Chaudhry, S. T.; Mei, J., In Advances in Heterocyclic Chemistry, Scriven, E. F. V.; Ramsden, C. A., Eds. Academic Press: chapter 1, Amsterdam, 2017,121, 133-171.

3. Rockett, A., The Materials Science of Semiconductors: chapter 9, Berlin, 2008; p 395-453.

4. Xu, R.-P.; Li, Y.-Q.; Tang, J.-X., *J. Mater. Chem.* ***2016,*** *4*, 9116-9142.

5. Burroughes, J. H.; Bradley, D. D. C.; Brown, A. R.; Marks, R. N.; Mackay, K.; Friend, R. H.; Burns, P. L.; Holmes, A. B., *Nature* **1990,** 347, 539-541.

6. Cheng, Y.-J.; Yang, S.-H.; Hsu, C.-S., *Chem. Rev*. **2009,** 109, 5868-5923.

7. Hedley, G. J.; Ruseckas, A.; Samuel, I. D. W.,*Chem. Rev.* **2017,** 117, 796-837.

8. Torsi, L.; Magliulo, M.; Manoli, K.; Palazzo, G., *Chem. Soc. Rev.* **2013,** 42, 8612-8628.

9. McQuade, D. T.; Pullen, A. E.; Swager, T. M., *Chem. Rev.* **2000,** *100*, 2537-2574.

10. Introduction to the Hybridizatio https://www.chemistrysteps.com/sp3-sp2-and-sp-hybridization-organic-chemistry/ (Accessed 7/11/2020)

11. Li, G.; Chang, W.-H.; Yang, Y., *Nat. Rev. Mater.* **2017,** 2, 17043.

12. Kim, S. H.; Jang, J.; Lee, J. Y., *Appl. Phys. Lett*.**2007,** 90, 223505.

13. Wu, S.; Li, S.; Sun, Q.; Huang, C.; Fung, M.-K., *Sci. Rep.* **2016,** *6*, 25821.

14. Du, L.; Luo, X.; Wen, Z.; Zhang, J.; Sun, L.; Lv, W.; Li, Y.; Zhao, F.; Zhong, J.; Ren, Q.; Huang, F.; Xia, H.; Peng, Y., *J. Phys. D: Appl. Phys.* **2015,** 48, 405105.

15. Yi, M.; Guo, J.; Li, W.; Xie, L.; Fan, Q.; Huang, W., *RSC Advances* **2015,** *5*, 95273-95279.

16. See reference 3

17. Facchetti, A., *Chem. Mater.* **2011,** 23, 733-758.

18. Bunz, U. H., *Chem. Rev.* **2000,** 100, 1605-44.

19. Shan, B.; Miao, Q., *Tetrahedron Lett.* **2017,** 58, 1903-1911.

20. Ando, S.; Nishida, J.-i.; Fujiwara, E.; Tada, H.; Inoue, Y.; Tokito, S.; Yamashita, Y., *Chem. Mater.* **2005,** 17, 1261-1264.

21. Schwarze, M.; Tress, W.; Beyer, B.; Gao, F.; Scholz, R.; Poelking, C.; Ortstein, K.; Günther, A. A.; Kasemann, D.; Andrienko, D.; Leo, K., *Science* **2016,** 352, 1446.

22. Quinn, J. T. E.; Zhu, J.; Li, X.; Wang, J.; Li, Y., *J. Mater. Chem. C.* **2017,** 5, 8654-8681.

23. Burke, D. J.; Lipomi, D. J., *Energy Environ. Sci.* **2013,** *6*, 2053-2066.

24. Ragan, J. A.; Raggon, J. W.; Hill, P. D.; Jones, B. P.; McDermott, R. E.; Munchhof, M. J.; Marx, M. A.; Casavant, J. M.; Cooper, B. A.; Doty, J. L.; Lu, Y., *Org Process Res Dev*. **2003,** 7, 676-683.

25. Leclerc. M, Morin. J.F, Suzuki Polycondensation. Synthetic Methods for Conjugated Polymers and Carbon Materials: chapter 2, Hoboken, 2017; 59-95.

26. Chinchilla, R.; Nájera, C., *Chem. Soc. Rev.* **2011,** 40, 5084-5121.

27. Phan, S.; Luscombe, C. K., *Trends Chem.* **2019,** 1, 670-681.

28. Kharissova, O. V.; Kharisov, B. I.; González, C. M. O.; Méndez, Y. P.; López, I., *R. Soc. Open Sci*. **2019,** *6*, 191378.

29. Rudenko, A. E.; Thompson, B. C., *J. Polym. Sci. A Polym. Chem.* **2015,** 53, 135-147.

30. Mercier, L. G.; Leclerc, M., *Acc. Chem. Res.* **2013,** 46, 1597-1605.

31. Marrocchi, A.; Facchetti, A.; Lanari, D.; Petrucci, C.; Vaccaro, L., *Energy Environ. Sci.* **2016,** 9, 763-786.

32. Berrouard, P.; Najari, A.; Pron, A.; Gendron, D.; Morin, P.-O.; Pouliot, J.-R.; Veilleux, J.; Leclerc, M., *Angew Chem Int Ed Engl.* **2012,** 51, 2068-2071.

33. Pouliot, J.-R.; Mercier, L. G.; Caron, S.; Leclerc, M., *Macromol. Chem. Phys.***2013,** *214*, 453-457.

34. Wang, Q.; Takita, R.; Kikuzaki, Y.; Ozawa, F., *J. Am. Chem. Soc.* **2010,** 132, 11420-11421.

35. Wakioka, M.; Kitano, Y.; Ozawa, F., *Macromolecules* **2013,** 46, 370-374.

36. Lu, W.; Kuwabara, J.; Kanbara, T., *Macromolecules* **2011,** 44, 1252-1255.

37. Pankow, R. M.; Ye, L.; Thompson, B. C., *ACS Macro Lett.* **2018,** 7, 1232-1236.

38. Ye, L.; Pankow, R. M.; Schmitt, A.; Thompson, B. C., *Polym. Chem.* **2019,** 10, 6545-6550.

39. Bannock, J. H.; Xu, W.; Baïssas, T.; Heeney, M.; de Mello, J. C., *Eur. Polym. J.* **2016,** *80*, 240-246.

40. Pankow, R. M.; Ye, L.; Thompson, B. C., *Polym. Chem.* **2019,** 10, 4561-4572.

41. Pankow, R. M.; Thompson, B. C., *Polym. Chem.* **2020,** 11, 630-640.

42. Pankow, R. M.; Ye, L.; Gobalasingham, N. S.; Salami, N.; Samal, S.; Thompson, B. C., *Polym. Chem.* **2018,** 9, 3885-3892.

43. Beydoun, K.; Doucet, H., *ChemSusChem.* **2011,** 4, 526-534.

44. Goto, E.; Nakamura, S.; Kawauchi, S.; Mori, H.; Ueda, M.; Higashihara, T., *J. Polym. Sci. A Polym. Chem* .**2014,** *52* (16), 2287-2296.

45. Qiu, Y.; Worch, J. C.; Fortney, A.; Gayathri, C.; Gil, R. R.; Noonan, K. J. T., *Macromolecules.* **2016,** 49, 4757-4762.

46. Pankow, R. M.; Ye, L.; Thompson, B. C., *Polym. Chem.* **2018,** 9, 4120-4124.

47. Christopherson, C. J.; Hackett, Z. S.; Sauvé, E. R.; Paisley, N. R.; Tonge, C. M.; Mayder, D. M.; Hudson, Z. M., *J. Polym. Sci. A Polym. Chem* **2018,** 56, 2539-2546.

48. Guan, J.; Daljeet, R.; Kieran, A.; Song, Y., J. *Condens. Matter Phys.* **2018,** 30, 224004.

49. Al-Hossainy, A. F.; Kh. Thabet, H.; Zoromba, M. S.; Ibrahim, A., *New J Chem.* **2018,** 42, 10386-10395.

50. Ichige, A.; Saito, H.; Kuwabara, J.; Yasuda, T.; Choi, J.-C.; Kanbara, T., *Macromolecules.* **2018,** 51, 6782-6788.

51. Faradhiyani, A.; Zhang, Q.; Maruyama, K.; Kuwabara, J.; Yasuda, T.; Kanbara, T., *Mater. Chem. Front.* **2018,** 2, 1306-1309.

52. Hoogenboom, R.; Schubert, U. S., *Macromol. Rapid Commun.* **2007,** 28, 368-386.

53. Kappe, C. O., *Angew. Chem. Int. Ed.***2004,** 43, 6250-6284.

54. de la Hoz, A.; Díaz-Ortiz, Á.; Moreno, A., *Chem. Soc. Rev.* **2005,** 34, 164-178.

55. Dallinger, D.; Kappe, C. O., *Chem. Rev.* **2007,** 107, 2563-2591.

56. Roberts, B. A.; Strauss, C. R., *Acc. Chem. Res.* **2005,** 38, 653-661.

57. Galbrecht, F.; Bünnagel, T. W.; Scherf, U.; Farrell, T., *Macromol. Rapid Commun.* **2007,** 28, 387-394.

58. Ebner, C.; Bodner, T.; Stelzer, F.; Wiesbrock, F., *Macromol. Rapid Commun.* **2011,** 32, 254-288.

59. Nehls, B. S.; Asawapirom, U.; Füldner, S.; Preis, E.; Farrell, T.; Scherf, U., *Adv. Funct. Mater*. **2004,** 14, 352-356.

60. Tierney, S.; Heeney, M.; McCulloch, I., *Synth. Met.* **2005,** 148, 195-198.

61. Jessop, P. G., *Green Chem.* **2011,** 13, 1391-1398.

62. James, S. L.; Adams, C. J.; Bolm, C.; Braga, D.; Collier, P.; Friščić, T.; Grepioni, F.; Harris, K. D. M.; Hyett, G.; Jones, W.; Krebs, A.; Mack, J.; Maini, L.; Orpen, A. G.; Parkin, I. P.; Shearouse, W. C.; Steed, J. W.; Waddell, D. C., *Chem. Soc. Rev.* **2012,** 41, 413-447.

63. Porcheddu, A.; Colacino, E.; De Luca, L.; Delogu, F., *ACS Catal.* **2020,** *10*, 8344-8394.

64. Andersen, J.; Mack, J., *Green Chem.* **2018,** 20, 1435-1443.

65. Declerck, V.; Nun, P.; Martinez, J.; Lamaty, F., *Angew. Chem. Int. Ed.* **2009,** 48, 9318-9321.

66. Balema, V. P.; Wiench, J. W.; Pruski, M.; Pecharsky, V. K., *Chem.Comm* **2002,** 7, 724-725.

67. Balema, V. P.; Wiench, J. W.; Pruski, M.; Pecharsky, V. K., *J. Am. Chem. Soc.***2002,** 124, 6244-6245.

68. Wang, G.-W., *Chem.Soc. Rev.* **2013,** 42, 7668-7700.

69. Thorwirth, R.; Stolle, A.; Ondruschka, B., *Green Chem.* **2010,** 12, 985-991.

70. Seo, T.; Ishiyama, T.; Kubota, K.; Ito, H., *Chem. Sci.* **2019,** 10, 8202-8210.

71. Kubota, K.; Seo, T.; Koide, K.; Hasegawa, Y.; Ito, H., *Nat. Commun.* **2019,** *10*, 111.

72. Yu, J.; Yang, X.; Wu, C.; Su, W., *J. Org. Chem.* **2020,** 85, 1009-1021.

73. Vogt, C. G.; Grätz, S.; Lukin, S.; Halasz, I.; Etter, M.; Evans, J. D.; Borchardt, L., *Angew. Chem. Int. Ed.* **2019,** 58, 18942-18947.

74. Lee, G. S.; Moon, B. R.; Jeong, H.; Shin, J.; Kim, J. G., *Polym.Chem.* **2019,** 10, 539-545.

75. Wang, Z.; Ayarza, J.; Esser-Kahn, A. P., *Angew. Chem. Int. Ed.* **2019,** *58*, 12023-12026.

76. Grätz, S.; Borchardt, L., *RSC Adv.* **2016,** 6, 64799-64802.

77. Grätz, S.; Wolfrum, B.; Borchardt, L., *Green Chem.* **2017,** 19, 2973-2979.

78. Ravnsbæk, J. B.; Swager, T. M., *ACS Macro Lett.* **2014,** 3, 305-309.

79. Cho, H. Y.; Bielawski, C. W., *Angew. Chem. Int. Ed.* **2020,** *59* (33), 13929-13935.

80. Ahmed, E.; Subramaniyan, S.; Kim, F. S.; Xin, H.; Jenekhe, S. A., *Macromolecules.* **2011,** 44, 7207-7219.

81. Bhuwalka, A.; Mike, J. F.; He, M.; Intemann, J. J.; Nelson, T.; Ewan, M. D.; Roggers, R. A.; Lin, Z.; Jeffries-El, M., *Macromolecules.* **2011,** 44, 9611-9617.

82. Zhou, J.; Zuo, Y.; Wan, X.; Long, G.; Zhang, Q.; Ni, W.; Liu, Y.; Li, Z.; He, G.; Li, C.; Kan, B.; Li, M.; Chen, Y., *J.Am.Chem.Soc.***2013,** 135, 8484-8487.

83. Chavez Iii, R.; Cai, M.; Tlach, B.; Wheeler, D. L.; Kaudal, R.; Tsyrenova, A.; Tomlinson, A. L.; Shinar, R.; Shinar, J.; Jeffries-El, M., *J. Mater. Chem. C.* **2016,** 4 , 3765-3773.

84. Nandakumar, M.; Karunakaran, J.; Mohanakrishnan, A. K., *Org. Lett.* **2014,** *16*, 3068-3071.

85. Pappenfus, T. M.; Seidenkranz, D. T.; Lovander, M. D.; Beck, T. L.; Karels, B. J.; Ogawa, K.; Janzen, D. E., *J. Org. Chem.* **2014,** 79, 9408-9412.

86. Khambhati, D. P.; Sachinthani, K. A. N.; Rheingold, A. L.; Nelson, T. L., *Chem.Comm.* **2017,** 53, 5107-5109.

87. Su, W.-F., Step Polymerization. Principles of Polymer Design and Synthesis. Berlin, Heidelberg, Springer Berlin Heidelberg**,** 2013111-136.

88. Jung, I. H.; Lo, W.-Y.; Jang, J.; Chen, W.; Zhao, D.; Landry, E. S.; Lu, L.; Talapin, D. V.; Yu, L., *Chem. Mater.* **2014,** 26, 3450-3459.

89. Zhen, S.; Wang, S.; Li, S.; Luo, W.; Gao, M.; Ng, L. G.; Goh, C. C.; Qin, A.; Zhao, Z.; Liu, B.; Tang, B. Z., *Adv. Funct. Mater.* **2018,** 28, 1706945.

90. Lei, T.; Peng, R.; Fan, X.; Wei, Q.; Liu, Z.; Guan, Q.; Song, W.; Hong, L.; Huang, J.; Yang, R.; Ge, Z., *Macromolecules* **2018,** 51, 4032-4039.

91. Santosh Adhikari, Y. X. R., Mihaela C. Stefan, and Toby L. Nelson., C-H Functionalization Approach to the Synthesis of Benzodithiophene-S,S-Tetraoxide-Based Polymer Acceptors *Polym. Chem*. 2020.

92. Kowalski, S.; Allard, S.; Scherf, U., *ACS Macro Lett.* **2012,** 1, 465-468.

93. Zhao, H.; Liu, C.-Y.; Luo, S.-C.; Zhu, B.; Wang, T.-H.; Hsu, H.-F.; Yu, H.-h., *Macromolecules.* **2012,** *45* (19), 7783-7790.

94. Culver, E. W.; Anderson, T. E.; López Navarrete, J. T.; Ruiz Delgado, M. C.; Rasmussen, S. C., *ACS Macro Lett.* **2018,** 7, 1215-1219.

95. Berrouard, P.; Najari, A.; Pron, A.; Gendron, D.; Morin, P.-O.; Pouliot, J.-R.; Veilleux, J.; Leclerc, M., *Angew. Chem. Int. Ed.***2012,** 51, 2068-2071.

96. Punzi, A.; Capozzi, M. A. M.; Di Noja, S.; Ragni, R.; Zappimbulso, N.; Farinola, G. M., *J. Org. Chem*. **2018,** 83, 9312-9321.

97. Ajitha, M. J.; Pary, F.; Nelson, T. L.; Musaev, D. G., *ACS Catal.* **2018,** 8, 4829-4837.

98. Ojha, N. K.; Zyryanov, G. V.; Majee, A.; Charushin, V. N.; Chupakhin, O. N.; Santra, S., *Coord. Chem. Rev.* **2017,** 353, 1-57.

99. Gawande, M. B.; Goswami, A.; Felpin, F.-X.; Asefa, T.; Huang, X.; Silva, R.; Zou, X.; Zboril, R.; Varma, R. S., *Chem.Rev.* **2016,** 116, 3722-3811.

100. Ranu, B. C.; Dey, R.; Chatterjee, T.; Ahammed, S., *ChemSusChem.* **2012,** 5, 22-44.

101. Zhang, W.; Zeng, Q.; Zhang, X.; Tian, Y.; Yue, Y.; Guo, Y.; Wang, Z., *J. Org. Chem.* **2011,** 76, 4741-4745.

102. Pla, D.; Gómez, M., *ACS Catal.* **2016,** 6, 3537-3552.

103. Debasree, S.; Chhanda, M., *Curr. Organocatal.* **2019,** 6, 79-91.

104 Boudreault, P.-L. T.; Beaupré, S.; Leclerc, M.,*Polym. Chem* **2010,** 1 , 127-136.

105 Jin, G.; Xia, L.; Liu, Z.; Lin, H.; Ling, J.; Wu, H.; Hou, L.; Mo, Y., *J. Mater. Chem. C.* **2016,** 4, 905-913.

106 Lin, Y.; Zhao, F.; He, Q.; Huo, L.; Wu, Y.; Parker, T. C.; Ma, W.; Sun, Y.; Wang, C.; Zhu, D.; Heeger, A. J.; Marder, S. R.; Zhan, X., *J. Am. Chem. Soc.* **2016,** 138, 4955-4961.

107. Jiang, D.; Xue, Z.; Li, Y.; Liu, H.; Yang, W., *J. Mater. Chem. C.* **2013,** 1, 5694-5700.

108. Zhu, Y.; Champion, R. D.; Jenekhe, S. A., *Macromolecules* **2006,** 39, 8712-8719.

109. Neophytou, M.; Bryant, D.; Lopatin, S.; Chen, H.; Hallani, R. K.; Cater, L.; McCulloch, I.; Yue, W., *Macromol. Rapid Commun.* **2018,** 39, 1700820.

110. Hou, J.; Park, M.-H.; Zhang, S.; Yao, Y.; Chen, L.-M.; Li, J.-H.; Yang, Y., *Macromolecules* **2008,** *41* (16), 6012-6018.

111 Wang, S.; Wang, Z.; Zha, Z., *Dalton Trans.* **2009,** 43, 9363-9373.

112 Ojha, N. K.; Zyryanov, G. V.; Majee, A.; Charushin, V. N.; Chupakhin, O. N.; Santra, S., *Coord. Chem. Rev.* **2017,** *353*, 1-57.

113 Cong, H.; Porco, J. A., *ACS Catalysis* **2012,** 2, 65-70.

114 Mohammadparast, F.; Dadgar, A. P.; Tirumala, R. T. A.; Mohammad, S.; Topal, C. O.; Kalkan, A. K.; Andiappan, M., *J. Phys. Chem. C.* **2019,** 123, 11539-11545.

115 Ouyang, G.; Wang, C. X.; Yang, G. W., *Chem. Rev.* **2009,** *109* (9), 4221-4247.

116 Ranu, B. C.; Dey, R.; Chatterjee, T.; Ahammed, S., *ChemSusChem*. **2012,** *5*, 22-44.

117 Gawande, M. B.; Goswami, A.; Felpin, F.-X.; Asefa, T.; Huang, X.; Silva, R.; Zou, X.; Zboril, R.; Varma, R. S., *Chem. Rev.* **2016,** 116, 3722-3811.

118 Haque, A.; Al-Balushi, R. A.; Al-Busaidi, I. J.; Khan, M. S.; Raithby, P. R., *Chem. Rev.* **2018,** 118, 8474-8597.

119 Broggi, A.; Tomasi, I.; Bianchi, L.; Marrocchi, A.; Vaccaro, L., *ChemPlusChem* **2014**, 79, 486-507.

120 Steiger, D.; Smith, P.; Weder, C., *Macromol. Rapid Commun*.**1997,** 18, 643-649.

121 Kijima, M.; Kinoshita, I.; Hattori, T.; Shirakawa, H, *Synth. Met*.**1999,** 100, 61-69.

122 Williams, V. E.; Swager, T. M., *J Polym Sci A Polym Chem***. 2000,** 38, 4669-4676.

123 Addanki Tirumala, R. T.; P. Dadgar, A.; Mohammadparast, F.; Ramakrishnan, S. B.; Mou, T.; Wang, B.; Andiappan, M., *Green Chem.* **2019,** 21, 5284-5290.

124 Pankow, R. M.; Ye, L.; Thompson, B. C., *ACS Macro Lett*. **2018,** 7, 1232-1236.

125 Isotope Distribution Calculator and Mass Spec Plotter. https://www.sisweb.com/mstools/isotope.htm. (Accessed: December 6, 2019).

126 Selvaraju, S.; Niradha Sachinthani, K. A.; Hopson, R. A.; McFarland, F. M.; Guo, S. Rheingold, A. L.; Nelson, T. L., *Chem. Comm.* **2015,** 51, 2957-2959.

127 Xu, R.-P.; Li, Y.-Q.; Tang, J.-X., *J. Mater. Chem.C,* **2016,** 4, 9116-9142.

128 Burroughes, J. H.; Bradley, D. D. C.; Brown, A. R.; Marks, R. N.; Mackay, K.; Friend, R. H.;Burns, P. L.; Holmes, A. B., *Nature* **1990,** *347*, 539-541.

129 Hedley, G. J.; Ruseckas, A.; Samuel, I. D. W., *Chem. Rev*. **2017,** *117*, 796-837.

130 McQuade, D. T.; Pullen, A. E.; Swager, T. M., *Chem. Rev* **2000,** *100*, 2537-2574.

131 Inal, S.; Rivnay, J.; Suiu, A.-O.; Malliaras, G. G.; McCulloch, I., *Acc. Chem. Res.* **2018,** 51, 1368-1376.

132 Kimbrough, R. D., *Environ Health Perspect*. **1976,** *14*, 51-56.

133 Suzuki, A., *J. Organomet. Chem.* **1999,** 576, 147-168.

134 Yokoyama, A.; Suzuki, H.; Kubota, Y.; Ohuchi, K.; Higashimura, H.; Yokozawa, T., *J. Am. Chem. Soc.* **2007,** 129, 7236-7237.

135 Kabalka, G. W.; Wang, L., *Tetrahedron Lett.* **2002,** *43*, 3067-3068

136 Parrish, J. P.; Jung, Y. C.; Floyd, R. J.; Jung, K. W., *Tetrahedron Lett.* **2002,** *43*, 7899-7902.

137 Lakmini, H.; Ciofini, I.; Jutand, A.; Amatore, C.; Adamo, C., *J. Phys. Chem. A*. **2008,** 112, 12896-12903.

138 Yuan, C.; Hong, J.; Liu, Y.; Lai, H.; Fang, Q. *J. Polym. Sci. A Polym. Chem*. **2011,** 49, 4098-4101.

139 Hinkes, S. P. A.; Klein, C. D. P., *Org. Lett.* **2019,** *21*, 3048-3052.

140 Kim, M.; Ryu, S. U.; Park, S. A.; Choi, K.; Kim, T.; Chung, D.; Park, T., *Adv. Funct. Mater*. **2020,** *30*, 1904545.

141 Su, Y.-W.; Lin, Y.-C.; Wei, K.-H., *J. Mater. Chem.* **2017,** *5*, 24051-24075.

142 Gomollón-Bel, F., *Int. J. Chem.***2019,** *41*, 12.

143 Tanaka, K.; Toda, F., *Chem. Rev*. **2000,** *100*, 1025-1074.

144 Li, J.; Nagamani, C.; Moore, J. S., *Acc. Chem. Res.* **2015,** 48, 2181-2190.

145 Chen, Z.; Mercer, J. A. M.; Zhu, X.; Romaniuk, J. A. H.; Pfattner, R.; Cegelski, L.; Martinez, T. J.; Burns, N. Z.; Xia, Y., *Science* **2017,** 357, 475.

146 Oh, C.; Choi, E. H.; Choi, E. J.; Premkumar, T.; Song, C., *ACS Sustain. Chem. Eng.* **2020,** 8, 4400-4406.

147 Peng, Q.; Lu, Z.-Y.; Huang, Y.; Xie, M.-G.; Han, S.-H.; Peng, J.-B.; Cao, Y., *Macromolecules.* **2004,** 37, 260-266.

148 Sandee, A. J.; Williams, C. K.; Evans, N. R.; Davies, J. E.; Boothby, C. E.; Köhler, A.; Friend, R. H.; Holmes, A. B., *J. Am. Chem. Soc*. **2004,** 126, 7041-7048.

149 Grisorio, R.; Suranna, G. P.; Mastrorilli, P.; Nobile, C. F., *Adv. Funct. Mater*. **2007,** 17, 538-548.

150 Leclerc, M., *Polym Sci A Polym Chem.* **2001,** 39, 2867-2873.

151 Donat-Bouillud, A.; Lévesque, I.; Tao, Y.; D'Iorio, M.; Beaupré, S.; Blondin, P.; Ranger, M.; Bouchard, J.; Leclerc, M., *Chem. Mater*. **2000,** 12, 1931-1936.

152 Peng, Q.; Lu, Z.; Huang, Y.; Xie, M.; Xiao, D.; Zou, D., *J. Mater. Chem.* **2003,** 13, 1570-1574.

153 Herguth, P.; Jiang, X.; Liu, M.; Jen, A. K. Y., *SPIE*. **2003**, 4800.

154 Herguth, P.; Jiang, X.; Liu, M. S.; Jen, A. K. Y., *Macromolecules* **2002,** 35, 6094-6100.

155. Pentsak, E. O.; Ananikov, V. P., *Eur. J. Org. Chem*.**2019,** 2019 , 4239-4247.

156. Karikomi, M.; Kitamura, C.; Tanaka, S.; Yamashita, Y., *J. Am. Chem. Soc*. ***1995,*** 117, 6791-6792.

157. Bundgaard, E.; Krebs, F. C., *Macromolecules* **2006,** 39, 2823-2831.

158. Bundgaard, E.; Krebs, F. C., *Sol. Energy Mater Sol. Cells*. **2007,** 91, 954-985.

VITA

Fathima Fazna Pary

Candidate for the Degree of

Doctor of Philosophy

Dissertation: GREENER AND FACILE APPROACHES TOWARDS SYNTHESIS OF ORGANIC SEMICONDUCTING MATERIALS

Major Field: Chemistry

Biographical:

Education:

Completed the requirements for the Doctor of Philosophy in Chemistry at Oklahoma State University, Stillwater, Oklahoma in December, 2020.

Completed the requirements for the Bachelor of Science in Chemistry at University of Kelaniya, Kelaniya, Sri Lanka in 2013.

Experience:

Graduate teaching and research assistant, Department of Chemistry, Oklahoma State University, Stillwater, Oklahoma 2015-2020.
Undergraduate Teaching Assistant, Department of Chemistry, University of Kelaniya, Sri Lanka 2013-2015

Professional Memberships:

American Chemical Society (Division of Polymer Chemistry)
Electrochemical Society, Oklahoma Chapter